THE ROLE OF MTOR IN CARDIAC FUNCTION

A DISSERTATION SUBMITTED TO THE GRADUATE DIVISION OF THE UNIVERSITY OF HAWAI`I AT MANOA IN PARIAL FULFILLMENT OF THE REQUIREMENTS FOR THE DEGREE OF

DOCTOR OF PHILOSOPHY

IN

CELL AND MOLECULAR BIOLOGY

AUGUST 2017

BY

BRIANA KIYOMI SHIMADA

Dissertation Committee:
Takashi Matsui, Chairperson
Marla J. Berry
Benjamin Fogelgren
Olivier Le Saux
George Hui

ACKNOWLEDGEMENTS

First and foremost, I would like to recognize my doctoral advisor, Dr. Takashi Matsui for his invaluable and immeasurable support and guidance during my time as a Ph.D. student here at the University of Hawaii, Manoa. Throughout the past five years he has provided me instrumental advice in science, in my career, and in life. He has been an incredible advisor for me and was always willing to give his time and energy in discussing experiments and teaching me in order to grow my knowledge of both cardiovascular research and basic science in general. I cannot thank him enough as without him, this thesis would not have been possible. I would like to also express my sincere gratitude for each member of my thesis committee, Dr. Marla Berry, Dr. Benjamin Fogelgren, Dr. Olivier Le Saux, and Dr. George Hui for his or her vital mentorship and willingness to serve on my committee. Each of them has given me key advice on both science and career throughout their time on my committee.

I would also like to especially acknowledge several members of the Matsui Lab for their assistance over the years, particularly Dr. Jason Higa for his advice and guidance, Dr. Yuichi Baba for his advice and assistance, MS Naaiko Yorichika, for teaching and assisting me, especially with the IonOptix system, and Dr. Toshinori Aoyagi for instructing me in using the *ex vivo* Langendorff system. I would also like to appreciate the numerous medical students, undergraduate, and high school students who assisted with various projects in the lab, especially genotyping and helping with the murine colony. I am very grateful to all Matsui Lab members for their help over the years.

I am also appreciative of all of my fellow students and colleagues at JABSOM for all of their help in navigating the PhD process whether it was providing information about a

class or just general advice about the program and life as a graduate student. Their input and support were vital to my progression as a student.

Next, I would like to acknowledge the NIH, as this dissertation would also not have been possible without funding from them and from the T32 Training Grant I received during the last year of my thesis work. I would like to express my thanks to the NIH who provided this backing and Dr. Ralph Shohet for accepting me as a T32 trainee.

Finally, I also want to acknowledge all of my friends and family for their support over the past five years of my graduate studies, especially my parents Michael and Robin Shimada. They have always encouraged me to follow my dreams and passion and without them, I would not have been able to pursue this career.

ABSTRACT

Despite many therapeutic advances, the rate of heart failure after myocardial infarction remains very high. Therefore, there is still significant need to develop better therapeutics to treat heart failure. One potential mark is the protein, mechanistic target of rapamycin (mTOR), a key signaling kinase for most cell types. Overexpression of mTOR has been previously shown by our lab as sufficient to protect the heart against different stressors including ischemia-reperfusion (I/R) injury, TAC-induced hypertrophy, and metabolic syndrome and obesity. As our laboratory is most concerned with the role of mTOR in I/R injury, in this dissertation I wanted to determine if mTOR was necessary for cardioprotection in I/R against various pathological settings, including diabetes mellitus (DM).

To do this, I generated a tamoxifen-inducible, cardiac muscle specific mTOR knockout (CKO) mouse model to evaluate the loss of mTOR in functional studies, especially I/R injury. I initially characterized heart physiology in the CKO mouse at baseline using echocardiography. Preliminary *in vivo* I/R injury and *ex vivo* Langendorff I/R using acute inhibition of mTOR by Torin1 administration suggested mTOR was necessary to protect the heart as the recovery of the CKO group was significantly worse than that of littermate controls in both settings. However, when CKO hearts were subjected to I/R using the *ex vivo* system, CKO hearts surprisingly exhibited had better cardiac function following I/R than control hearts. This was also the case in a mouse model of obesity and hyperglycemia. CKO hearts also had irregular contractility, a finding that led to the investigation of Ca^{2+} handling in these CKO mice. Cardiomyocytes (CM) isolated from CKO mice displayed weaker contractions and smaller calcium (Ca^{2+})

transients as well as a reduction in relative SR Ca^{2+} content. Insulin also blunted the recovery of these mice, showing mTOR is at least partially necessary for cardioprotection against I/R injury. The findings in this study may be caused by decreased expression of the IP3R, which plays an important role in regulating Ca^{2+} transfer from the ER to the mitochondria, since that was found to be lower in the SR/mitochondria fraction of CKO hearts. However, a clear mechanism for explaining these results still needs to be identified. A novel role for mTOR in Ca^{2+} handling and contraction could bring new insights into potential therapeutics for treating and managing heart failure.

TABLE OF CONTENTS

ACKNOWLEDGEMENTS.....II

ABSTRACT IV

LIST OF FIGURES..... XII

LIST OF TABLES XV

LIST OF ABBREVIATIONS.....XVI

CHAPTER ONE: INTRODUCTION

1.1. Introduction 1

1.2. Myocardial infarction, cardiac remodeling, and the development of subsequent heart failure 3

1.3. Background and signaling pathway of mTOR 5

1.4. The role of mTOR in cardiac function and cell survival 9

1.5. Regulation of cardiac muscle contraction and calcium transients physiological and heart failure settings 12

1.6. Calcium regulation of cell death in the cardiomyocyte.....15

1.7. mTOR and calcium signaling and regulation 16

1.8. The role of mTOR in cardiac metabolism and the metabolic syndrome 18

1.9. Research Objectives.....21

CHAPTER TWO: THE ROLE OF MTOR IN AN EX VIVO LANGENDORFF I/R INJURY MODEL

2.1. Introduction 22

2.1.1. Specific Aim 1: To determine the necessity of mTOR in I/R injury by using ..22

ex vivo Langendorff. 22

2.1.2. Rationale for using tomato reporter mice 23

2.1.3. Rationale for using ex vivo Langendorff 23

2.2.1. Animal Models 24

2.2.1.1. Generation of cardiac specific mTOR knockout 24

2.2.1.2. Generation of tomato reporter mice 25

2.2.3. Tamoxifen administration 27

2.2.4. Echocardiography 27

2.2.5. Isolation of adult murine ventricular myocytes 27

2.2.6. Western blot analysis 29

2.2.7. Analysis of tomato reporter mice. 29

2.2.8. Ex vivo I/R in Langendorff perfused hearts. 30

2.2.9. Drug treatment protocol for ex vivo Langendorff perfused hearts. 31

2.2.10. Pacing protocol for ex vivo Langendorff perfused hearts. 31

2.2.11. Isoproterenol challenge of ex vivo Langendorff perfused hearts 32

2.2.12. Biological analysis of ex vivo perfused hearts 32

2.2.14. Calculation for peak ischemic contracture (Δ mmHg) and time to peak ischemic contracture. 33

2.2.15. Insulin stimulation of ex vivo Langendorff perfused hearts. 33

2.2.16. Subcellular fractionation of whole heart tissue. 33
2.2.17. Statistical analysis 34
2.3. Results 34
2.3.1. Knockout of mTOR is cardiomyocyte specific. 34
2.3.2. mTOR-KO mice have normal heart sizes and baseline function. 36
2.3.3. Torin1 significantly decreases the percent left ventricular developed pressure (%LVDP) recovery of wild-type Langendorff perfused hearts. 38
2.3.4. Torin1 treatment decreases downstream mTOR signaling. 39
2.3.5. Baseline ex vivo Langendorff parameters show control and mTOR-KO mice hearts have similar cardiac function prior to I/R injury. 40
2.3.6. Hearts from mTOR-KO mice exhibit better percent left ventricular developed pressure recovery (%LVDP) after I/R injury but increased variance of contractions compared to controls. 41
2.3.7. mTOR-KO hearts have significantly less cell death than controls after ex vivo I/R. 43
2.3.8. Isoproterenol challenge of CKO hearts does not significantly affect LVDP recovery 44
2.3.9. mTOR-KO hearts exhibit cardiac alternans at baseline. 46
2.3.10. Pacing has no effect on LVDP recovery of control and CKO hearts. 48
2.3.11. Pacing before reperfusion results in decreased ischemic contracture of CKO hearts. 49
2.3.12. mTOR-KO mice hearts recover worse when treated with insulin during reperfusion. 51

2.3.13. IP3R2 expression is significantly decreased in the SR/mito fractions of mTOR-KO hearts. 52
2.4. Discussion....54
2.4.1. Summary and interpretation of results 54

CHAPTER THREE: THE ROLE OF MTOR IN VITRO IN CALCIUM SIGNALING AND EC-COUPLING

3.1. Introduction 57
3.1.2. Specific Aim 2: To determine the role of mTOR in cardiomyocyte Ca^{2+} signaling and EC-coupling. 57
3.1.3. Rationale for measuring contraction and Ca^{2+} transients using Fura-2-AM and the IonOptix system 58
3.1.4. Rationale for using isoproterenol and ryanodine....59
3.1.5. Rationale for using caffeine....59
3.2. Methods 60
3.2.1. Subcellular fractionation of whole heart tissue. 60
3.2.2. Western Blot analysis....60
3.2.3. Isolation of adult murine ventricular myocytes for Ionoptix 60
3.2.4. Measurement of Ca^{2+} transients and sarcomere length shortening....60
3.2.5. Isoproterenol challenge of isolated adult murine ventricular myocytes and ryanodine treatment 63
3.2.6. Caffeine stimulation of isolated adult murine ventricular myocytes....64
3.2.7. Calculation of %spontaneous calcium waves (%SCW) 64

3.2.8. Statistical analysis 65
3.3. Results 65
3.3.1. mTOR is localized in both cytosolic and subcellular fractions 65
3.3.2. Cardiomyocytes isolated from mTOR-CKO mice have decreased contractility and a smaller calcium transient ratio. 66
3.3.3. Isoproterenol challenge of CKO cardiomyocytes did not show an increase in the percent of spontaneous Ca^{2+} waves (SCWs) and ryanodine inhibition of the ryanodine receptor did not decrease the amount of SCWs. 69
3.3.4. mTOR-CKO CMs do not show a change in any major EC-Coupling protein. 70
3.3.5. Caffeine stimulation of control and CKO cardiomyocytes showed CKO CMs have decreased relative SR Ca^{2+} content 72
3.4. Discussion 74
3.4.1. Summary and interpretation of results 74

CHAPTER FOUR: THE ROLE OF MTOR IN OTHER PATHOLOGICAL SETTINGS

4.1. Introduction 76
4.1.1. Specific Aim 3: To determine the role of mTOR in other pathological settings such as diabetes mellitus (DM). 76
4.1.2. Rationale for using a diet-induced obesity mouse model 77
4.2. Methods 77
4.2.1. Tamoxifen administration (injections) 77
4.2.2. High-fat diet administration. 78

4.2.3. Collection of blood glucose levels. 78
4.2.4. Statistical analysis 78
4.3. Results 79
4.3.1. Mice on a HFD exhibit large body weights and high blood glucose levels relative to mice on a NCD. 79
4.3.2. CKO mice hearts recover significantly better than CON on both a NCD and a HFD. 80
4.4. Discussion 81
4.4.1. Summary and interpretation of results 81

CHAPTER FIVE: CONCLUDING REMARKS

5.1. Summary and discussion of results 83
5.2. Conclusion 86
5.3. Limitations and future directions 88
LITERATURE CITED 90

LIST OF FIGURES

CHAPTER ONE

Figure 1.1. The structure of mTOR. 6

Figure 1.2. mTOR complexes 1 and 2 and their associated proteins. 7

Figure 1.3. The mTOR-signaling pathway.....9

Figure 1.4. mTOR-KO have significantly increased fibrosis and decreased % fractional shortening (%FS) 7 days after in vivo I/R injury. 11

Figure 1.5. EC-Coupling under normal physiological conditions. 13

Figure 1.6. Mechanisms behind reduced SR Ca^{2+} content in heart failure. 15

Figure 1.7. Overexpression of cardiac mTOR prevents cardiac dysfunction after transient ischemia in HFD hearts. 20

CHAPTER TWO

Figure 2.1. mTOR-KO breeding scheme. 25

Figure 2.2. Generation of tomato reporter mice. 26

Figure 2.3. Adult murine CMs isolated from C57BL6 mice. 28

Figure 2.4. Picture of a heart hung on the ex vivo Langendorff apparatus with balloon inserted into the LV. 31

Figure 2.5 Knockout of mTOR is cardiomyocyte specific. 35

Figure 2.6. mTOR-CKO mice have normal sized hearts and normal baseline cardiac function. 37

Figure 2.7. Torin1 treatment significantly decreases %LVDP recovery in wild-type mice. 38
Figure 2.8. Torin1 treatment decreases downstream signaling of both mTORC complexes. 40
Figure 2.9. mTOR-CKO hearts have better %LVDP recovery after *ex vivo* I/R. 42
Figure 2.10. mTOR-KO hearts have significantly increased average variance of contractions. 43
Figure 2.11. mTOR-KO hearts have a significantly decreased marker of myocardial damage compared with controls. 44
Figure 2.12. Isoproterenol stimulation decreased recovery of both control and CKO hearts but does not cause CKO hearts to recover significantly worse than controls. 45
Figure 2.13. mTOR-CKO hearts display cardiac alternans at baseline. 48
Figure 2.14. Pacing does not affect %LVDP recovery of mTOR-CKO hearts. 49
Figure 2.15. CKO hearts have significantly decreased peak ischemic contracture as well as well as significantly increased time to peak ischemic contracture. 50
Figure 2.16. Insulin administered at reperfusion significantly decreases recovery of the mTOR-KO hearts. 52
Figure 2.17. IP3R protein level is reduced in the SR/mito fraction of CKO hearts. 53
and p-PLN. VDAC was used as a loading control for the SR/mito fraction while Gapdh was used as the loading control for the cytosolic fraction. N = 6 for all groups. 71

CHAPTER THREE

Figure 3.1. Picture of our IonOptix system including the inverted microscope used in these experiments. 62

Figure 3.2. Measurements of cardiac function by IonOptix. 63

Figure 3.3. Scheme of isoproterenol treatment and subsequent pacing protocol using the IonOptix system. 64

Figure 3.4. mTOR is localized in both cytosolic and subcellular fractions 66

Figure 3.5. Cardiomyocytes isolated from mTOR-KO mice have weaker contractility and a smaller calcium transient ratio. 68

Figure 3.6. mTOR-KO CMs do not have significantly more %SCW than controls and ryanodine did not significantly decrease the percentage of SCWs. 70

Figure 3.7. CKO hearts do not show a change in any major EC-Coupling protein. 71

Figure 3.8. mTOR-CKO CMs have lower relative SR calcium content than controls. 73

CHAPTER FOUR

Figure 4.1. Body weight and fasting blood glucose levels are significantly higher in control mice on a HFD. 80

Figure 4.2. mTOR-CKO mice on a NCD and HFD recover better after I/R injury in the *ex vivo* Langendorff model. 81

CHAPTER FIVE

Figure 5.1. Scheme of our speculated mechanism for the findings in this dissertation. . 88

LIST OF TABLES

Table 1. Body weight, heart weight, and heart weight:tibia length (HW:TB) ratio of control and mTOR-KO mice. 36

Table 2. Baseline echocardiograph parameters. 37

Table 3. Baseline *ex vivo* Langendorff parameters. 41

Table 4. CKO hearts display cardiac alternans more consistently and at lower frequencies versus controls. 47

Table 5. Comparison of body weight, heart weight, and HW:TB between control and CKO mice on a NCD and a HFD 79

LIST OF ABBREVIATIONS

%FS:	% fractional shortening
4E-BP1:	Eukaryotic translation initiation factor 4E-binding protein 1
ANT:	Adenine nucleotide translocase
BDM:	Butanedione monoxime
BW:	Body weight
Ca^{2+}:	Calcium
CAMKIIδ:	Calcium/calmodulin dependent serine/threonine kinase IIδ
CHF:	Congestive heart failure
CICR:	Calcium-induced calcium release
CK:	Creatine kinase
CKO:	Cardiac specific mTOR-KO mice
CKO:	Cardiac-specific mTOR knockdown mice
CM:	Cardiomyocyte
CON:	Control mice
CON:	Littermate control mice
CVD:	Cardiovascular disease
CypD:	Cyclophilin D
DAPI:	4',6-diamidino-2-phenylindole
DEPTOR:	DEP domain containing mTOR-interacting protein
DM:	Diabetes mellitus
eIF4E:	Eukaryotic translation initiation factor 4E
ER:	Endoplasmic reticulum
HF:	Heart failure
HFD:	High fat diet
HW:	Heart weight
I/R:	Ischemia-reperfusion injury
IMM:	Inner mitochondrial membrane
IP3R:	Inositol 1,4,5-trisphosphate receptor
IRS-1:	Insulin receptor substrate 1

LAD:	Left anterior descending coronary artery
LV:	Left ventricular
LVDP:	Left ventricular developed pressure
LVEDP:	Left ventricular end diastolic pressure
LVIDd:	Left ventricular interior diameter dimension
LVPWd:	Left ventricular posterior wall diameter
MAMs:	Mitochondrial associated membranes
MI:	Myocardial infarction
mLST8:	Mammalian lethal with SEC13 protein 8
mPTP:	Mitochondria permeability transition pore
mPTP:	Mitochondria permeability transition pore
mSIN1:	Mammalian stress-activated protein kinase interacting protein 1
mTOR:	Mechanistic target of rapamycin
mTORC1:	mTOR complex 1
mTORC2:	mTOR complex 2
NCD:	Normal chow diet
NCX-1:	Sodium-calcium exchanger 1
NO:	Nitric oxide
NZO:	New Zealand Obese mice
OMM:	Outer mitochondrial membrane
p-PLN:	Phospho-phospholamban
p-RYR:	Phospho-ryanodine receptor
p70S6K:	Ribosomal protein S6 kinase
PDK1:	Phosphoinositide-dependent kinase-1
PI3K:	Phosphoinositide-3 kinase
PIKK:	Phosphatidylinositol 3-kinase-related kinase
PIP_3:	Phosphatidylinositol (3,4,5)-trisphosphate
PKA:	Protein kinase A
PLN:	Phospholamban
PRAS40:	Proline-rich Akt substrate of 40
RAPTOR:	Regulatory associated protein of mTOR

RHEB:	Ras homolog enriched in brain
RICTOR:	Rapamycin-insensitive companion of mTOR
RYR:	Ryanodine receptor
S6:	Ribosomal protein S6
S6K1:	Ribosomal protein S6 kinase beta-1
SCW:	Spontaneous calcium waves
SERCA:	Sarco-endoplasmic reticulum calcium ATPase
SL:	Sarcomere length
SR:	Sarcoplasmic reticulum
TAC:	Transverse aortic constriction
TB:	Tibia length
TBE:	2,2,2-tribromoethanol
Tg:	mTOR-transgenic
TNF:	Tumor necrosis factor
TPS:	Time to peak shortening
TR90:	Time to 90% re-lengthening
TSC1/2:	Tuber sclerosis complex 1 and 2
VDAC:	Voltage dependent anion channel
WT:	Wild-type
αMHC:	Alpha myosin heavy chain

Chapter One

INTRODUCTION

1.1 Introduction

Myocardial infarction (MI) and later heart failure (HF) continue to be among the leading causes of morbidity and mortality for patients in the United States. Despite therapeutic advances such as coronary stents and bypass surgery, HF prevalence in the United States has actually increased from 5.7 million people to 6.5 million from 2009 to 2014 although the five-year survival rate improved [1]. Therefore, there is still significant need to discover potential therapeutic targets in order to prevent and treat HF and cardiovascular disease (CVD) in general.

The mechanistic target of rapamycin (mTOR) kinase plays a key role in the insulin-signaling pathway and is known to protect the heart against ischemia/reperfusion (I/R) injury [2-4]. **However, the mechanism behind the cardioprotective effects of mTOR in I/R injury remains unknown**. A recent study suggested mTOR may be localized between the sarcoplasmic reticulum (SR) and the mitochondria and may have a role in regulating calcium (Ca^{2+}) transients [5]. Intracellular Ca^{2+} plays a central role in Excitation-Contraction (EC) Coupling for muscle contraction and in cell death by Ca^{2+} overload through the mitochondrial permeability transition pore (mPTP) [6]. A role for mTOR in Ca^{2+} transients may explain the cardioprotective effects of mTOR in I/R injury.

To further investigate the role of mTOR in cardioprotection, I generated cardiomyocyte (CM) specific, tamoxifen-inducible Cre mTOR knockout (CKO) mice and

assessed the cardiac function of their hearts using *ex vivo* Langendorff to generate global ischemia, and *in vitro* using IonOptix. IonOptix is specialized software that uses a dual excitation photometer system and an edge detector to evaluate contraction and Ca^{2+} transients. Preliminary data showed that the CKO mice displayed significantly worse recovery after *in vivo* I/R injury. Our previous studies using our mice with cardiac specific mTOR overexpressing transgene (mTOR-Tg) demonstrated mTOR was cardioprotective in a variety of pathologies. mTOR overexpression resulted in improved cardiac function post I/R injury, after transverse aortic constriction (TAC) induced hypertrophy, and in a mouse model of obesity [2, 7, 8]. These studies all suggested mTOR was *sufficient* to protect the heart against these certain stressors. A previous report using cardiac-specific mTOR knockout mice showed that deletion of cardiac mTOR accelerates heart failure progression in TAC-induced hypertrophy [9]. However, a mechanism of how mTOR regulates cardioprotective effects in I/R injury remains undefined. *Therefore, my overall hypothesis is that mTOR is necessary to protect the heart against I/R in various pathological settings including diabetes mellitus (DM).* To test this hypothesis, I performed experiments addressing the following three specific aims that will be addressed in the specified chapters:

Specific Aim 1 (Chapter Two): To determine the necessity of mTOR in I/R injury by using *the ex vivo* Langendorff method.

For this aim, I investigated the effects of loss of mTOR by generating and validating a CM specific, tamoxifen-inducible Cre mTOR knockdown (CKO) line. I evaluated the CKO mice versus their littermate controls (CON) at baseline and after *ex*

vivo I/R injury to determine whether mTOR was necessary to protect CMs from cell death.

Specific Aim 2 (Chapter Three): To define the role of mTOR in cardiomyocyte Ca^{2+} signaling and EC-coupling.

By isolating CMs from adult mTOR-CKO mice, I was able to measure how contractility and Ca^{2+} transients were affected by the loss of mTOR. Sarcomere length (SL) shortening and intracellular Ca^{2+} transients were assessed as indicators of cardiac function using the IonOptix technology. To determine if release or reuptake was affected in mTOR-CKO CMs, I analyzed Ca^{2+} upon stimulation with isoproterenol and caffeine.

Specific Aim 3 (Chapter Four): To define the role of mTOR in ischemia-reperfusion injury in a mouse model of diabetes mellitus (DM).

For this section, I measured the cardiac function of our CKO and CON mice in a mouse model of obesity. I placed the CKO and CON mice on a high fat diet (HFD) for 12 weeks beginning at 6-8 weeks of age. At the end of the 12 weeks, the mice were weighed and fasting blood glucose was measured. I subjected hearts from CON and CKO mice to I/R injury using the *ex vivo* Langendorff system. I also evaluated the effects of insulin on the CKO and CON mice using the *ex vivo* system.

1.2 Myocardial infarction, cardiac remodeling, and the development of subsequent heart failure

Myocardial infarction and subsequent heart failure still remains a significant cause of mortality in the United States with an estimated 5 million Americans diagnosed with

congestive heart failure (CHF). Epidemiological reports estimate the rate of heart failure after MI to be around 25% [10]. The post-MI development of heart failure depends on multiple factors including size of infarct, location, and time to reperfusion or revascularization.

Cardiac remodeling is the underlying molecular mechanism by which heart failure occurs after an MI and is also influenced by many factors such as hemodynamic load, neurohormonal activation, cytokines such as tumor necrosis factor (TNF) and nitric oxide (NO), and oxidative stress [11]. The process of left ventricular (LV) remodeling begins rapidly, usually within the first few hours after an infarct and continues to progress over time due to a variety of cellular changes involving many different components and factors [12, 13]. The major contributors to cardiac remodeling are cardiac myocyte cell death, fibroblast proliferation, and collagen deposition [14-17]. Previous clinical studies strongly suggest that the magnitude of LV remodeling in patients is directly proportional to the initial infarct size following acute MI, including reperfusion injury [18, 19]. Thus, the CM cell death is perhaps one of the most important components in LV remodeling. After an MI, CMs die and cause the surviving myocytes to become elongated or hypertrophied as a compensatory mechanism. This in turn leads to increased ventricular wall thickness, altered loading conditions, and wall stress. These changes result in energy imbalance and further ischemia and feeding a vicious cycle of continual ventricular remodeling [20].

Eventually, all of these changes lead to a progressive worsening of cardiac function and heart failure. Generally, patients with a greater extent of remodeling have a poorer prognosis and outcome than those that do not, especially those with a reduced

LV ejection fraction [21]. This is especially true in the post-MI population where LV end-systolic volume (LVESV) is the strongest prognostic indicator. Those with the lowest LVESV are correlated with the patients having the highest morbidity [22].

1.3 Background and signaling pathway of mTOR

The mechanistic target of rapamycin (mTOR) was originally discovered through a genetic screen in budding yeasts as a target of the drug rapamycin in 1993 [23, 24]. Shortly thereafter, mTOR was purified and characterized in mammalian cells by three independent studies [25-27]. Following these pioneer studies, mTOR has been found to be a very important cell regulator with multiple different functions. It is a large (289 kDa), atypical serine/threonine kinase, and belongs to the phosphatidylinositol kinase-related family (PIKK) [28]. Structural studies revealed that it contains several tandem HEAT repeats, a central focal adhesion targeting (FAT) domain, a FRB domain, a catalytic kinase domain and the c-terminal FAT (FATC) domain [29] (Figure 1.1).

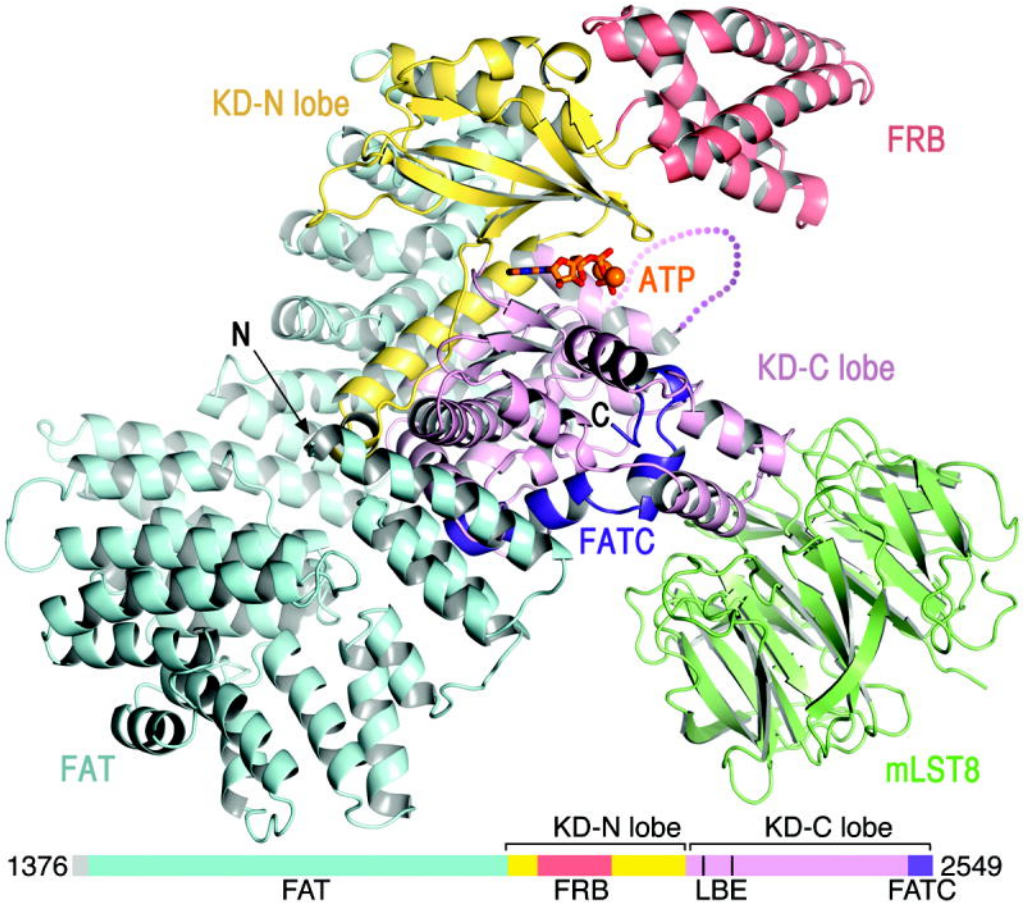

Figure 1.1. The structure of mTOR.
Crystallography structure of a N-terminally truncated mTOR showing its FAT, FRB, kinase, and FATC domains. *Yang, et. al 2013.*

mTOR forms two multi-protein complexes, mTORC1 and mTORC2 [4, 30]. mTORC1 is the rapamycin sensitive complex and is activated by amino acids, especially leucine, and by stress, oxygen, energy, and growth factors [4, 30, 31]. mTORC1 binding proteins consist of regulatory associated protein of mTOR (RAPTOR), mammalian lethal with Sec13 protein (mLST8), proline-rich Akt/PKB substrate 40 kDa (PRAS40), and DEP-domain-containing mTOR interacting protein (DEPTOR) [32-35]. mTORC1 is downstream of Akt and activates the p70S6 kinase (p70S6K) and 4E-binding protein1 (4E-BP1). Central to many signaling pathways, mTORC1 regulates

aspects of protein synthesis, cell growth, proliferation, ribosomal and mitochondrial biogenesis, autophagy, and metabolism.

mTORC2 is the rapamycin insensitive complex and is upstream of Akt. mTORC2 activates Akt by phosphorylating Akt at its Ser473 site. Its binding partners consist of rapamycin-insensitive companion of mTOR (RICTOR), mammalian stress-activated protein kinase [SAPK]-interacting protein (mSin1), protein observed with rictor-1 (PROTOR), DEPTOR, and mLST8 [36-38]. mTORC2 has been shown to regulate cell survival and actin organization [4, 30, 39-42] (Figure 1.2 and 1.3).

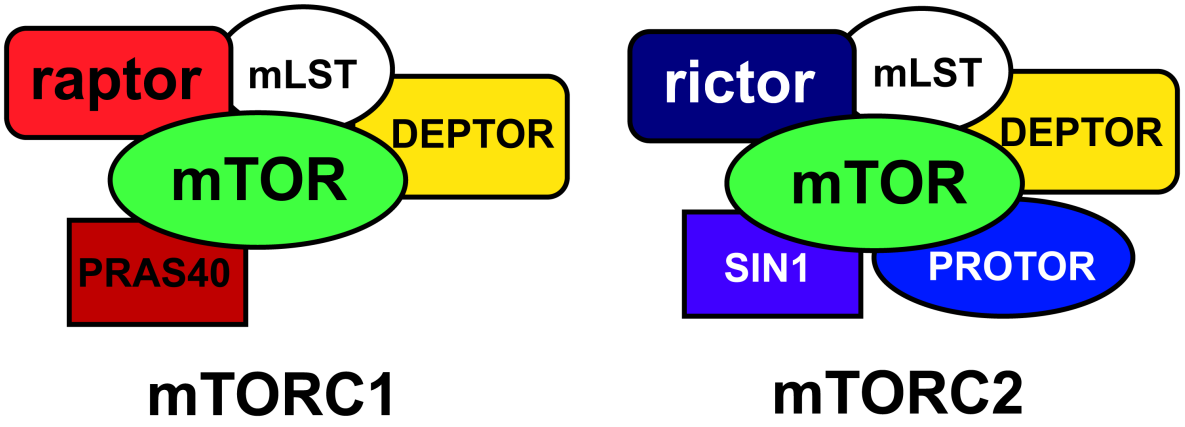

Figure 1.2. mTOR complexes 1 and 2 and their associated proteins.
mTORC1 is associated with raptor, mLST8, DEPTOR, and PRAS40. mTORC2 is associated with rictor, mLST, DEPTOR, PROTOR, and SIN1.

Originally mTOR was found to be a downstream target of the insulin-signaling pathway. However, it can also be activated by amino acids, especially leucine and arginine, through the activation of Rag GTPases associated with ras homolog enriched in brain (Rheb) [43-45]. The binding of insulin to its receptor causes the receptor to undergo a conformational change activating the tyrosine kinase activity on the intracellular side of the receptor. This promotes the recruitment of insulin receptor substrate 1 (IRS1), leading to activation of phosphoinositide 3-kinase (PI3K) and the

production of phosphatidylinositol (3,4,5)-triphosphate (PIP_3). This in turn recruits and activates Akt at the plasma membrane [46]. Akt activation by growth factors can also activate mTORC1 in a tuber sclerosis complex 1 and 2 (TSC1/2) independent manner by promoting the phosphorylation and dissociation of PRAS from mTORC1 [34, 47]. Akt regulates mTORC1 activity via the tuberous sclerosis complex 1 and 2 (TSC-1/2) and Rheb [48, 49]. Akt inhibits TSC2 by phosphorylating it, thereby activating Rheb. This in turn activates mTORC1. mTORC1 phosphorylates p70S6K activating ribosomal protein S6 (S6). mTORC1 also inactivates 4E-BPs, thereby activating the eukaryotic translation initiation factor 4E (eIF4E) and promoting translation (Figure 1.3).

On the other hand, less is known about mTORC2 regulation and signaling although it is known that mTORC2 can control survival by phosphorylating several members of the AGC (PKA/PKG/PKC) family of protein kinases [50-52]. However, the most important and primary role of mTORC2 is to directly phosphorylate Akt on its Ser473 site, with this phosphorylation event, and with phosphoinositide-dependent kinase 1 (PDK1), phosphorylating the Thr308 site, Akt becomes activated [53]. Akt is an extremely important cell regulator responsible for controlling cell survival, proliferation, and growth (Figure 1.3).

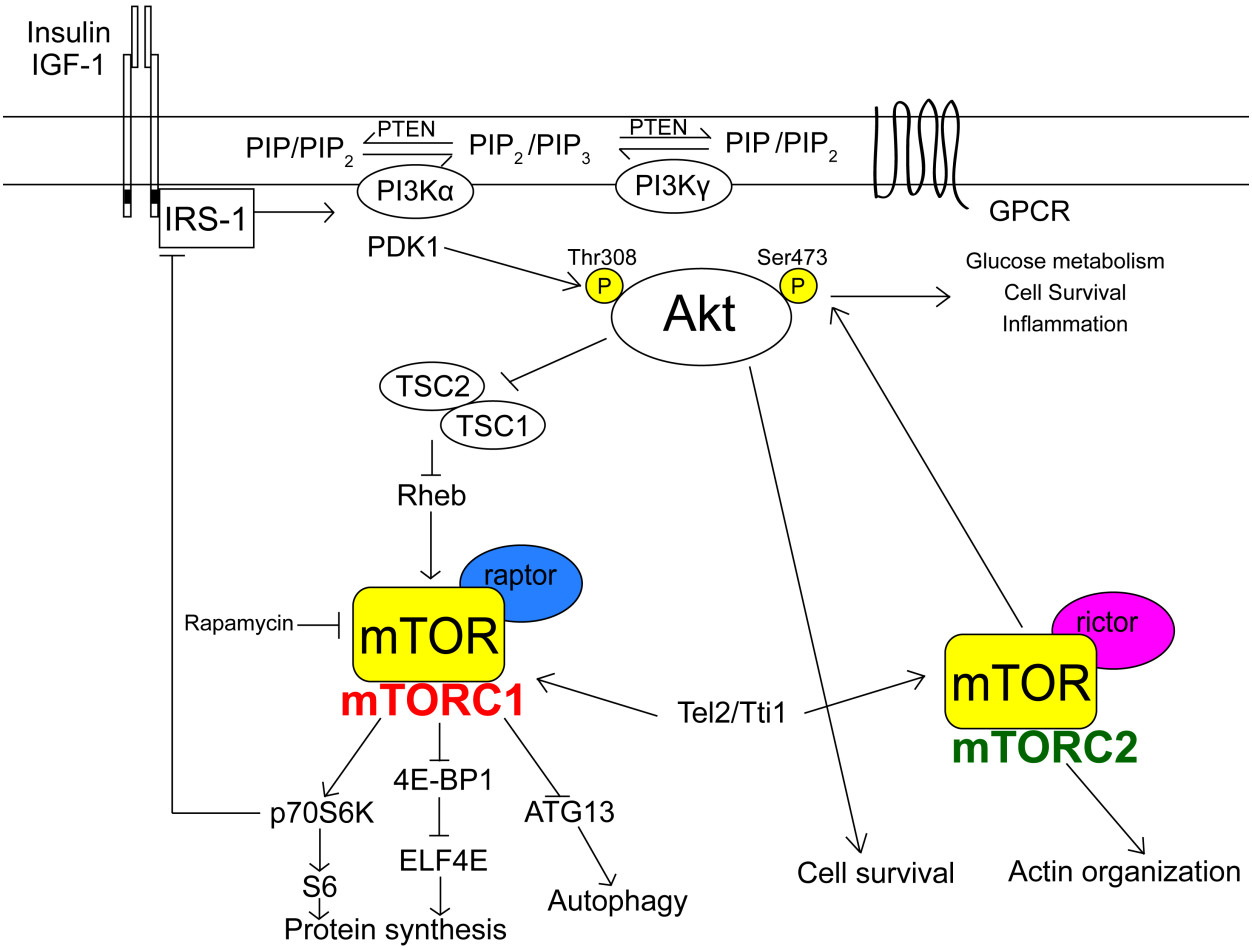

Figure 1.3. The mTOR-signaling pathway
mTOR is a central subunit in two complexes, mTORC1 and mTORC2. mTORC1 is the rapamycin sensitive complex and is activated by insulin, IGF-1 and other growth factors by an Akt dependent mechanism. mTORC1 activates p70S6k which forms a negative feedback loop on IRS-1. mTORC2 is the rapamycin insensitive complex and activates Akt on its serine473 site. Tel2/Tti1 stabilize both complexes. mTORC1 is involved in protein synthesis, proliferation and autophagy whereas mTORC2 is involved in cell survival and actin organization.

1.4 The role of mTOR in cardiac function and cell survival

Physiological and pathophysiological roles of mTOR in the heart is complicated due to the dual complexes mTOR forms. Several studies using mouse models of pathological cardiac hypertrophy reported that treating with rapamycin and its derivatives (e.g. sirolimus and everolimus) inhibited cardiac hypertrophy and preserved

cardiac function [54, 55]. Other groups showed pretreatment with rapamycin also protects the heart against I/R injury in an *ex vivo* Langendorff model. Mice treated with rapamycin had lower infarct sizes, improved cardiac function, and had significantly lower rates of both necrosis and apoptosis [56, 57]. Another group confirmed this finding using a model of *in vivo* I/R injury and found everolimus (a rapamycin derivative) to once again be beneficial by applying the drug on the day or three days after the I/R surgery [58].

However, in contrast to these findings, our group reported a protective effect of mTOR in I/R injury. Using cardiac-specific transgenic mice overexpressing wild-type mTOR driven by an α-myosin heavy chain (αMHC) promoter (mTOR-Tg), we subjected these mice to both *in vivo* and *ex vivo* I/R injury. Both models of I/R demonstrated improved cardiac function compared to littermate controls after I/R injury as well as decreased CM cell death as indicated by the amount of creatine kinase (CK) released into the perfusate post I/R. Masson's trichrome staining showed that 28 days after *in vivo* I/R, mTOR-Tg mice had a significantly smaller area of interstitial fibrosis compared to wild-type (WT) mice. Consistent with this finding, mTOR-Tg hearts subjected to *ex vivo* I/R had less necrosis as indicated by Evans blue dye staining [2]. Other groups have also shown that insulin-mediated protection against CM cell death is largely dependent on the activation of PI3K, Akt, and mTOR; again indicating mTOR activation is beneficial for cardioprotection [59, 60]. Further supporting mTOR as cardioprotective is our preliminary data using a tamoxifen inducible, cardiac specific mTOR knockout (CKO) mouse. We subjected these mice and their littermate controls to *in vivo* I/R injury by left anterior descending coronary artery (LAD) ligation and found that the CKO mice

had significantly worse cardiac function and substantially more fibrosis just seven days after the surgery (Figure 1.4).

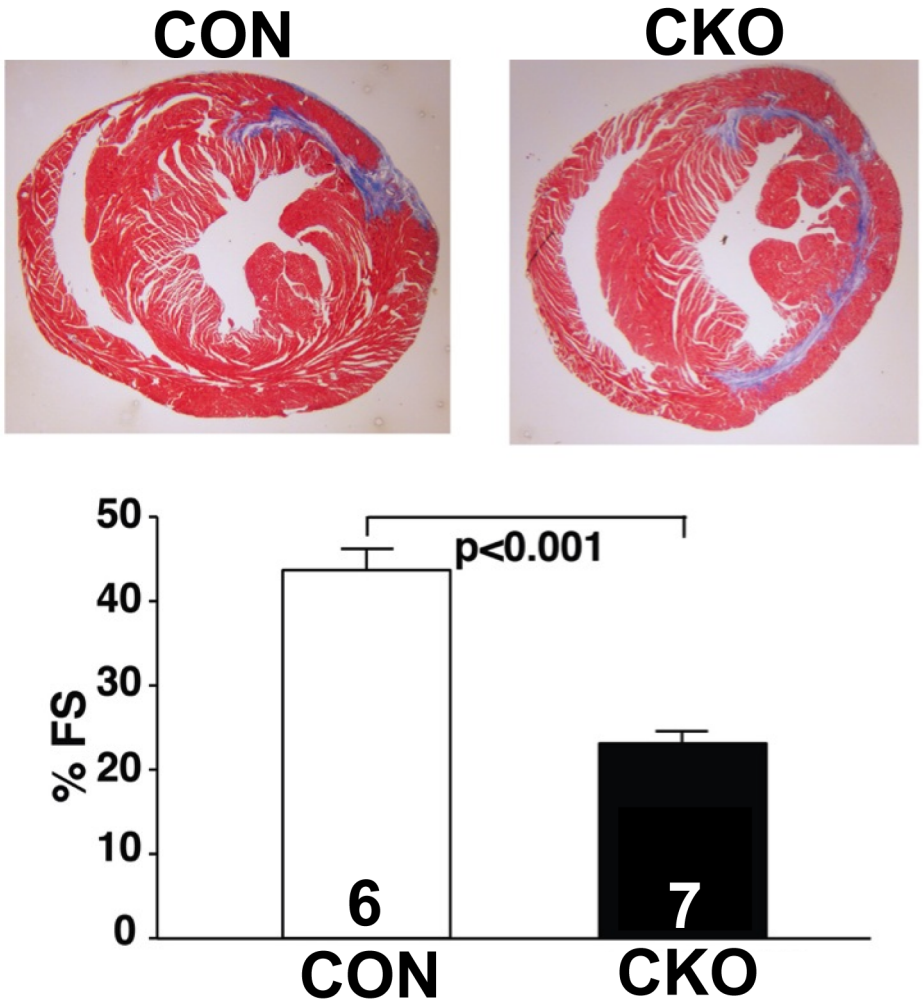

Figure 1.4. mTOR-KO have significantly increased fibrosis and decreased % fractional shortening (%FS) 7 days after in vivo I/R injury.
Top. Representative Masson's trichrome staining showing a significantly larger area of fibrosis in CKO hearts compared to controls. Bottom. Quantification of %FS using echocardiography showing CKO hearts have significantly decreased %FS compared to controls. N= 6 (CON) and 7 (CKO). p-values displayed on graph.

These opposing findings may be explained by a negative feedback loop where mTORC1 signaling through S6K1 negatively regulates Akt by inhibiting insulin receptor substrate-1 (IRS-1) [61, 62]. Several groups have demonstrated rapamycin inhibits this

negative feedback loop leading to the activation of Akt via mTORC2 and suppresses apoptosis in post-MI hearts and other pathological stimuli [56, 63, 64]. On the other hand, overexpression of mTOR increased the phosphorylation of both S6 and Akt following I/R injury [2]. Increased phosphorylation of S6 and Akt indicates mTORC1 and mTORC2 signaling are increased in mTOR-Tg mice. Therefore, the signaling pathways that lead to cardiac protection by rapamycin and the genetic mTOR-Tg mice are different and may explain the contradictory findings.

1.5 Regulation of cardiac muscle contraction and calcium transients physiological and heart failure settings

Ca^{2+} is the key element for controlling and regulating cardiac muscle contraction [65]. In normal conditions, during the cardiac action potential, the myocyte membrane depolarizes leading extracellular Ca^{2+} to enter the cell through the L-type voltage dependent Ca^{2+} channel. This inward Ca^{2+} current is insufficient to cause contraction by itself [66]. However, this initial inward movement of Ca^{2+} acts as an amplification signal for the release of Ca^{2+} from the SR and triggers Ca^{2+}-induced Ca^{2+} release (CICR) from adjacent type 2 ryanodine receptors (RyR2s) on the SR membrane [67]. RyR activity is closely tied to cytosolic Ca^{2+} levels with low concentrations (1-10 μM) being activatory while high concentrations (> 10 μM) are inhibitory [68]. Activation of the RyRs and Ca^{2+} release from the SR produces a Ca^{2+} release signal known as a "Ca^{2+} spark" [69]. Multiple Ca^{2+} sparks produces enough intracellular Ca^{2+} in order to trigger contraction (Figure 1.5).

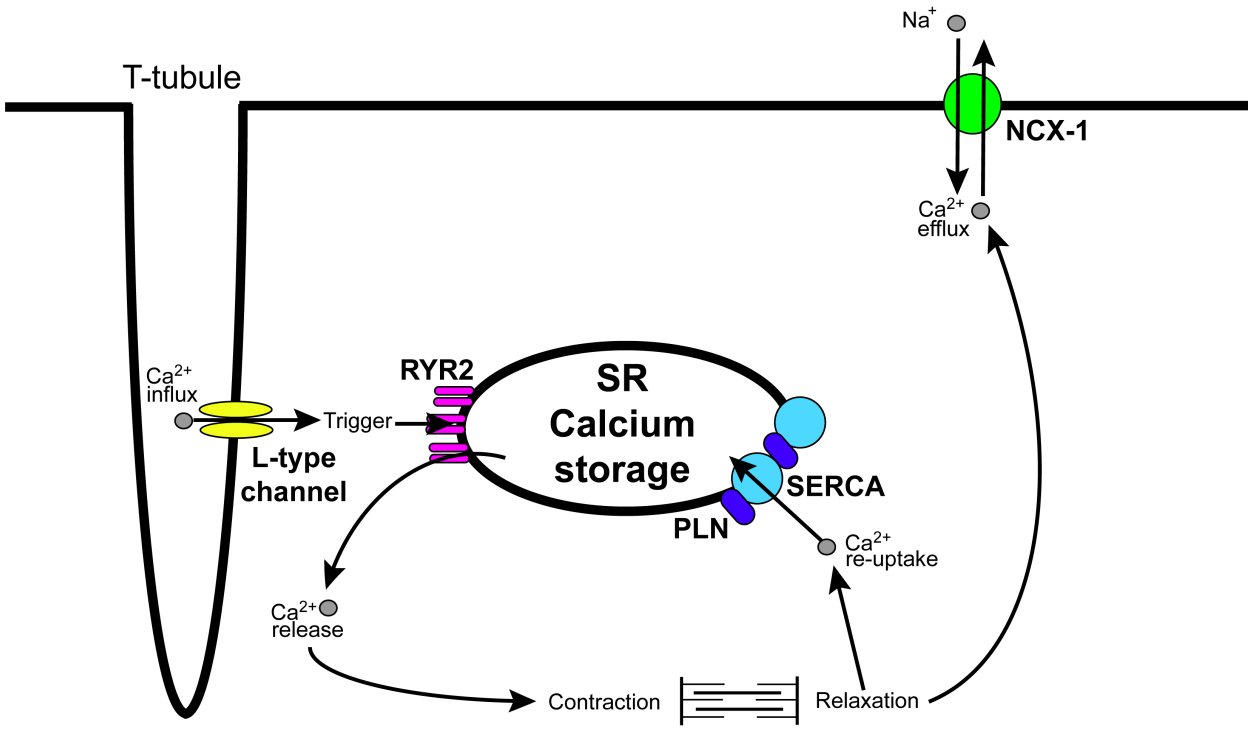

Figure 1.5. EC-Coupling under normal physiological conditions.
Under normal physiological conditions, Ca^{2+} enters the cell through L-type Ca^{2+} channels triggering Ca^{2+} induced Ca^{2+} release from the SR and contraction. Following contraction, Ca^{2+} returns to the SR by SERCA or is effluxed out of the cell through the NCX-1.

Contraction is triggered when the Ca^{2+} released from the SR travels to the adjacent myofibrils where it binds to troponin C on the troponin-tropomyosin complex [70]. Myofilaments consist of an array of thick and thin filaments [71]. The sarcomere is composed of one unit of interacting thin and thick filaments. Thick filaments are composed of myosin heavy chains and two pairs of light chains. Ca^{2+} binding causes tropomyosin to move away from binding sites allows the formation of cross-bridges between actin and myosin [72]. This facilitates the “power-stroke” causing the myocyte to contract [73]. Following contraction, the Ca^{2+} is then returned to the SR by the sarco/endoplasmic reticulum Ca^{2+}-ATPase (SERCA) or is effluxed out of the cell via the Na^{+}/Ca^{2+} exchanger (NCX-1) [74]. A small amount of Ca^{2+} also goes into the mitochondria.

In heart failure, reduced SR Ca^{2+} and Ca^{2+} release is the central cause of contractile dysfunction and arrhythmias [75]. This results in the generation of a smaller contractile force. There are multiple factors that can lower SR Ca^{2+} in heart failure although a major cause is the down-regulation of the SERCA pump [76]. Reduced SR Ca^{2+} uptake can also be attributed to the decreased activity of phospholamban (PLN) [77-80]. Dephosphorylated PLN inhibits SERCA, and some studies have shown that phosphorylation of PLN is decreased in the failing human heart [77, 79]. Another potential cause is the up-regulation of NCX resulting in more Ca^{2+} being removed from the cell [81]. Increased phosphorylation of RYRs also causes further depletion of Ca^{2+} stores due to diastolic leak of SR Ca^{2+} through RYR2 channels [82]. Additionally, diastolic leak of SR Ca^{2+} is also the primary mechanism resulting in delayed afterdepolarizations, triggered ventricular arrhythmias and sudden death in heart failure, though NCX upregulation is also a contributing factor [83-85] (Figure 1.6). Overall, these changes in proteins typically involved with EC-coupling result in reduced SR Ca^{2+} load and smaller Ca^{2+} transients [86]. All of these factors contribute to the contractile dysfunction typically seen in heart failure.

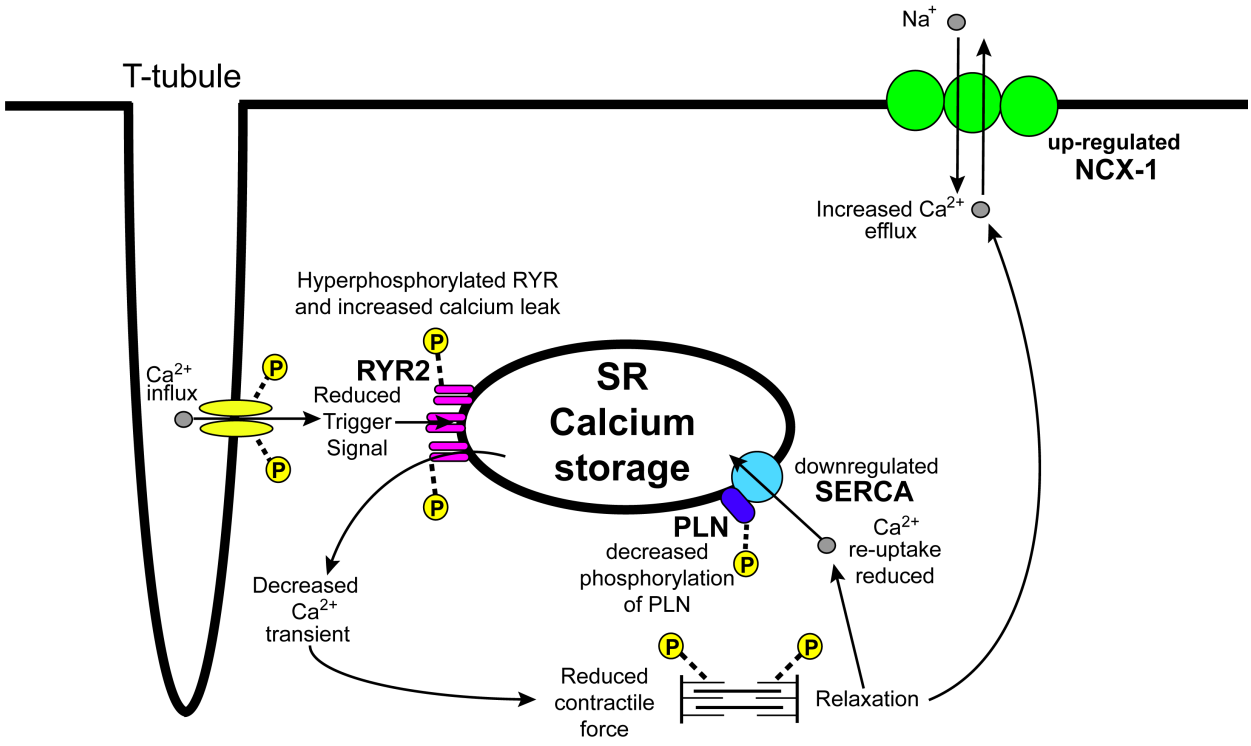

Figure 1.6. Mechanisms behind reduced SR Ca^{2+} content in heart failure.
In heart failure, hyper-phosphorylated ryanodine receptor leads to increased Ca^{2+} leak and arrhythmias and decreased Ca^{2+} transients. This results in a reduced contractile force. SERCA is downregulated leading to reduced reuptake of Ca^{2+} and further contractile and Ca^{2+} dysfunction. Other contributors to reduced SR Ca^{2+} include decreased phosphorylation of PLN and up-regulated NCX-1.

1.6 Calcium regulation of cell death in the cardiomyocyte

Ca^{2+} also plays an important role in mitochondria-mediated cell death and is an important regulator of the mitochondrial permeability transition pore (mPTP). Previously, majority of studies focused on apoptosis as a key pathogenesis of I/R injury-induced heart failure. However, recent studies suggested that programmed necrosis is actually the dominant form of cell death in CMs after I/R injury [6, 87]. Programmed necrosis is induced mainly by Ca^{2+} overload through the opening of the mPTP on the inner mitochondrial membrane (IMM) whereas in apoptosis, the central mitochondrial event is the permeabilization of the outer mitochondrial membrane (OMM) [6, 88].

The mPTP is a multi-protein complex that spans both the outer and inner mitochondrial membrane [89]. Main components of the mPTP include the voltage-dependent anion channel (VDAC) in the outer membrane, the adenine nucleotide translocase (ANT) in the inner mitochondrial membrane, and cyclophilin-D (CypD) in the matrix [90-92]. mPTP opening leads to the following features: collapse of the mitochondrial membrane, cessation of ATP synthesis, redistribution of ions across the inner mitochondrial membrane (IMM) and increased water entry [6]. This causes swelling of the mitochondrial matrix and expansion of the IMM that can eventually lead to the rupture of the OMM and eventual cell death or programmed necrosis.

The cellular mechanisms that contribute to the opening of the mPTP during ischemia are anaerobic metabolism, lactate production, and intracellular acidosis. These cause H+ ions to be pumped out of the cell by the Na^+/H^+ exchanger. The Na^+/K^+ ATPase results in increased intracellular Na^+ that is then exchanged for Ca^{2+} resulting in Ca^{2+} overload. The SR also contributes to increased intracellular Ca^{2+} due to CICR [6, 93]. Ca^{2+} overload of the mitochondria then triggers programmed necrosis and is the major mechanism by which programmed necrosis occurs [88].

1.7 mTOR and calcium signaling and regulation

mTOR plays a role in Ca^{2+} signaling via indirect regulation of the inositol 1,4,5-trisphosphate receptor (IP3R) [94-96]. A few reports demonstrated inhibiting mTOR with rapamycin or a rapamycin derivative resulted in a decrease in IP3-evoked intracellular Ca^{2+} rise [95, 97]. Another study using non-excitable cells suggested that mTOR directly phosphorylated and activated the IP3R2 [98]. Most of these studies focused on mTOR's

association with the FK506-binding proteins (FKBPs). FKBPs are accessory proteins that regulate both ryanodine receptors and the IP3R. Both FK506 and rapamycin disrupted the association between FKBPs and the IP3R and RYR by displacing FKBP from the channels [99]. However, fairly recently it was also discovered that mTORC2 is localized to the endoplasmic reticulum (ER) sub-compartment they termed mitochondria-associated ER membrane (MAM) and interacts with the IP3R-Grp75-voltage dependent anion-selective channel 1 ER-mitochondrial tethering complex [5]. Knockdown of mTORC2 disrupted the MAM and resulted in mitochondrial defects such as increases in ATP production and Ca^{2+} uptake due to an increase in mitochondrial membrane potential.

There is also additional evidence for mTOR having a role in Ca^{2+} signaling and regulation. Intracellular Ca^{2+} is known to regulate autophagy, a process also regulated by mTOR. One group reported that mTOR inhibition by rapamycin altered intracellular Ca^{2+} signaling resulting in increased ER Ca^{2+}-store content, decreased ER Ca^{2+} leak rate, and increased Ca^{2+} release through IP3Rs [100]. Another study demonstrated that amino acids could induce a rise in intracellular Ca^{2+} and activate mTORC1. All of these studies show mTOR may have a key role in the regulation of Ca^{2+} signaling, though the studies were performed mainly in non-excitable cells. There is yet to be a demonstration of a role for mTOR in Ca^{2+} signaling in CMs though there is substantial evidence to suggest mTOR has one.

1.8 The role of mTOR in cardiac metabolism and the metabolic syndrome

The metabolic syndrome has been defined as a set of metabolic risk factors including obesity, insulin resistance, and glucose intolerance [101]. These risk factors are the key factors for the later development of type 2 DM and CVD. DM is a powerful risk factor for the development of post-MI HF and is a common co-morbidity of HF accounting for 66% of mortality during the first year [102]. The Framingham study established the epidemiologic link between diabetes and HF demonstrating the risk of HF was increased 2.4 fold in men and 5-fold in woman with diabetes compared to those without [103]. Therefore, there is a significant need for developing therapeutics to prevent heart failure in diabetic patients.

The insulin-signaling pathway is a major potential target for therapeutic development as it is known to be the main cellular pathway controlling energy and glucose metabolism [30]. A key molecule of this pathway, mTOR may be a possible target for developing such therapies. mTOR has been previously shown to be cardioprotective and is one of the key molecules in the insulin-signaling pathway (Figure 1.3) [2]. Dysregulated mTOR has also been implicated in both metabolic syndrome and DM [104]. A number of studies have shown mTOR to be involved in the regulation of cardiac metabolism and suggest it is upregulated in conditions of nutritional excess, obesity, and the metabolic syndrome [30, 39-41]. These reports seem to suggest that increased activation of mTOR is detrimental to the heart in these conditions; however, they primarily focused on mTORC1 activation and the inhibition of mTOR with rapamycin. In contrast, a conflicting report also using rapamycin seemed to suggest inhibition of mTOR with rapamycin actually prevented pancreatic beta-cell adaptation to

hyperglycemia and exacerbated the metabolic state in DM [105]. Supporting this study that mTOR is beneficial to CMs in DM is our own publication using wild type and mTOR-Tg mice on a high fat diet. We again demonstrated that the overexpression of mTOR in CMs to be cardioprotective against I/R injury in a mouse model of obesity (Figure 1.7). Our study demonstrated that mTOR-Tg hearts were resistant to the detrimental effects of a HFD as the %LVDP recovery after *ex vivo* I/R injury was better than littermate controls. Peak ischemic contracture, a phenomenon resulting from increased intracellular Ca^{2+} levels and ATP depletion, and indicative of decreased recovery after I/R [106], was also lower in mTOR-Tg mice on a HFD than WT on a HFD [8].

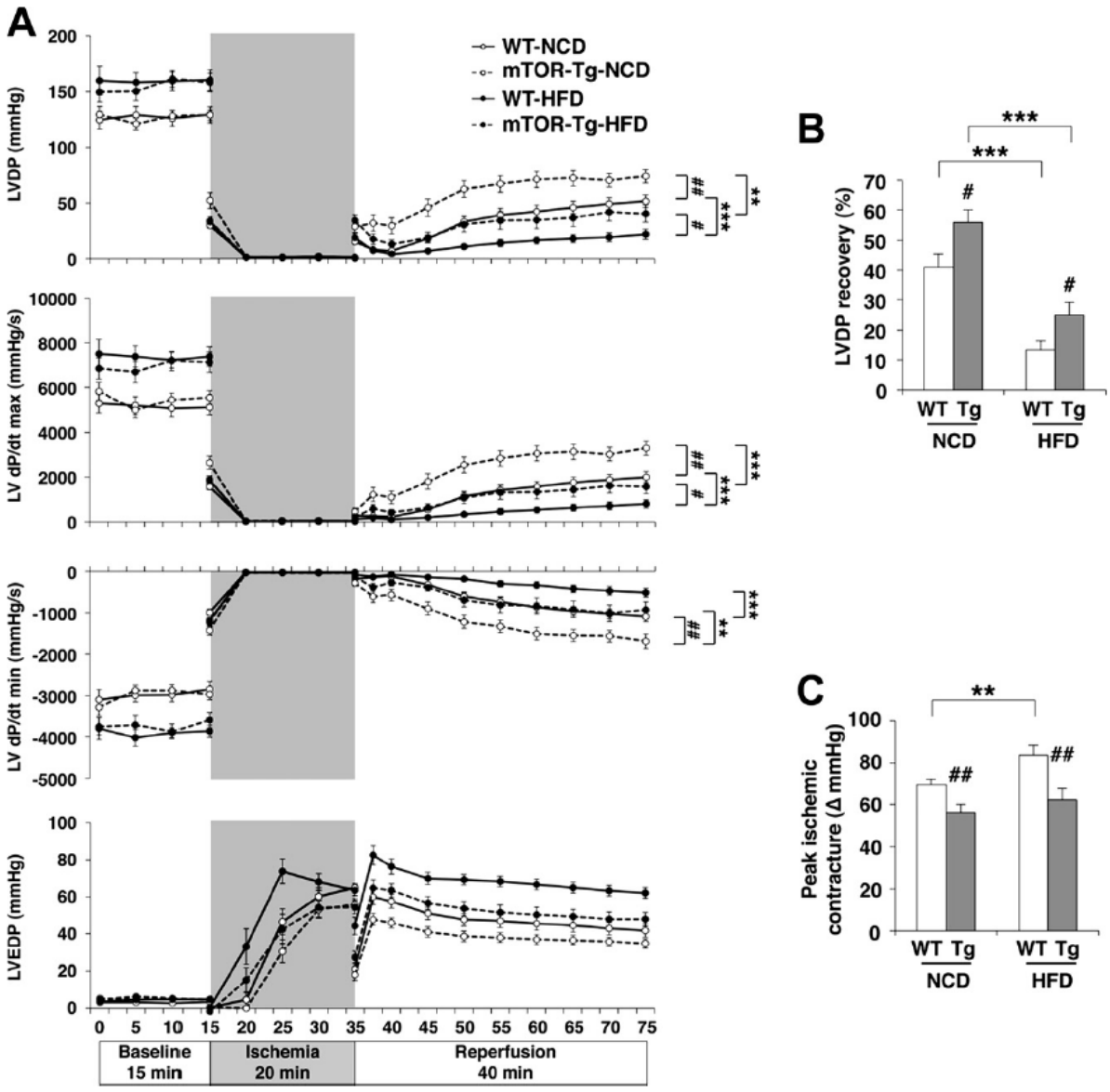

Figure 1.7. Overexpression of cardiac mTOR prevents cardiac dysfunction after transient ischemia in HFD hearts.

A. LVDP, LV dp/dt(max), LV dp/dt(min), and LVEDP over the course of the ex vivo Langendorff experiment. B. Quantification of the LVDP after 40 min of reperfusion compared to baseline to determine %LVDP recovery. C. Ischemic contracture during the 20-min ischemia period as determined by peak ischemic contracture (ΔLVEDP from 0 min of ischemia). N = 24 (WT-NCD), 28 (Tg NCD), 24 (WT HFD), and 26 (Tg HFD). * $p < 0.05$, ** $p < 0.01$, and *** $p < 0.001$. # $p < 0.05$ and ## $p < 0.01$. *Aoyagi, et. al 2015.*

As previously explained in section 1.4, the reason for the conflicting reports may again be due to the negative feedback loop where mTORC1 signaling through S6K1 negatively regulates Akt by inhibiting insulin receptor substrate-1.

1.9 Research Objectives

The overarching hypothesis for my dissertation is that mTOR is necessary for cardioprotection against pathological stressors, especially I/R injury and DM. In the following chapters, I will discuss the following:

1) Determine if mTOR is necessary to protect the heart against I/R injury (Chapter 2). To achieve this, I studied the loss of mTOR using an ex vivo I/R injury model.
2) Determine if mTOR is necessary to maintain normal contractions and Ca^{2+} transients (Chapter 3). In this study I measured single CM function and intracellular Ca^{2+} using IonOptix.
3) Determine if mTOR is necessary to protect the heart against I/R injury in a mouse model of obesity (Chapter 4). For this study, I employed the same ex vivo I/R model as in Chapter 2, but examined the effects of an mTOR knockout on cardiac function in mice that were on a high-fat diet.
4) Discuss my findings and main conclusions from this dissertation and comment on future directions for this research (Chapter 5).

Chapter Two

THE ROLE OF mTOR IN AN *EX VIVO* LANGENDORFF I/R INJURY MODEL

2.1. Introduction

2.1.1. Specific Aim 1: To determine the necessity of mTOR in I/R injury by using *Ex vivo* Langendorff.

Previous studies by our laboratory using a mTOR transgenic mouse model that overexpressed mTOR in the CMs demonstrated that increased mTOR was sufficient to protect the heart against I/R injury [2]. I next wanted to demonstrate that loss of mTOR was necessary for cardioprotection against I/R injury. Therefore, I generated cardiac specific mTOR-KO (CKO) mice using a mouse strain with Cre expression under control of the alpha myosin heavy chain (α-MHC) promoter. To show specificity of the knockout I also used a tdtomato allele as a Cre reporter in the mTOR-CKO line. I then characterized heart function of the CKO mice at baseline by using echocardiography. Next, to determine whether mTOR was protective against I/R injury, I subjected these hearts to global ischemia using *ex vivo* Langendorff. Surprisingly, I found the hearts from the CKO mice recovered better than controls. However, CKO hearts also had irregular contractility that indicated they might have dysfunctional Ca^{2+} signaling. Based on these results, I investigated a functional role for mTOR in EC-coupling by using different stimuli such as isoproterenol and pacing.

2.1.2. Rationale for using tomato reporter mice

Determining the specificity of the knockout in CMs is difficult because the whole heart consists of multiple different cell types including fibroblasts, smooth muscle cells, and endothelial cells. In our mice, mTOR is knocked out only in the CM, which means the specificity is difficult to discern in the whole heart. Therefore, I also generated a tomato reporter mouse line in which a stop cassette behind the Rosa26 promoter prevents transcription of the tomato reporter gene [107]. When Cre recombinase is present, the *LoxP* sites recombine, excising the stop cassette. This then allows the tomato fluorescent protein to be expressed only in the cells where Cre is active. Breeding the reporter line with the $mTOR^{flox/flox}$ line, this results in tomato only being expressed in the CMs after tamoxifen administration.

2.1.3. Rationale for using ex vivo Langendorff

In vivo I/R injury is influenced by external factors such as neuronal, hormonal, and immune factors. In order to investigate the loss of mTOR alone without the influence of these factors, I used the *ex vivo* Langendorff system to determine whether mTOR was protective against I/R injury. *Ex vivo* Langendorff has several advantages that make it an attractive method, including its relative simplicity, experimental reproducibility and the ability to investigate myocardial responses in the absence of confounding peripheral neurohormonal factors [108].

2.2. Methods

2.2.1. Animal Models

2.2.1.1. Generation of cardiac specific mTOR knockout

Animal experiments in this study were approved by the Institution Animal Care and Use Committees of the University of Hawaii (Honolulu, HI). This investigation conformed with the National Institutes of Health *Guide for the Care and Use of Laboratory Animals* (NIH Pub. No. 85-23, Revised 1996). Breeding pairs of floxed mTOR mice ($mTOR^{fl}$; B6.129S4-$mTOR^{tm1.2Koz}$/J) were obtained from Jackson Laboratories and inbred to generate $mTOR^{fl/fl}$ mice, and were further inbred for more than ten generations before use. These mice contain *LoxP* sites that flank exons 1-5 of the mTOR gene [109] (Figure 2.1). Since these exons contain the transcription start site, Cre-mediated deletion of these exons results in the loss of mTOR. CM specific mTOR-KO mice were then generated by crossing homozygous $mTOR^{fl/fl}$ mice with homozygous transgenic $mTOR^{fl/fl}$ mice expressing a tamoxifen-inducible Cre recombinase fused to two mutated estrogen receptors under the transcriptional control of the α-myosin heavy chain promoter (α-MHCmerCremer; Tg(Myh6-cre/Esr1)1Jmk/J).

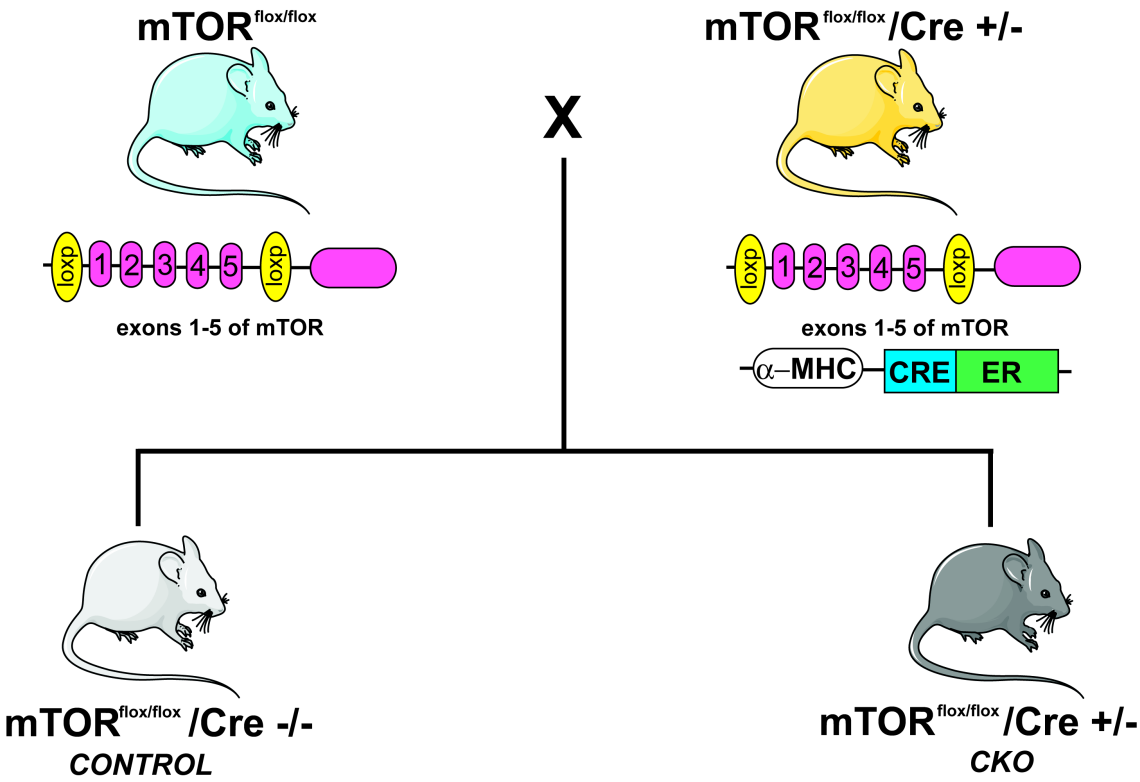

Figure 2.1. mTOR-KO breeding scheme.
Homozygous mTOR$^{flox/flox}$ with *LoxP* sites flanking exons 1-5 of mTOR were bred to homozygous mTOR$^{flox/flox}$ and heterozygous Cre$^{+/-}$ mice to generate homozygous mTOR$^{fllox/flox}$ mice either with or without a tamoxifen inducible Cre under control of the cardiac specific, α-MHC promoter. These mice were then treated with tamoxifen at 6-8 weeks of age to generate cardiac specific mTOR-KO mice and their littermate controls.

2.2.1.2. Generation of tomato reporter mice

Breeding pairs of homozygous tomato mice (tomato$^{R/R}$) were obtained from Dr. Michelle Tallquist's laboratory and bred with mTOR$^{fl/fl}$ mice to create heterozygous tomato^{R}/mTOR^{fl} mice. Heterozygous tomato^{R}/mTOR^{fl} mice were then bred together to generate homozygous tomato$^{R/R}$/mTOR$^{fl/fl}$ mice. These mice were further interbred for 4 generations before being crossed with mTOR$^{fl/fl}$/Cre$^{+/-}$. The tomato mice contain *LoxP* sites that flank a stop cassette preventing transcription of the tomato gene by the endogenous Rosa26 promoter [107]. When Cre is active, the stop cassette is excised and the fluorescent tomato gene is expressed (Figure 2.2).

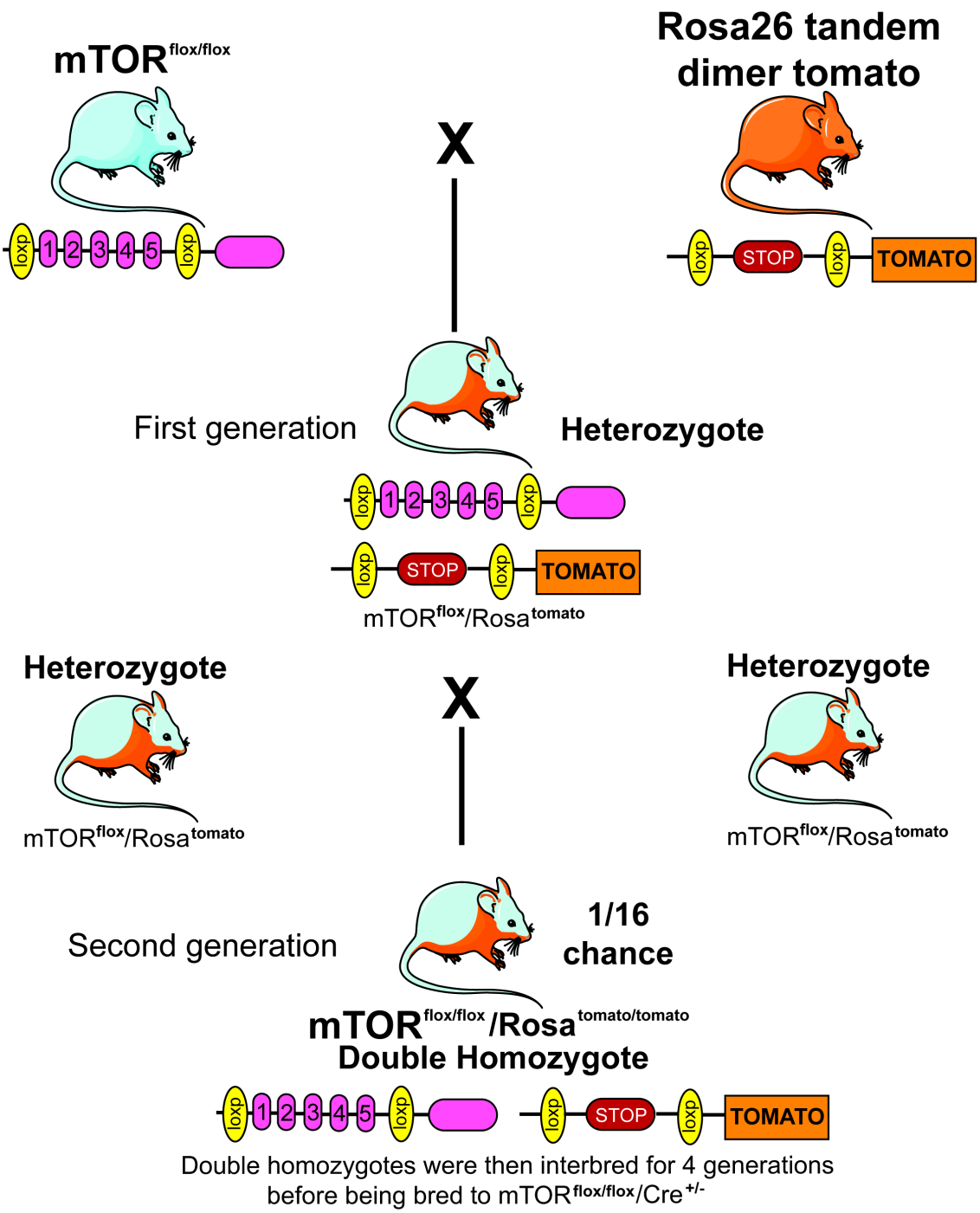

Figure 2.2. Generation of tomato reporter mice.
Homozygous mTOR$^{flox/flox}$ mice and homozygous Rosa$^{tomato/tomato}$ mice were bred to generate double heterozygous mice (mTOR^{flox} and Rosa^{tomato}). These heterozygotes were then bred together to generate a 1/16th chance of getting a double homozygous (mTOR$^{flox/flox}$ and Rosa$^{tomato/tomato}$). These double homozygous mice were then further inbred to generate the mTOR$^{flox/flox}$/Rosa$^{tomato/tomato}$ line.

2.2.3. Tamoxifen administration

Knockout of mTOR was induced by administering tamoxifen chow (Harlan Laboratories) to male mice ages 6-8 weeks. The chow consisted of 250 mg/kg of tamoxifen which provided 40 mg tamoxifen per kg body weight assuming a normal 20-25 g body weight and 3-4 g intake. Mice were kept on this diet for two weeks before a normal chow diet was resumed.

2.2.4. Echocardiography

Echocardiography was performed on non-anesthetized mice using a 13L high-frequency linear transducer (10 MHz, VingMed 5, GE Medical Services) as previously described [7]. I measured left ventricular interior diameter dimension (LVIDd) and % fractional shortening (%FS) as analysis of cardiac structure and function for control and mTOR-CKO mice at baseline.

2.2.5. Isolation of adult murine ventricular myocytes

Control or mTOR-KO male mice (8-12 weeks of age) were anesthetized with 2,2,2-tribromoethanol (TBE). The heart was quickly removed from the chest and retrograde perfused at a constant flow rate of 3 mL/min at 37°C for 2-3 minutes with a Ca^{2+}-free bicarbonate based buffer containing 120 mM NaCl, 5.4 mM KCl, 1.2 mM $MgSO_4$, 1.2 NaH_2PO_4, 5.6 mM glucose, 20 mM $NaHCO_3$, 10 mM 2,3-butanedione monoxime (BDM; Sigma) and 5 mM taurine (Sigma), gassed with 95% O_2-5%CO_2 to washout remaining Ca^{2+} in the heart. Following perfusion with the Ca^{2+}-free buffer, enzymatic digestion was initiated by perfusing with a collagenase buffer containing 0.4

mg/mL collagenase type B (Roche), 0.3 mg/mL collagenase type D (Roche), and 0.03 mg/mL protease type XIV (Sigma Aldrich) in 50 mL of Ca^{2+} free perfusion buffer. All solutions were filtered with a 0.2 μM filter. Hearts were perfused with the collagenase buffer for 15-20 minutes until the heart was fully digested. Collagenase buffer was then washed out by perfusing again with Ca^{2+}-free buffer for 2-3 minutes. CMs were isolated by mechanically teasing the cells apart. They were then gently triturated with a plastic transfer pipette and were filtered using a sterile 100 μM filter [110]. Myocytes were then allowed to settle by gravity. CMs were then snap frozen in liquid nitrogen for later use in Western blot analysis.

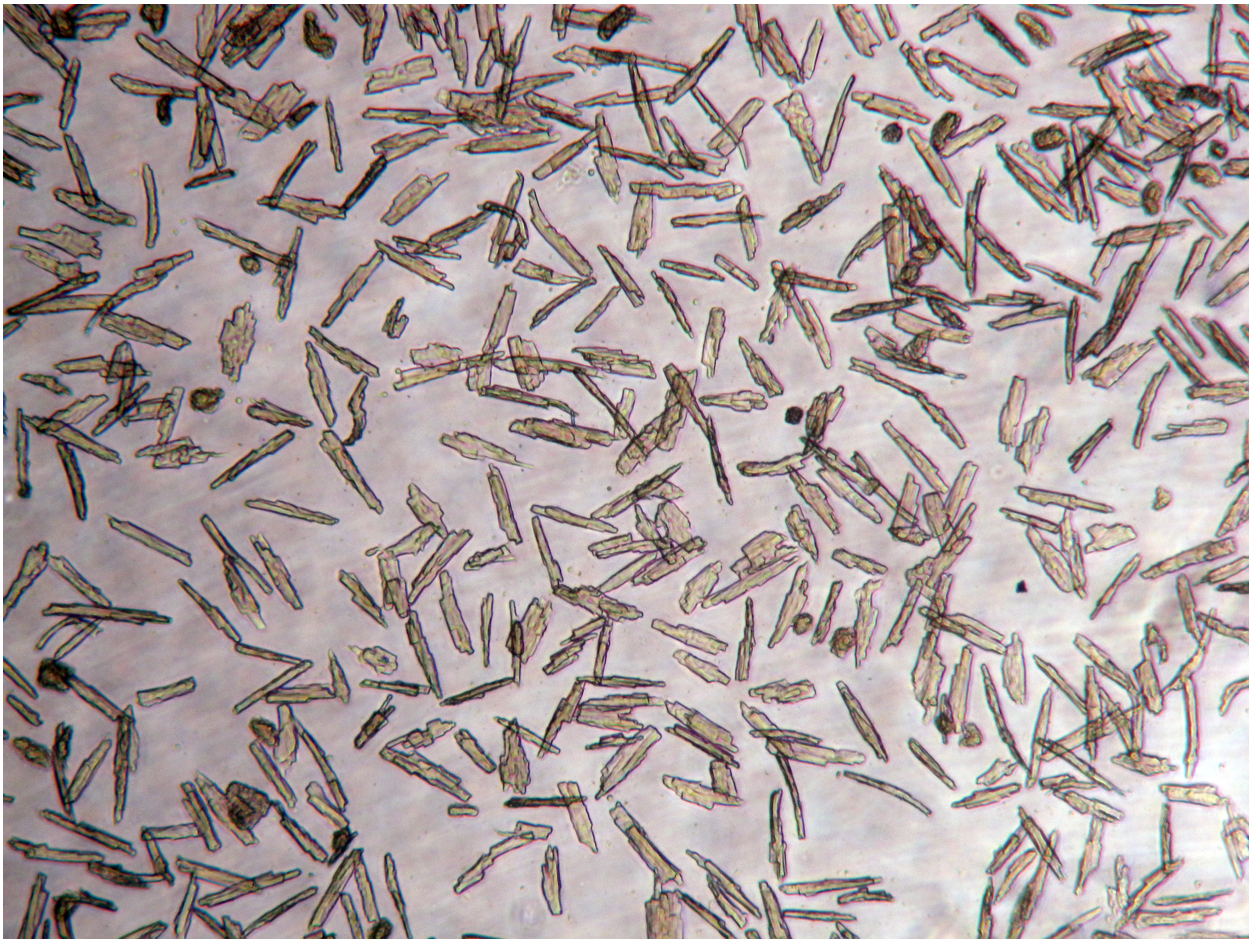

Figure 2.3. Adult murine CMs isolated from C57BL6 mice.

2.2.6. Western blot analysis

Hearts were harvested, snap frozen, and crushed in liquid nitrogen. Tissue was homogenized in ice-cold lysis buffer (Cell Signaling, Danvers, MA) as previously described [2, 7]. Isolated CMs were obtained as described above. The CMs were snap frozen and lysed in ice-cold lysis buffer (Cell Signaling, Danvers, MA). Protein concentrations were measure using the Bradford method (BioRad, Hercules, CA). SDS-PAGE was performed under reducing conditions on 4-20% gradient gels (Bio-Rad). Proteins were then transferred to a polyvinylidene fluoride (PVDF) transfer membrane with fluorescent capability (Millipore). Blots were then incubated with primary antibodies overnight for 18-20 h at 4°C followed by incubating with either a green fluorescent donkey anti-mouse secondary antibody or a red fluorescent goat anti-rabbit secondary antibody. Signal was detected using a fluorescent reader and Image Studio by Licor. Primary antibodies to mTOR (Cell Signaling), phospho and total S6 (Cell Signaling), phospho-Akt (Cell Signaling), Akt (Santa Cruz), IP3R2 (Millipore), VDAC (Cell Signaling), Cre (Millipore), and Gapdh (Santa Cruz) were used for immunoblot analysis.

2.2.7. Analysis of tomato reporter mice.

Tomato reporter mice ages 12-20 weeks were heparinized with 1000 IU/kg and anesthetized with 250 mg/kg 2,2,2-tribromoethanol (TBE). Whole hearts were excised and placed in optimal cutting temperature (O.C.T.) compound and snap-frozen at -80°C. Five μM sections were cut and placed on Superfrost Plus microscope slides (Thermo Scientific). Slides were stained with the nuclear stain 4',6-diamidino-2-phenylindole [(DAPI), Life Technologies]. They were then covered with Fluoromount-G (Southern

Biotech) in order to protect the fluorescent expression of the sections and visualized using an immunofluorescence microscope.

2.2.8. Ex vivo I/R in Langendorff perfused hearts.

Male controls and mTOR-CKO mice ages 12-20 weeks old were heparinized with 1000IU/kg and anesthetized with 250 mg/kg 2,2,2-tribromoethanol (TBE) diluted in sterile PBS. Hearts were excised and subjected to an *ex vivo* Langendorff perfusion model as previously described (Figure 2.4) [2, 111]. After retrograde perfusion was established at a constant pressure (80 mmHg), hearts were perfused with a modified Krebs-Henseleit buffer (11 mM glucose, 118 mM NaCl, 4.7 mM KCl, 2.0 mM $CaCl_2$, 1.2 mM $MgSO_4$, 1.2 mM KH_2PO_4, 25 mM $NaHCO_3$, and 0.5 mM EDTA) equilibrated with 95% O_2-5%CO_2 at 37°C to yield a pH of 7.4. A water-filled balloon catheter was introduced into the left ventricle (LV) to record LV pressure (PowerLab, AD Instruments, Denver, CO). I measured the volume of the coronary sinus effluent in the collected perfusate to determine the coronary flow rate. For the *ex vivo* I/R model, hearts were perfused for 15 min, and the flow was eliminated for 20 min, followed by reperfusion for 40 min. The peak ischemic contracture during the 20-min ischemia period was determined by the alteration of LV end-diastolic pressure (LVEDP) as previously reported [2, 112]. To calculate the percent left ventricular developed pressure recovery (%LVDP), the LVDP was compared at baseline and at 10, 20, 30, and 40 minutes of reperfusion.

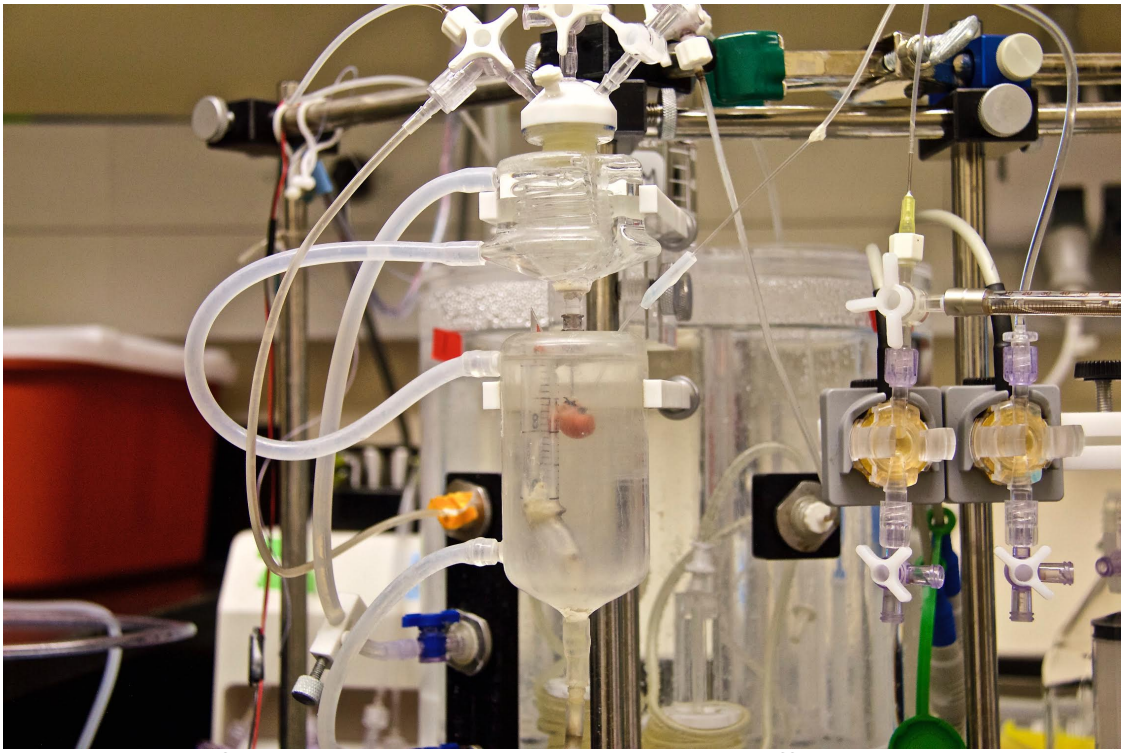

Figure 2.4. Picture of a heart hung on the ex vivo Langendorff apparatus with balloon inserted into the LV.

2.2.9. Drug treatment protocol for ex vivo Langendorff perfused hearts.

Wild-type (C57BL/6) mice were treated as described above in section 2.2.8. Hearts were perfused for 10 minutes and treated with 100 nM Torin1 for 20 minutes. The flow was eliminated for 20 minutes followed by 40 minutes of reperfusion.

2.2.10. Pacing protocol for ex vivo Langendorff perfused hearts.

Hearts from CKO and control mice were subjected to *ex vivo* Langendorff as described in 2.2.8. They were paced prior to ischemia at increasing pacing rates of 5, 6, 7, 8, 9, and 10 Hz for 15 seconds each at each pacing frequency followed by a recovery period of one minute. After the recovery period, the hearts were subjected to global ischemia for 20 minutes followed by 40 minutes of reperfusion.

2.2.11. Isoproterenol challenge of ex vivo Langendorff perfused hearts

Hearts were harvested from CKO and control mice and subjected to *ex vivo* Langendorff as described above in 2.2.8. The hearts were treated with 1 μM isoproterenol at the start of equilibration for 15 minutes. The hearts were subjected to the normal 20 minutes of ischemia before being perfused again with 1 μM isoproterenol at the start of reperfusion for 30 minutes. After 30 minutes, the hearts were switched to a buffer without isoproterenol for 10 minutes.

2.2.12. Biological analysis of ex vivo perfused hearts

Effluent was collected at 40 minutes of reperfusion and concentrated with an Amicon Ultra-0.5 centrifugal filter (3K device, Millipore, Billerica, MA). Samples concentrated from the effluent were analyzed with an enzyme activity kit for creatine kinase (RayBiotech).

2.2.13. Calculation for average variance of contractions

To calculate the average variance of contraction, I took the average LVDP and then took the change from that average to determine the variance for four 10-minute intervals during reperfusion. The formula I used was as follows:

$$\text{Sample Variance} = s^2 = \frac{\Sigma(X - \overline{X})^2}{n - 1}$$

The variance for each group was averaged.

2.2.14. Calculation for peak ischemic contracture (Δ mmHg) and time to peak ischemic contracture.

To calculate the peak ischemia contracture, I took the change in ΔLVEDP from 0 min of ischemia to the peak LVEDP as previously described [106]. To determine the time to peak ischemic contracture, I found the time it took to reach the peak ischemic contracture using the start of ischemia as time 0.

2.2.15. Insulin stimulation of ex vivo Langendorff perfused hearts.

Mice 12-20 weeks of age were again subjected to *ex vivo* Langendorff as described in section 2.2.7. At the start of reperfusion they were treated with 0.1 μg/mL of insulin for the entire duration of reperfusion.

2.2.16. Subcellular fractionation of whole heart tissue.

Hearts were isolated from control or mTOR-KO mice 12-20 weeks of age and placed in fiber relaxation buffer (100 mM KCl/5 mM EGTA/5 mM HEPES/KOH, pH=7.5) for 10 minutes. Hearts were dried and homogenized with a glass dunce homogenizer in SPHEM-A buffer (250 mM sucrose/20 mM HEPES/KOH, pH=7.5/10 mM KCl, 1.5 mM MgCl/1.5 mM Na EGTA/2.5 mM Na EDTA/1 mM DTT/0.1 mM PMSF). The homogenate was centrifuged at 2,700 rpm for 10 min at 4C. The result supernatant was collected and pellets were washed with sucrose-free buffer (SPHEM-A buffer without sucrose). This pellet was saved and labeled as the “nuclear fraction.” The supernatant was then centrifuged at 10,200 rpm for 15 min at 4C. Again the resulting supernatant was collected and the pellet was washed and resuspended with 1 mL SPHEM-A buffer. This

fraction was centrifuged at 6,137 rpm for 15 min at 4°C. The supernatant from this fraction was discarded and the pellet was saved as the “mito heavy fraction.” The supernatant that was collected in the previous step was then centrifuged at 29,000 rpm. The resulting supernatant was collected and labeled as the “cytosolic fraction” while the pellet was labeled as the “mito/SR fraction” [113].

2.2.17. Statistical analysis

Results were analyzed using Graph Pad’s PRISM software. Statistical tests were applied according to the experimental design as indicated in the figure legends. For comparisons of two groups, a student t-test was applied. For comparison of multiple groups, one-way ANOVA was used. Tukey’s post hoc test was used as a post-test for one-way ANOVA. *P* values are also shown in the figures or graphs. All results are reported as means ± SEM.

2.3. Results

2.3.1. Knockout of mTOR is cardiomyocyte specific.

First, in order to confirm lower levels of cardiac mTOR expression in our tamoxifen inducible mTOR-CKO mice, I isolated CMs from control and CKO mice using the method described in section 2.2.4. Western blot analysis of control and CKO mice using whole heart tissue and isolated CMs showed significantly lower levels of mTOR in CKO hearts in both the whole heart and isolated CMs as compared to controls (Figure 2.3A). For further confirmation, I also generated a tomato reporter line as explained in section 2.2.1.2. At 12-14 weeks of age, I excised whole hearts from these mice as

described in section 2.2.6 and examined the tomato expression using a fluorescent microscope. This further demonstrated that only CKO mice expressed the tomato reporter and that expression of tomato was only in the CMs (Figure 2.3B). Smooth muscle cells, fibroblasts, and other cell types within the heart did not express the tomato gene.

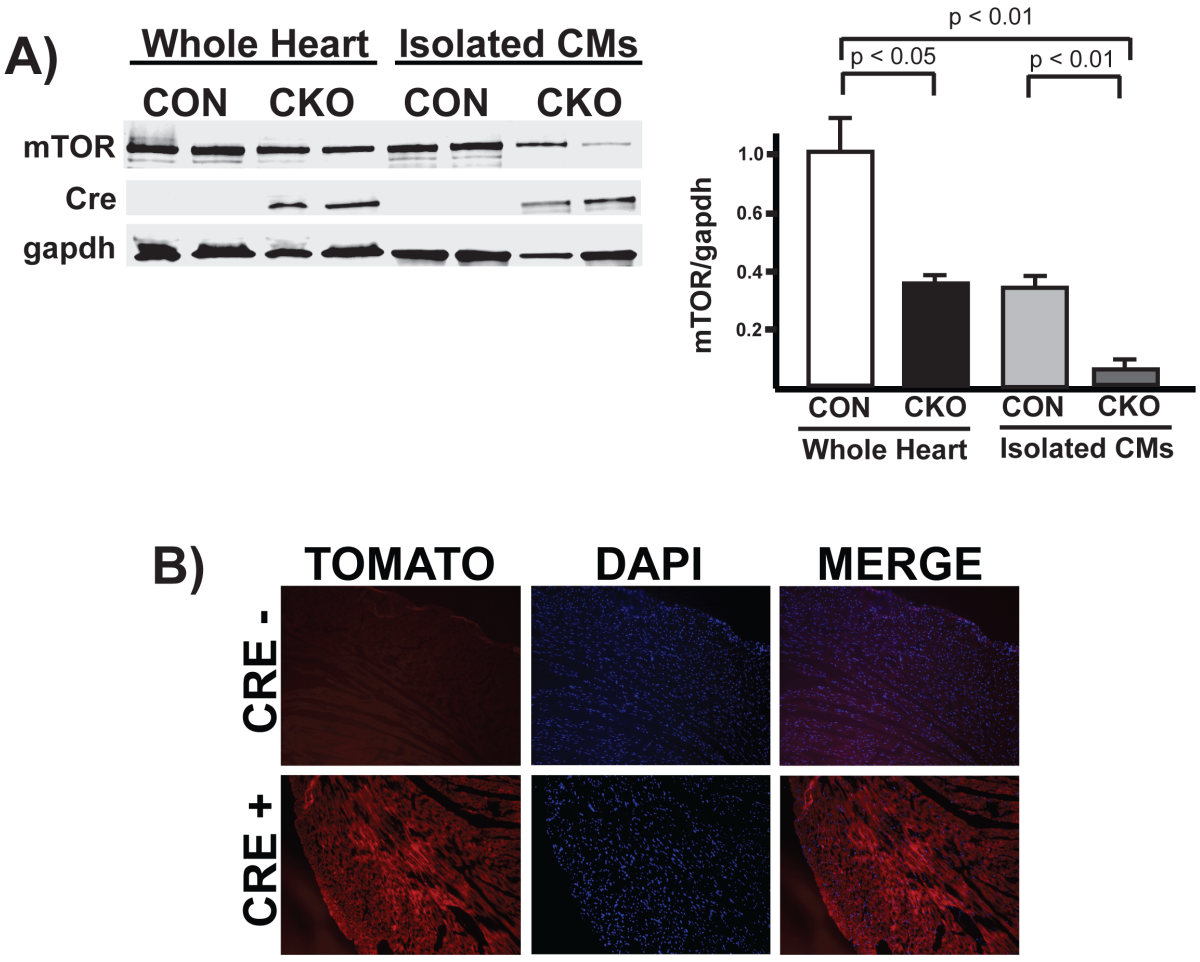

Figure 2.5 Knockout of mTOR is cardiomyocyte specific.
A) *Right.* Representative immunoblot showing a small decrease in mTOR expression in whole hearts and a significant decrease in the expression of mTOR in isolated CMs and in the whole heart compared to control. *Left.* Quantification of the amount of mTOR in whole heart and isolated CMs. N = 6 for all groups. B) Fluorescent images demonstrated expression of the tomato reporter gene is only in mice with Cre. Cre negative mice did not express the tomato gene.

2.3.2. mTOR-KO mice have normal heart sizes and baseline function.

To determine if mTOR knockout affects cardiac structure and function, I measured the size of mTOR-CKO heart versus body size, and baseline physiology, and compared them to littermate controls. Hearts were weighed and normalized to tibia length. mTOR-CKO mice showed no difference in heart size or body weight compared to controls (Table 2.1 and Figure 2.6A). Control and CKO mice were then also evaluated for baseline function via echocardiography (Table 2 and Figure 2.6B). There was no significant difference in percent fractional shortening (%FS) or left ventricular end diastolic internal dimension (LVIDd) (Figure 2.6C). However, left ventricular posterior wall diameter (LVPWd) was significantly decreased in CKO mice, potentially showing a decrease in ventricular wall thickness after mTOR knockout. Nevertheless, it did not appear to significantly affect cardiac function of the mice at baseline as there was no significant difference in %FS or ejection fraction (EF). Overall, these results show the cardiac structure and function of CKO mice are normal at baseline.

Table 1. Body weight, heart weight, and heart weight:tibia length (HW:TB) ratio of control and mTOR-KO mice.

	Control	**mTOR-CKO**
Body Weight	26.93 ± 0.39	26.18 ± 0.42
Heart Weight	0.198 ± 0.006	0.193 ± 0.006
HW:TB	0.00883 ± 0.00032	0.00845 ± 0.00024

There was no significant difference in body weight, heart weight, and HW:TB between controls and CKO mice. N = 24 for both groups.

Table 2. Baseline echocardiograph parameters.

	Control	mTOR-KO
E'-Vel	37.28 ± 2.45	35.32 ± 1.02
MV Decel Time	19.39 ± 1.57	18.33 ± 1.04
MV E-Vel	790.28 ± 23.79	764.41 ± 23.92
E/E'	21.87 ± 1.38	21.39 ± 0.65
IVSD	0.690 ± 0.014	0.657 ± 0.025
LVIDd	3.03 ± 0.028	3.02 ± 0.069
LVPWd	0.803 ± 0.014	0.716 ± 0.017 * **p < 0.01**
LVIDs	1.19 ± 0.078	1.39 ± 0.97
EF	91.14 ± 1.40	84.91 ± 1.75
%FS	61.13% ± 2.28	53.39% ± 2.90
HR	710.71 ± 10.48	710.62 ± 4.57

A list of baseline echocardiograph parameters from control and mTOR-KO mice. Only LVPWd of the knockdown mice was significantly different although functional parameters such as EF and %FS were not significantly different between the two groups. N = 7 in each group.

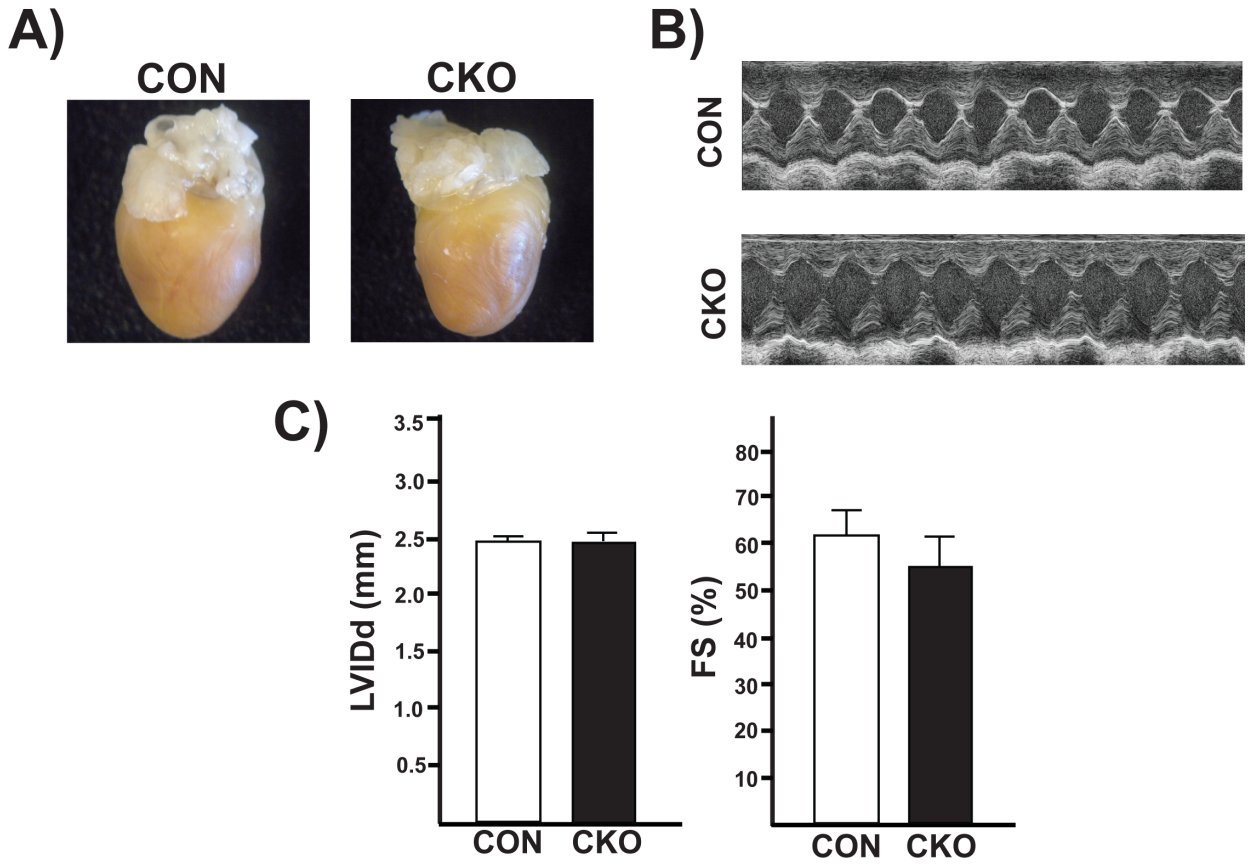

Figure 2.6. mTOR-CKO mice have normal sized hearts and normal baseline cardiac function.

A. Representative pictures of whole hearts isolated from control and CKO mice. CKO mice exhibited no gross abnormalities and are normal in size. B. Representative M-mode traces from baseline echocardiography analysis of control and CKO mice. CKO mice had normal

contractions that were similar to controls. C. *Left.* CKO mice LVIDd was comparable to controls. *Right.* %FS was similar between control and CKO mice. N = 7 in each group.

2.3.3. Torin1 significantly decreases the percent left ventricular developed pressure (%LVDP) recovery of wild-type Langendorff perfused hearts.

To show the effects that acute inhibition of mTOR has on the recovery of C57BL/6 wild-type hearts after I/R injury, I treated wild-type mice with Torin1, an mTORC1 and mTORC2 inhibitor [114]. I subjected the mice to *ex vivo* Langendorff and treated them with 100 nM of Torin1 for 10 minutes prior to ischemia as described in section 2.2.7. Treatment of wild-type mice with Torin1 resulted in significantly decreased %LVDP recovery (Figure 2.7). This showed that acute inhibition of mTORC1 and mTORC2 was detrimental to the heart post-I/R injury and was consistent with our *in vivo* data (Figure 1.4).

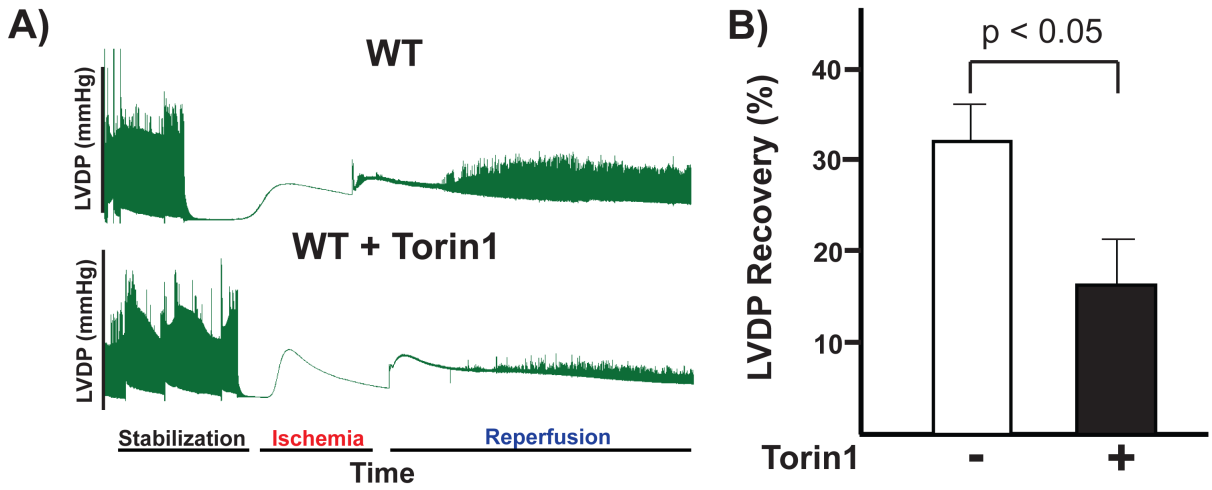

Figure 2.7. Torin1 treatment significantly decreases %LVDP recovery in wild-type mice. Wild-type C57Bl6 mice were subjected to *ex vivo* Langendorff and were either treated with 100 nM Torin1 or not treated. A) Representative tracings from the torin1 experiments. B) Quantification of the %LVDP recovery of wild-type mice treated with or without Torin1. The LVDP at baseline and reperfusion were compared to calculate the %LVDP. Torin1 treatment significantly decreased the recovery of wild-type Langendorff perfused hearts N=7 (WT) and 8 (WT + torin1). $p < 0.05$ by student T-test.

2.3.4. Torin1 treatment decreases downstream mTOR signaling.

To verify that Torin1 treatment was effective, I performed immunoblotting to determine if activation of both mTORC1 and mTORC2 were diminished in the wild-type mice that were given insulin as p-Akt is downstream of mTORC2 and p-S6 is downstream of mTORC1. I found that both p-Akt and p-S6 expression was significantly decreased in wild-type mice treated with Torin1 (Figure 2.8). This demonstrated my treatment with Torin1 was effective even though expression of mTOR was not significantly decreased between the two groups.

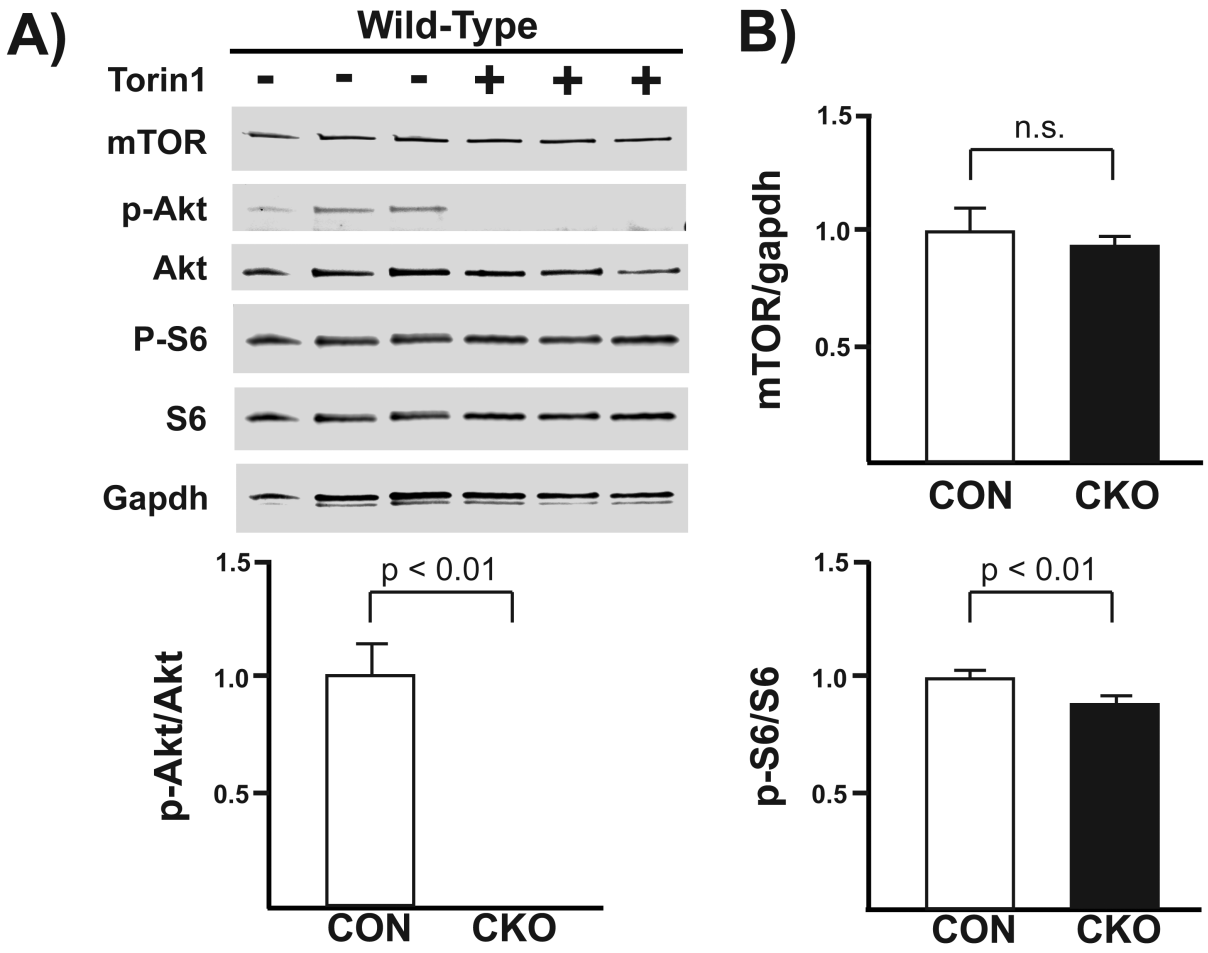

Figure 2.8. Torin1 treatment decreases downstream signaling of both mTORC complexes.
A) Immunoblot showing downstream targets (p-Akt and p-S6) of mTORC1 and mTORC2 are significantly decreased in hearts treated with Torin1. B) Densitrometric analysis of mTOR, p-Akt, and p-S6. mTOR was normalized to Gapdh. p-Akt was normalized to total Akt and p-S6 was normalized to total S6. *P*-values are displayed on graphs as determined by student's t-test. N = 3 for all groups.

2.3.5. Baseline ex vivo Langendorff parameters show control and mTOR-KO mice hearts have similar cardiac function prior to I/R injury.

Torin1 treatment of WT mice appeared to suggest mTOR was cardioprotective against I/R injury. Therefore, I used a genetic model to determine if mTOR activation in both complexes is required for protecting the heart against I/R injury. For this I

subjected cardiac specific mTOR-KO mice and littermate controls to *ex vivo* Langendorff. To ensure there were no gross abnormalities between the control and CKO hearts at baseline, I examined both baseline parameters prior to subjecting them to global ischemia (Table 3).

Table 3. Baseline *ex vivo* Langendorff parameters.

	Control	**mTOR-CKO**
Dp/Dt (max)	5824.36 ± 1040.97	5288.40 ± 630.57
Dp/Dt (min)	-3544.57 ± 242.41	-3238.95 ± 347.38
LVSP (base) mmHg	113.04 ± 13.56	113.07 ± 8.93
LVEDP (base) mmHg	6.45 ± 1.01	5.81 ± 1.15
LVDP (base) mmHg	106.67 ± 13.95	107.26 ± 9.83
Heart Rate (bpm)	369.83 ± 31.92	343.45 ± 18.32
Coronary Flow (mL/min)	4.30 ± 0.967	6.41 ± 0.856

Control and mTOR-CKO hearts have relatively the same cardiac function at baseline, prior to I/R injury. There was no statistically significant difference in beginning LVDP, heart rate, dp/dt (max) or dp/dt (min), or coronary flow rate.

2.3.6. Hearts from mTOR-KO mice exhibit better percent left ventricular developed pressure recovery (%LVDP) after I/R injury but increased variance of contractions compared to controls.

Baseline analysis of mTOR-KO and control hearts showed no significant difference prior to I/R injury. Therefore, I evaluated the loss of mTOR in I/R injury using *ex vivo* Langendorff. Unexpectedly, CKO and control hearts displayed significantly *better* LVDP recovery versus controls (Figure 2.9). This was a surprising result as the *in vivo* data clearly shows the CKO mice do not recover as well after I/R injury and acute inhibition of mTOR was also shown to be harmful to the heart in a global ischemia-reperfusion model. However, I did notice that the CKO hearts appeared to have increased irregular contractility compared to controls (Figure 2.10). I calculated the average variance of contractions (Section 2.2.11) and determined that mTOR-CKO

hearts had significantly increased variance during the first ten minutes and during the last ten minutes of reperfusion. The increased variance I observed in the CKO mice during reperfusion allowed me to formulate the hypothesis that mTOR has a possible role in EC-coupling and Ca^{2+} signaling.

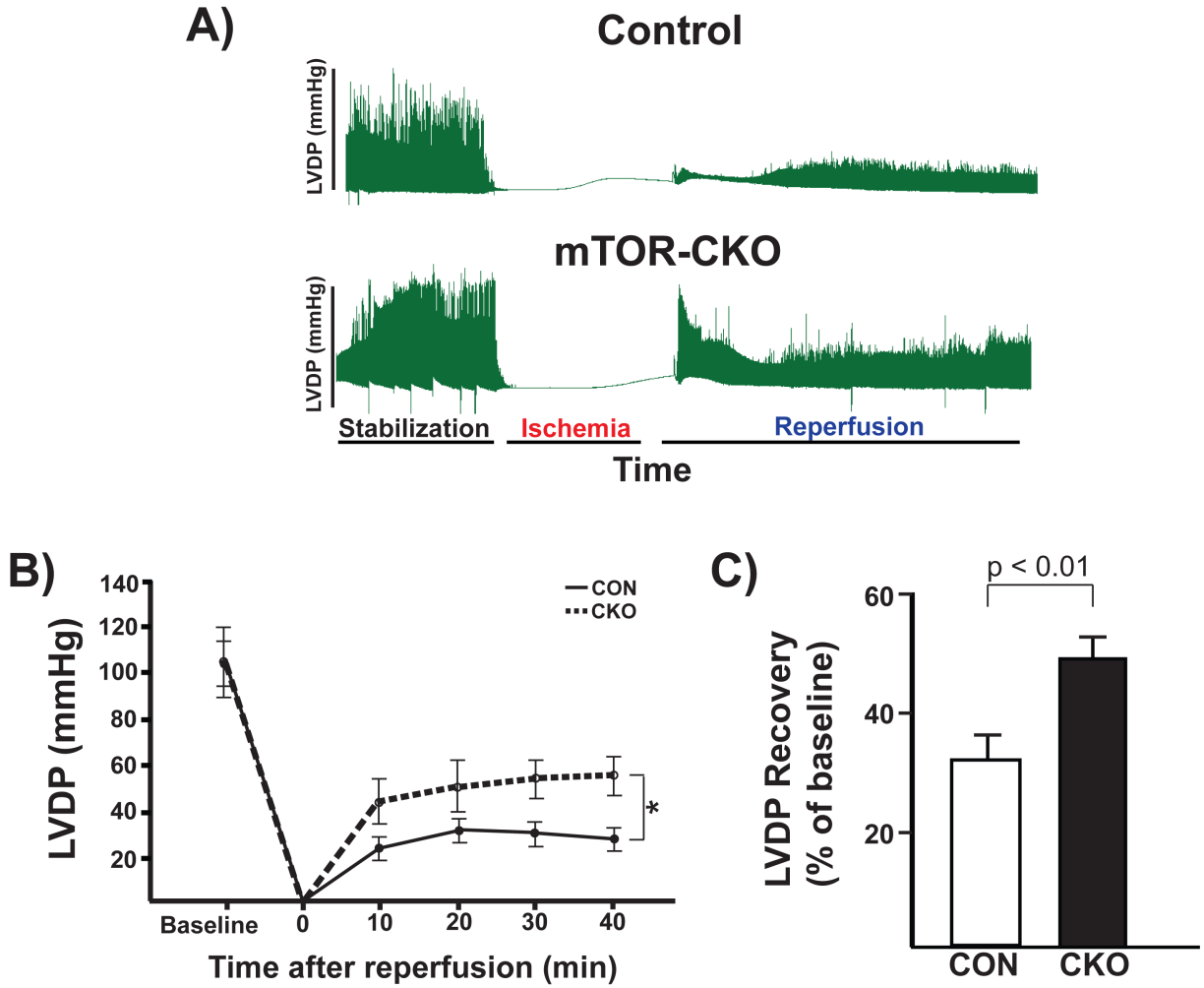

Figure 2.9. mTOR-CKO hearts have better %LVDP recovery after *ex vivo* I/R.
A. *Left.* Representative tracing showing LVDP throughout the Langendorff experiment. B. Quantification of LVDP at baseline and after every 10 min of reperfusion. C. Quantification of the %LVDP recovery for control vs. CKO. CKO hearts recover significantly better than controls. *$p < 0.05$ by student t-test. All other p-values displayed on graphs. N = 7 for each group.

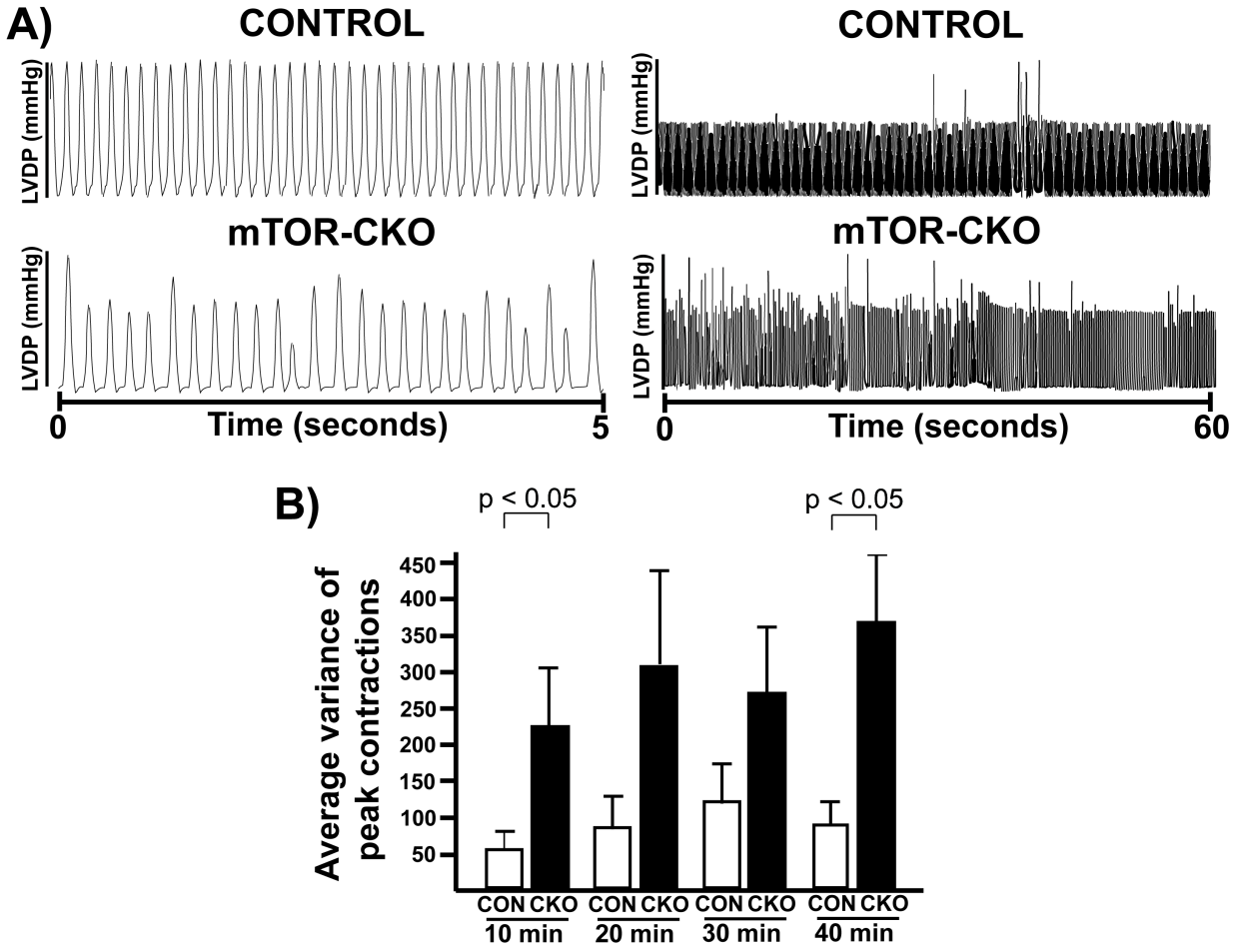

Figure 2.10. mTOR-KO hearts have significantly increased average variance of contractions.
A) *Left.* Representative tracing showing the difference in peak sizes between the control and CKO hearts taken over a 5 second period. mTOR-KO hearts had noticeably different sized peaks while controls were relatively the same. *Right.* Representative tracing showing the increased variance of contractions mTOR-KO hearts have after I/R injury. Representative tracings were taken over a 1-minute period during the last ten minutes of reperfusion. B) Quantification of the average variance of contractions. mTOR-KO hearts had significantly increased average variance during the first 10 minutes and last 10 minutes of reperfusion compared to controls. N=7 for each group. P-values listed on graph as determined by student's t-test.

2.3.7. mTOR-KO hearts have significantly less cell death than controls after ex vivo I/R.

To verify that the decrease in recovery was not artificial due to the Langendorff system, I determined the amount of the myocardial injury marker, creatine kinase (CK) released during the *ex vivo* experiment. Using an enzyme assay kit, I measured the

amount of creatine kinase in the buffer collected from control and CKO hearts. I found mTOR-CKO hearts significantly released less CK released than controls indicating less cell death than control hearts (Figure 2.11).

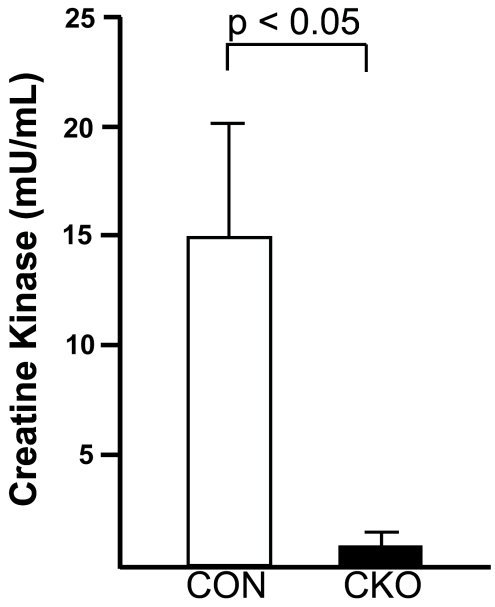

Figure 2.11. mTOR-KO hearts have a significantly decreased marker of myocardial damage compared with controls.
The amount of the myocardial injury marker, creatine kinase released after ischemia and 40 minutes of reperfusion was measured using an enzyme assay kit. CKO mice produced significantly less creatine kinase than controls. N=7 for each group. P-value shown on graph as determined by student's t-test.

2.3.8. Isoproterenol challenge of CKO hearts does not significantly affect LVDP recovery.

Due to the discrepancy between the *in vivo* I/R and *ex vivo* data, I challenged the mice using the β-adrenergic stimulator, isoproterenol. *Ex vivo* models do not have neuronal or hormonal stimulation and I hypothesized beta-adrenergic stimulation may be a missing factor that could explain the better recovery of the CKO mice using *ex vivo* Langendorff. Additionally, because of the increased variance of contractions, I speculated there might be a potential role for mTOR in Ca^{2+} signaling. Binding of

isoproterenol to both β1 and β2 adrenergic receptors activates PKA, which in turn causes increased phosphorylation of the RYR and can result in "leaky" channels that deplete SR Ca^{2+} stores. Isoproterenol has been used by other researchers in *ex vivo* Langendorff to investigate Ca^{2+} leakage through the RYR [115, 116]. I gave the hearts 1 μM isoproterenol at the start of equilibration and then again at the start of reperfusion until the last ten minutes. Then the buffer was switched to a normal KHB buffer without isoproterenol. The CKO hearts had decreased LVDP recovery when stimulated with isoproterenol. However, the recovery of the CKO hearts was relatively the same as controls (Figure 2.12).

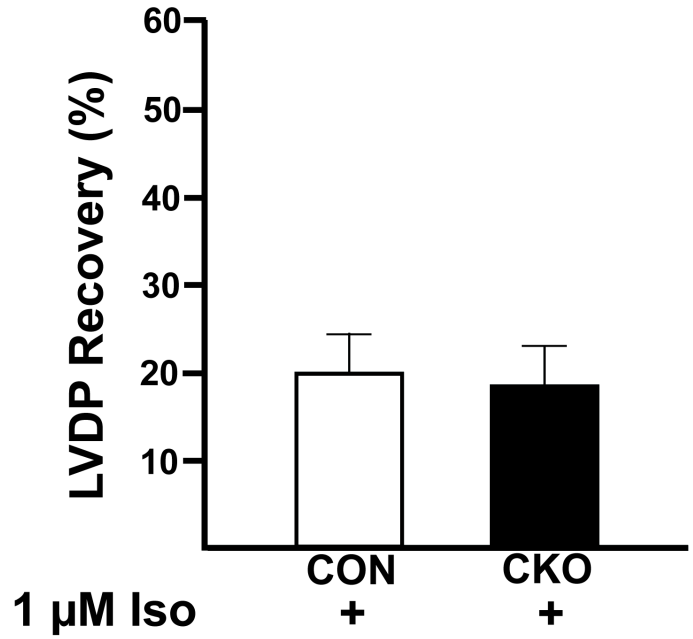

Figure 2.12. Isoproterenol stimulation decreased recovery of both control and CKO hearts but does not cause CKO hearts to recover significantly worse than controls.
Quantification of %LVDP recovery of CON and CKO hearts with and without 1 μM isoproterenol stimulation. N = 4 (CON) and N = 5 (CKO). There was no significant statistical difference between the control and CKO groups. P-value = 0.77

2.3.9. mTOR-KO hearts exhibit cardiac alternans at baseline.

Pacing also affects EC-Coupling and results in the increased activation of calcium/calmodulin-dependent serine/threonine kinase-δ (CAMKIIδ) and increased phosphorylation of PLN [117]. Therefore, I next decided to pace the hearts to determine if pacing would reveal any alterations in Ca^{2+} handling and/or contractility. CON and CKO hearts were again subjected to *ex vivo* Langendorff. Hearts were paced prior to ischemia for 15 seconds at each frequency (5 to 10 Hz). Hearts were then allowed to recover with no pacing for 1 minute before undergoing the normal 20 minutes of ischemia, followed by 40 min of reperfusion. mTOR-CKO hearts exhibited cardiac alternans at baseline (Table 4 and Figure 2.13). Cardiac alternans is a periodic beat-to-beat oscillation in electrical activity at a constant heart rate. It is caused by a number of different factors; however, alternans always originate from disturbances of the coupling of the membrane voltage and intracellular Ca^{2+} [118]. As shown in Table 4, on average, CKO mice displayed cardiac alternans more consistently and at lower frequencies than controls.

Table 4. CKO hearts display cardiac alternans more consistently and at lower frequencies versus controls.

	5 Hz	6 Hz	7 Hz	8 Hz	9 Hz	10 Hz
CONTROL #1	N	N	N	N	N	N
CONTROL #2	N	N	N	N	N	N
CONTROL #3	N	N	N	N	N	N
CONTROL #4	N	N	N	N	Y	Y
CONTROL #5	N	N	N	N	Y	Y
mTOR-CKO #1	N	N	Y	Y	Y	Y
mTOR-CKO #2	N	N	N	Y	Y	Y
mTOR-CKO #3	N	N	Y	Y	Y	Y
mTOR-CKO #4	N	N	N	N	Y	Y

Table showing each heart used in this experiment. N is for no cardiac alternans, Y is for cardiac alternans.

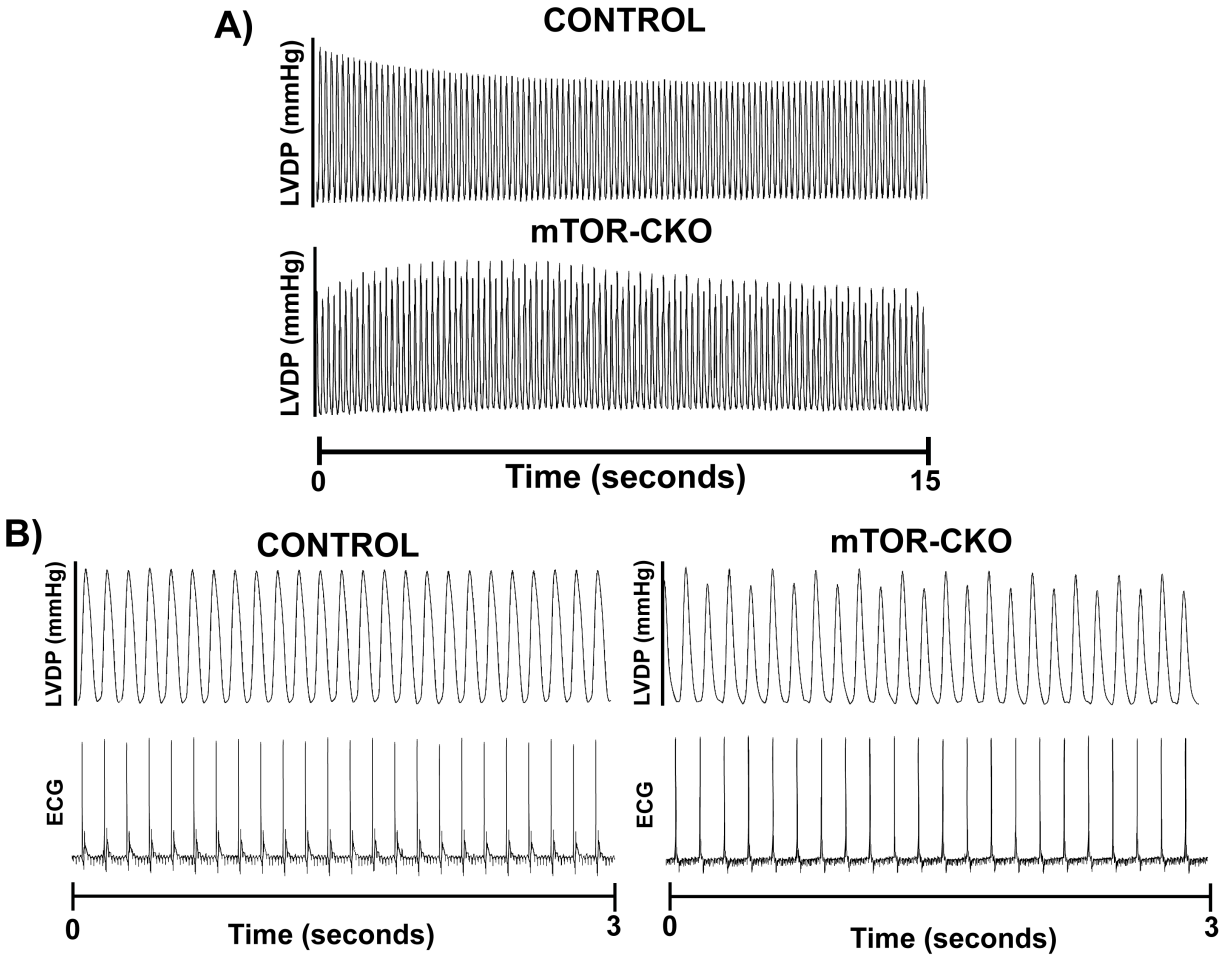

Figure 2.13. mTOR-CKO hearts display cardiac alternans at baseline.
Hearts were paced at increasing frequencies from 5 to 10 Hz for 15 seconds at each frequency. A) Representative tracing of the changes in LVDP during 8 Hz pacing. Pacing revealed CKO hearts had cardiac alternans when paced at 8 Hz or higher. B) Close up view of the traces shown above along with the ECG tracings. N=5 for each group.

2.3.10. Pacing has no effect on LVDP recovery of control and CKO hearts.

To determine if pacing had any effect on the LVDP recovery of control and CKO hearts I compared the baseline LVDP to the LVDP at the end of 40 minutes of reperfusion to determine the %LVDP recovery. I found that pacing had no effect overall on the recovery of the control and CKO hearts as the CKO hearts still recovered

significantly better than the controls despite displaying cardiac alternans at baseline (Figure 2.14).

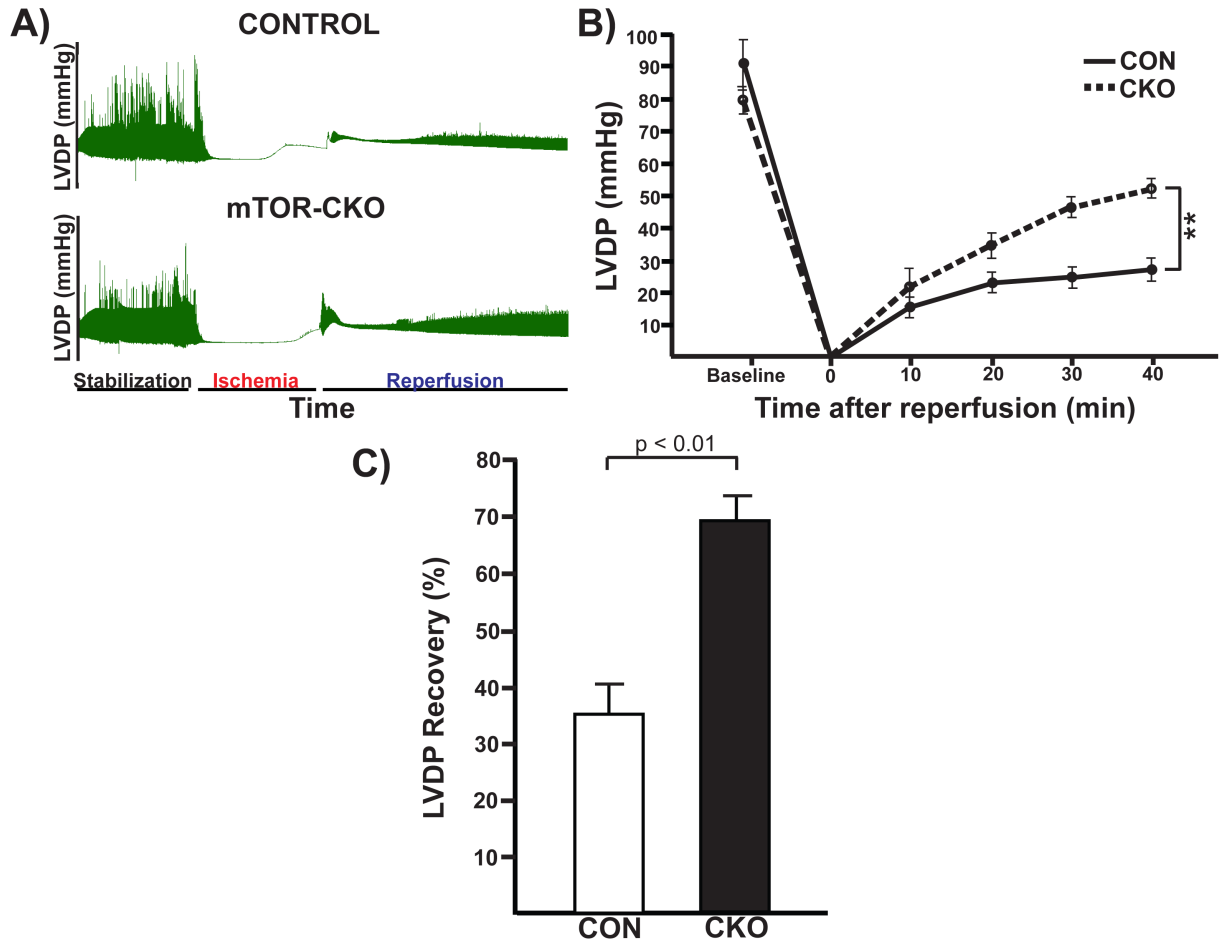

Figure 2.14. Pacing does not affect %LVDP recovery of mTOR-CKO hearts.
A) Representative tracings of a full Langendorff experiment from a control heart and an mTOR-CKO heart. B) Quantification of the change in LVDP from baseline over the course of reperfusion. C) Comparison of the LVDP after 40 minutes of reperfusion to baseline LVDP to determine %LVDP. ** $p < 0.01$. P-value for %LVDP is displayed on graph. N = 9 (CON) and 8 (CKO).

2.3.11. Pacing before reperfusion results in decreased ischemic contracture of CKO hearts.

The cardiac alternans displayed at baseline by the CKO hearts suggested that the SR Ca^{2+} concentration of the CKO hearts was different than the control hearts. Consequently, I examined the ischemic contracture of hearts on the pacing protocol. I

found the CKO hearts had significantly decreased peak ischemic contracture (Δ mmHg) and significantly increased time to peak ischemic contracture (Figure 2.15). The significance of ischemic contracture is that it is due to the depletion of ATP but also the rise of intracellular Ca^{2+} [119, 120]. Lower baseline SR Ca^{2+} levels could be a reason for the decreased peak ischemic contracture I observed in the CKO hearts.

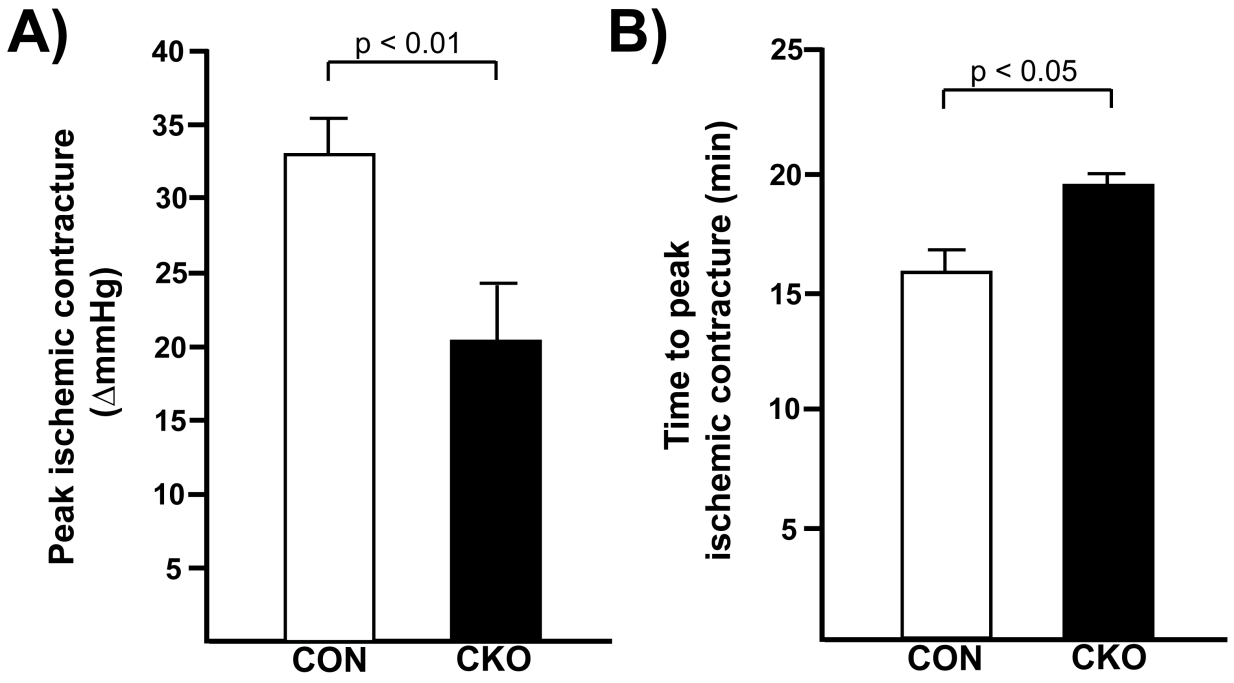

Figure 2.15. CKO hearts have significantly decreased peak ischemic contracture as well as well as significantly increased time to peak ischemic contracture.
A) Quantification of peak ischemic contracture. B) Quantification of time to peak ischemic contracture. N = 9 (CON) and 8 (CKO). P-values are displayed on graphs.

2.3.12. mTOR-KO mice hearts recover worse when treated with insulin during reperfusion.

As mentioned in section 2.1.3, hearts subjected to *ex vivo* Langendorff are missing a number of systemic factors. Therefore, because mTOR is part of the insulin-signaling pathway, I tested the effect of insulin on our mTOR-CKO mice. I subjected control and CKO mice to the same insulin and *ex vivo* protocol (Section 2.2.4). I found insulin to be slightly cardioprotective in our control mice though the result was not significant. However, in the CKO mice I found that insulin appeared to significantly decrease the %LVDP recovery when given at reperfusion although it did not lower the recovery significantly more than the controls (Figure 2.16).

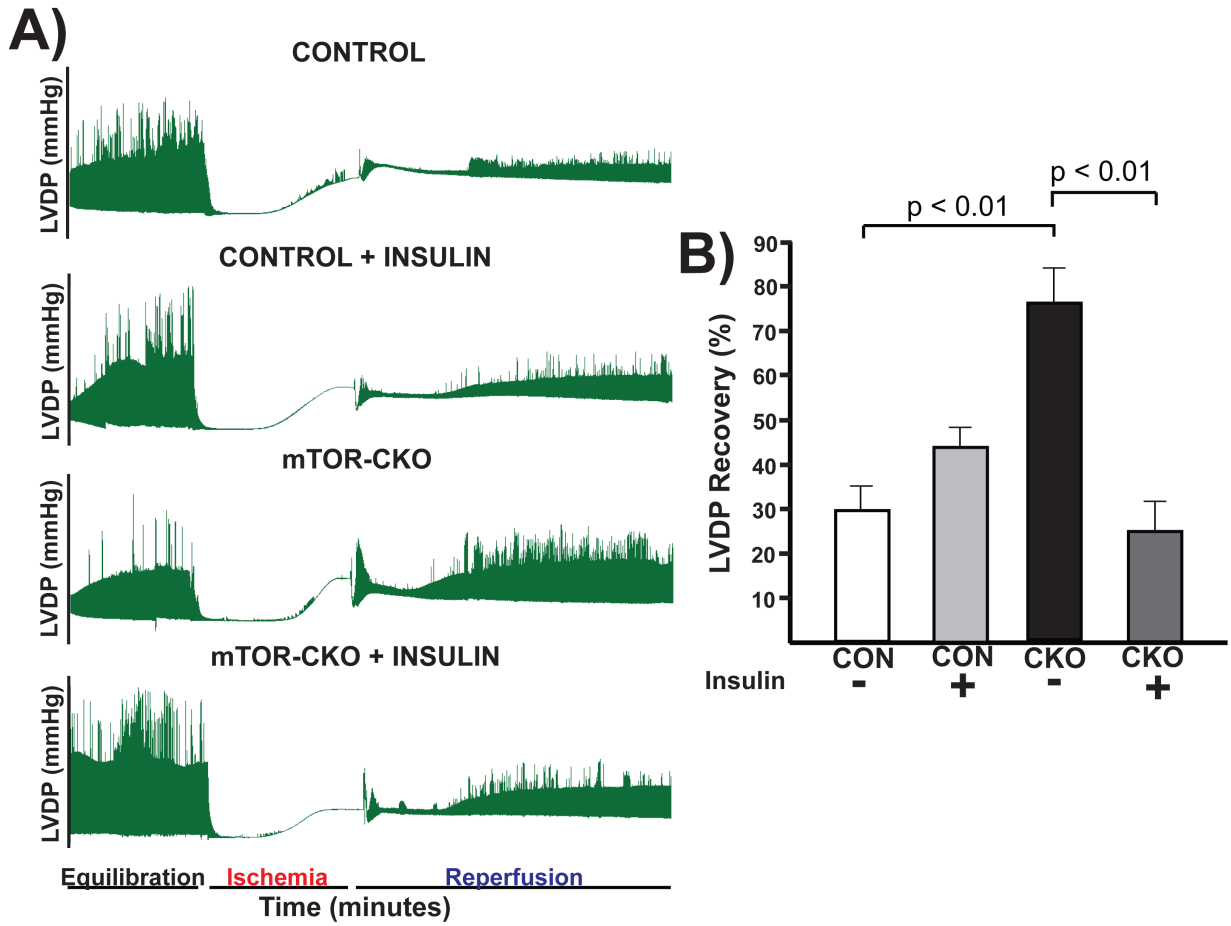

Figure 2.16. Insulin administered at reperfusion significantly decreases recovery of the mTOR-KO hearts.
A) Representative tracings of LVDP over the course of the Langendorff experiment. Insulin administered at reperfusion appeared to decrease the recovery of mTOR-KO hearts. B) Comparison of LVDP at baseline and after 40 minutes of reperfusion to determine %LVDP. CKO N = 6 (CON), 3 (CKO), 6 (CON + Insulin), and 4 (CKO + Insulin). P-values are listed on graph as determined by one-way ANOVA and Tukey's post hoc test.

2.3.13. IP3R2 expression is significantly decreased in the SR/mito fractions of mTOR-KO hearts.

It is known that insulin activates Ca^{2+} release through the IP3R and promotes mitochondrial Ca^{2+} uptake [121, 122]. Since mTOR is known to localize at mitochondria associated membranes, I investigated the other Ca^{2+} release channel in the heart, the IP3R2 to determine if the expression was changed. Decreased expression of IP3R2 at the SR/mito has previously been shown to be downregulated at MAMs in mouse

embryonic fibroblasts (MEFs) that have RICTOR knocked down [5]. mTOR has also been shown to phosphorylate the IP3R2 in non-excitable pancreatic AR4-2J cells [98]. Therefore, alteration of the IP3R may be the reason for the improved recovery I saw initially without insulin stimulation but substantially mitigated function with insulin treatment at reperfusion. To assess the IP3R expression in CKO and control hearts, I followed the subcellular fractionation protocol detailed in section 2.2.16 to obtain the SR/mito fraction. I immunoblotted IP3R2 and found the expression of the IP3R2 to be significantly decreased in mTOR-KO hearts when normalized to VDAC (Figure 2.17).

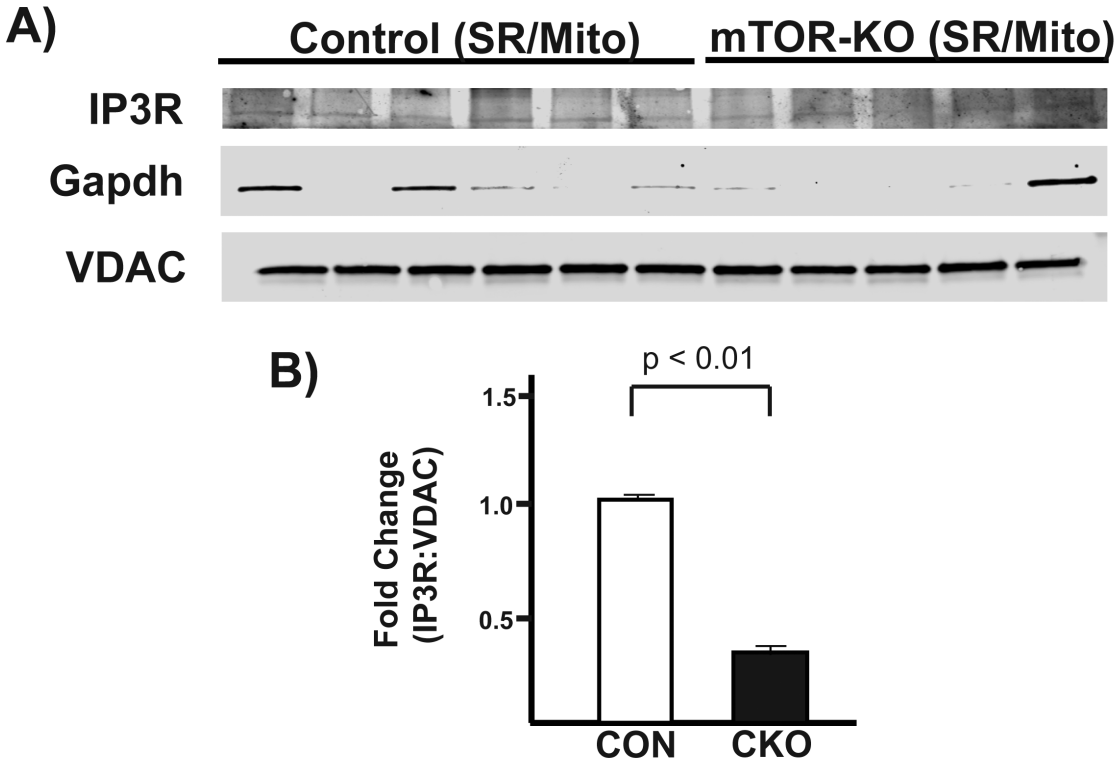

Figure 2.17. IP3R protein level is reduced in the SR/mito fraction of CKO hearts.
Hearts from CKO and control mice were harvested and subjected to a subcellular fractionation protocol. A) Western blot showing decreased IP3R expression in the SR/mito fraction of mTOR-KO hearts. B) Quantification of the fold change decrease of IP3R expression. Gapdh was used to determine the purity of the fractions while VDAC was used as a loading control. Blots were analyzed using ImageJ software. N=6 (control) and 5 (CKO). *p*-value displayed on graph as determined by student t-test.

2.4. Discussion

2.4.1. Summary and interpretation of results

Based on our previous studies using mTOR-Tg mice in *in vivo* and *ex vivo* I/R injury, in the study using the mTOR-CKO, I anticipated that mTOR was *necessary* for cardioprotection against I/R injury. The *in vivo* data clearly demonstrated mTOR was necessary for protecting CMs from cell death following I/R injury (Figure 1.4). Accordingly, I also anticipated the mTOR-CKO mice would have significantly worse recovery after *ex vivo* I/R injury. Acute inhibition of mTOR with Torin1 in our *ex vivo* model supported our *in vivo* findings (Figure 2.7). However, I was surprised to find the CKO hearts had significantly better recovery after *ex vivo* I/R injury as well as a significant decrease in release of the myocardial injury marker, creatine kinase (Figures 2.9 and 2.11). I hypothesized the reason for this discrepancy between the *in vivo* and *ex vivo* models could be due to either a lack of systemic stimulation in the *ex vivo* system or due to a change in one or more of the proteins involved in EC-Coupling. Several publications have already suggested a role for mTOR in Ca^{2+} signaling in other cell types [5, 97, 100, 123, 124] and one report has shown mTOR to be localized at mitochondrial associated ER membranes [5, 97, 100, 123, 124]. Additionally, my own data showing the CKO hearts had irregular contractility following I/R injury was another clue hearts from mTOR-CKO mice may have abnormal contractile function and Ca^{2+} transients (Figure 2.10).

Based on previous studies and my data, I examined the role of mTOR in EC-coupling in the CKO hearts treated with isoproterenol that stimulates SR Ca^{2+} release. I observed no difference in the recovery between control and CKO hearts using this

method of stimulation although isoproterenol resulted in a lower recovery for both control and CKO hearts than normal (Figure 2.12). This suggested that hyper-phosphorylation of the ryanodine receptor is not the major EC-coupling protein alteration in CKO CMs. Therefore, I applied electrical stimulation to pace the hearts to investigate another potential mechanism responsible for the irregular contractility of the CKO hearts. Pacing has been shown to activate CAMKIIδ and also increase phosphorylation of PLN [117, 125]. This would allow me to assess if there was an alteration in PLN in CKO hearts. I noticed that the mTOR-KO hearts displayed cardiac alternans at baseline but also had significantly decreased peak ischemic contracture as well as time to peak ischemic contracture (Figures 2.13 and 2.15). Ischemic contracture is the result of decreased ATP and increased Ca^{2+} levels during ischemia. However, I did not find any evidence to suggest that PLN was altered in the CKO hearts and was responsible for the decreased peak ischemic contracture and time to peak ischemic contracture. It is likely that mechanisms other than the hyper-phosphorylation of the RYR2 and PLN result in the improved recovery for the CKO hearts.

One possible mechanism may involve insulin since mTOR is a major component of insulin signaling. It is known that insulin stimulates mitochondrial fusion and function in CMs via the Akt-mTOR-NFkB-Opa-1 signaling pathway [121, 122, 126]. As a result, I stimulated the hearts with insulin at reperfusion (Figure 2.16). As expected, insulin was detrimental to the CKO hearts but in the same proportion as control hearts.

After the insulin study, I investigated the IP3R since none of the traditional proteins involved in EC-coupling and Ca^{2+} handling seemed to be altered in our mouse models. In addition, insulin has been shown to activate Ca^{2+} release from the IP3R in

striated muscle cell promoting mitochondrial Ca^{2+} uptake [121]. mTOR is known to associate with MAMs and I hypothesized that decreased IP3R expression could lead to MAM destabilization. The additional Ca^{2+} entering the cytosol should increase uptake into the mitochondria due to insulin stimulation. Since the MAM is already destabilized, this should result in increased cell death due to Ca^{2+} overload, which may explain the lowered recovery I observed in our CKO hearts after insulin was given at reperfusion. Lowered IP3R expression could also explain the better recovery in the initial *ex vivo* studies, as there would be less Ca^{2+} released due to a decrease in IP3R expression. Indeed, when I compared the SR/mito fractions of the CKO hearts compared with controls, I found IP3R expression to be significantly decreased (Figure 2.17). As this was a preliminary study, I did not verify creatine kinase release from the hearts stimulated with insulin, nor did I check the mRNA levels of the IP3R. More thorough and stringent investigation is therefore needed to determine if this really is the mechanism behind the improved recovery *ex vivo*.

In conclusion, even though the CKO hearts recovered better than control hearts in a Langendorff model of global ischemia and reperfusion, it does not indicate that less expression of mTOR is cardioprotective against I/R injury. Since there are no neurohormonal factors such as insulin in *ex vivo* hearts, in certain condition, missing systemic factors would affect cardiac recover after I/R injury in this model. The decreased recovery of the CKO hearts seen after insulin stimulation and the *in vivo* data suggests mTOR plays an important cardioprotective role against I/R injury, although its mechanism remains unclear.

Chapter Three

THE ROLE OF mTOR *IN VITRO* IN CALCIUM SIGNALING AND EC-COUPLING

3.1. Introduction

3.1.2. Specific Aim 2: To define the role of mTOR in cardiomyocyte Ca^{2+} signaling and EC-coupling.

I next determined if cardiac mTOR regulates Ca^{2+} transients and contraction in adult murine CMs, a necessity in the heart. A key marker of heart failure is defective Ca^{2+} handling leading to arrhythmias and contractile dysfunction [127]. Defective Ca^{2+} transients are the result of many different pathogenic mechanisms including hyper-phosphorylation of the ryanodine receptor, decreased SERCA expression, and increased phosphorylation of PLN [128]. mTOR, an important cell regulator of many processes, has already been shown to be involved in Ca^{2+} regulation as previously mentioned in section 1.7. In mouse embryonic fibroblasts, mTORC2 has been shown to associate with the ER and mitochondrial associated membranes (MAMs). Disruption of mTORC2 was associated with a number of mitochondrial defects including an increased Ca^{2+} uptake [5]. Another group demonstrated that rapamycin inhibition of mTOR impaired Ca^{2+} release from inositol 1,4,5-trisphophate receptors (IP3Rs) in vascular smooth muscle [95]. Several other groups also confirmed mTOR's role in modulating the IP3R (section 1.7).

Therefore, based on this literature and on our preliminary data, I hypothesized that mTOR is *necessary* to maintain normal Ca^{2+} transients and EC-coupling [5]. Accordingly, I investigated Ca^{2+} transients in the control and CKO CMs. To do this, I isolated CMs as specified in section 2.2.4 and 3.2.2. The cells were loaded with the Ca^{2+} indicator, Fura-2-AM as described in section 3.2.3 and measured sarcomere length and Ca^{2+} transients were measured using the IonOptix system. Then, to determine if Ca^{2+} release or reuptake was impaired in the CKO CMs, I stimulated the CMs with the β-adrenergic stimulator, isoproterenol. Finally, I assessed the *relative* SR content using the ryanodine receptor stimulator, caffeine.

3.1.3 Rationale for measuring contraction and Ca^{2+} transients using Fura-2-AM and the IonOptix system

The IonOptix system is ideal and well suited for studying contraction and Ca^{2+} transients due to its video edge detector and IonWizard Core Analysis Software as well as its dual-excitation fluorescence photomultiplier system. This is especially ideal for measuring Ca^{2+} transients with the fluorescent Ca^{2+} indicator, Fura-2 pentacetoxymethyl AM ester (Fura-2-AM, Molecular Probes). Fura-2 is advantageous as the endogenous esterase enzymes inside the cell cleave the AM groups attached to fura-2 leaving it free to bind intracellular Ca^{2+}. The Ca^{2+} bound by Fura-2 can then be measured by the dual-excitation photomultiplier system that detects fluorescence at an emission of 510 nm. In the presence of intracellular Ca^{2+}, fura-2 is excited at 340 nm and in its absence; it is excited at 380 nm [129, 130]. The ratio of fluorescence at

340/380 allows for the determination of the relative concentration of free intracellular Ca^{2+}.

3.1.4. Rationale for using isoproterenol and ryanodine

Isoproterenol is known to stimulate β-adrenergic receptors, which in turn activate PKA. PKA and CAMKII are the two major proteins responsible for phosphorylating the ryanodine receptor. I hypothesized that the mTOR-KO CMs may exhibit dysfunction in one or more components involved in EC-Coupling. Consequently, I challenged the CKO CMs using isoproterenol. Several groups use isoproterenol to induce what is termed spontaneous Ca^{2+} waves (SCW) or Ca^{2+} sparks [131, 132]. I treated control and CKO CMs with isoproterenol to evaluate any differences between those two groups. Simultaneously, I also used the ryanodine receptor inhibitor, ryanodine to assess if that decreased the amount of SCWs [69].

3.1.5. Rationale for using caffeine

Caffeine is a well-known stimulator for Ca^{2+}-induced Ca^{2+} release (CICR) from RYRs on the SR. It has become a useful tool to determine the Ca^{2+} content of intracellular membrane storage organelles such as the SR of intact cardiac muscle cells [133, 134]. It is an advantageous pharmacological tool because it has a dual mechanism of action depending on what concentration of caffeine is given. At low concentrations (< 1 mM), activation of RYR occurs mainly from the sensitivity of the channel to cytosolic Ca^{2+}. However, high concentrations such as the 10 mM

concentration I used in this study, increase the sensitivity of the ryanodine receptor to luminal Ca^{2+} [135].

3.2. Methods

3.2.1. Subcellular fractionation of whole heart tissue.

Subcellular fractionation was carried out as specified in section 2.2.16.

3.2.2. Western Blot analysis

After the fractionation protocol described in the above section (3.2.1), I performed immunoblotting exactly the same way as described in section 2.2.4. I used the following primary antibodies: phospho serine 2808-RYR (Badrilla), RYR (Thermo Scientific), SERCA2a (Santa Cruz), IP3R (Millipore), VDAC (Cell Signaling), GAPDH (Santa Cruz), p-PLN (Cell Signaling), and PLN (Cell Signaling).

3.2.3. Isolation of adult murine ventricular myocytes for Ionoptix

CMs from CKO and CON mice were isolated as described in section 2.2.5. CMs were re-loaded with Ca^{2+} using increasing concentrations of Ca^{2+} (0.06 mM, 0.24 mM, 0.6 mM, 1.2 mM) for 10 minutes each before using them for Ca^{2+} transients and contraction measurements.

3.2.4. Measurement of Ca^{2+} transients and sarcomere length shortening

Myocytes were loaded with Ca^{2+} indicator Fura 2-AM (5 μM) for 15 minutes at 25°C. Myocytes attached to a coverslip were placed in a chamber mounted on the stage

of an inverted microscope (Nikon Eclipse, Figure 3.1) and superfused at approximately 2 mL/min at 37°C with a buffer containing 10 mM glucose, 137 mM NaCl, 5.4 mM KCl, 0.5 mM $MgCl_2$, 10 mM HEPES (pH = 7.4), and 1.2 mM $CaCl_2$. The cells were field-stimulated at a frequency of 2 Hz. A video-based edge detector was used to capture and convert changes in cell length during shortening and re-lengthening into an analog voltage signal. Cell contractions were assessed using the following indicators: peak shortening, time to 90% PS (TPS), time to 90% re-lengthening (TR90) and maximal velocities or shortening and re-lengthening (± dL/dt) (Figure 3.2A). Ca^{2+} was evaluated by examining the Fura-2 emission ratio of intracellular to extracellular Ca^{2+} as previously described [136](Figure 3.2B).

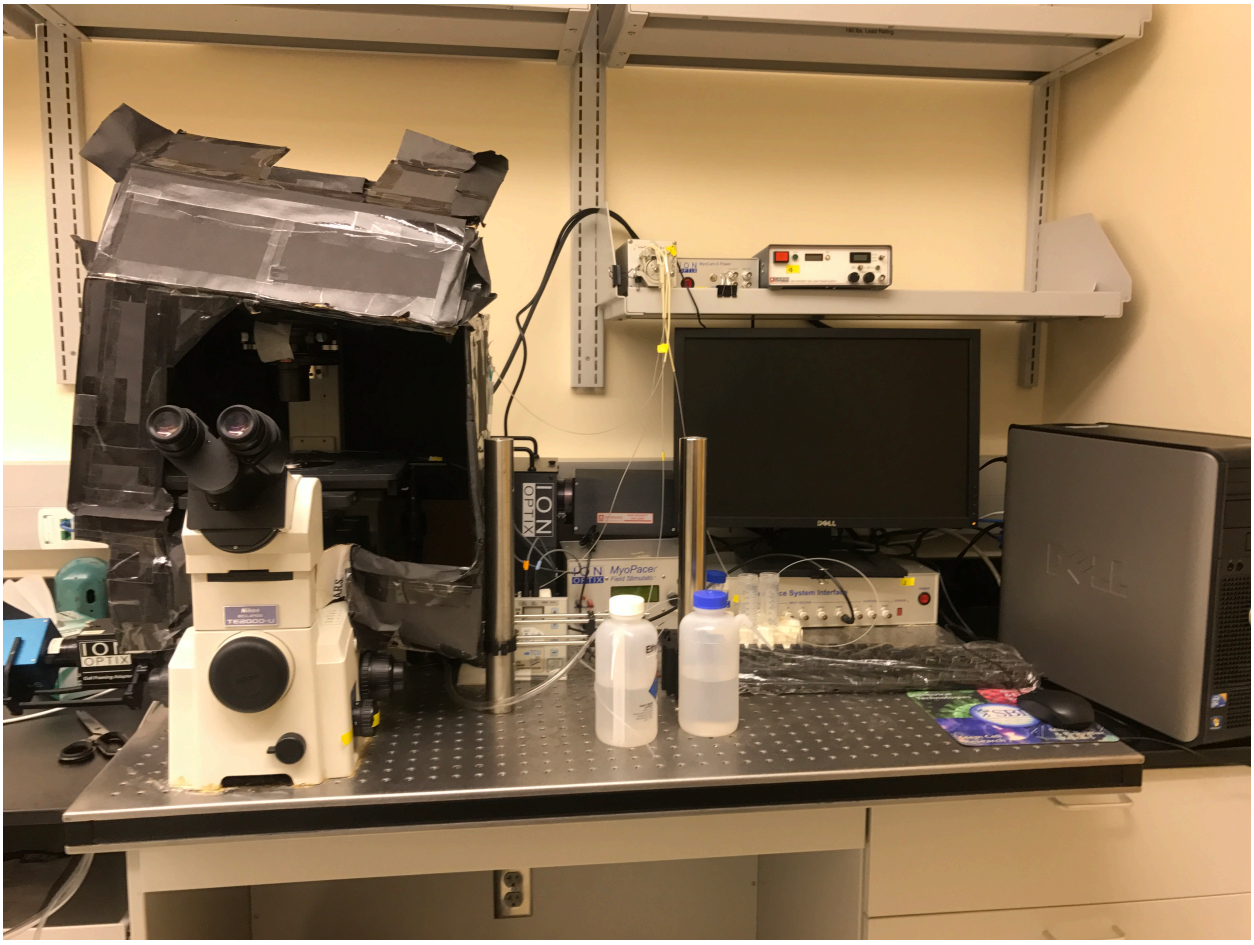

Figure 3.1. Picture of our IonOptix system including the inverted microscope used in these experiments.

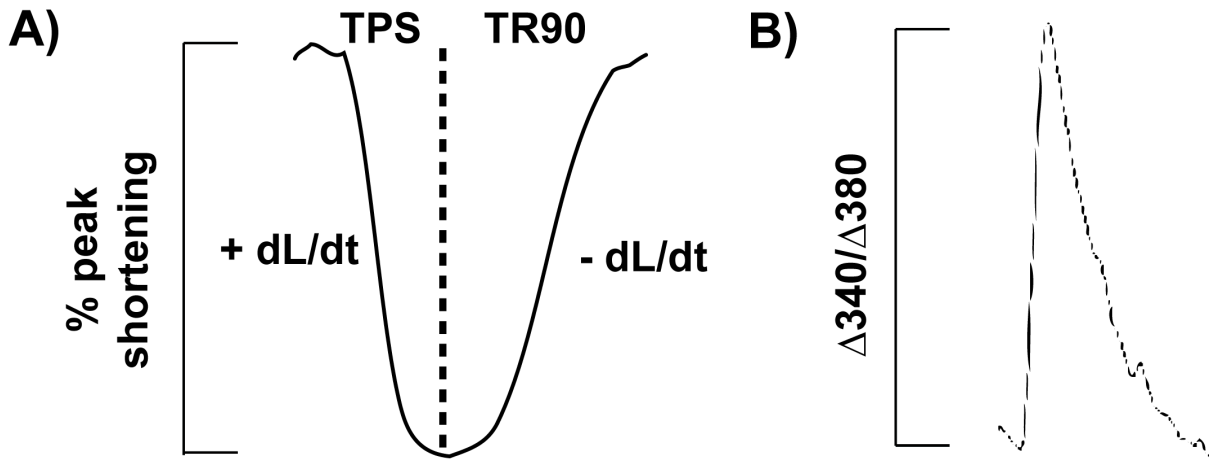

Figure 3.2. Measurements of cardiac function by IonOptix.
Diagram of measurements used to evaluate cardiac function using the IonOptix system. A) Measurements of sarcomere length shortening. TPS (time to peak shortening), TR90 (time to 90% relaxation), ± dL/dt (departure and return velocity) B) Measurement of Ca^{2+} transients using the ratio of intracellular and extracellular Ca^{2+}.

3.2.5. Isoproterenol challenge of isolated adult murine ventricular myocytes and ryanodine treatment

CMs were inoculated with or without 1 μM ryanodine prior to pacing. The cells were then perfused with the buffer containing the components listed in section 3.2.3 and 1 μM isoproterenol. CMs were stimulated at 0.5 Hz for 5 minutes to allow equilibration to the isoproterenol and the stimulation. Increased pacing rates (0.5, 1.0, and 2.0 Hz) were used to field-stimulate CMs for one minute to induce spontaneous Ca^{2+} waves (SCW). Pacing was stopped at each frequency for 10 seconds to determine delayed after depolarizations (DADs). The scheme for the isoproterenol experiment is displayed below (Figure 3.3).

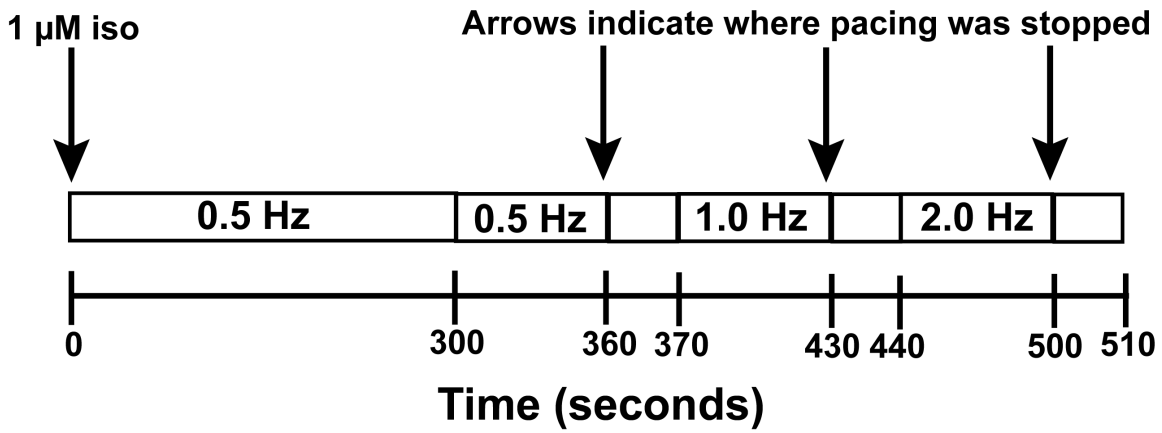

Figure 3.3. Scheme of isoproterenol treatment and subsequent pacing protocol using the IonOptix system.

3.2.6. Caffeine stimulation in isolated adult murine ventricular CMs

CMs were field stimulated at 0.5 Hz to steady state for 1 minute before pacing was stopped for 30 seconds and 10 mmol/L caffeine was rapidly applied. The caffeine was allowed to washout for another 30 seconds and the CMs were paced again at 0.5 Hz to re-attain the same steady state [137].

3.2.7. Calculation of %spontaneous calcium waves (%SCW)

The number of Ca^{2+} peaks in a one-minute time period was counted for each pacing frequency to determine the regular amount of peaks in each pacing frequency. The spontaneous, extra Ca^{2+} peaks were counted and compared to the number of regular peaks to determine the % spontaneous Ca^{2+} waves. To calculate the DADs I counted the number of peaks after pacing was stopped for that 10-second period.

3.2.8. Statistical analysis

Results were analyzed using Graph Pad's PRISM software. Statistical tests were applied according to the experimental design as indicated in the figure legends. For comparisons of two groups, a student t-test was applied. For comparison of multiple groups, one-way ANOVA was used. Tukey's post hoc test was used as a post-test for one-way ANOVA. *P* values are also shown in the figures or graphs. All results are reported as means ± SEM.

3.3. Results

3.3.1. mTOR is localized in both cytosolic and subcellular fractions

To confirm the localization of mTOR to the SR/mitochondria, I used the subcellular fractionation method described in section 3.2.1 and obtained a cytosolic and an SR/mito fraction for both control and CKO hearts. Western blot analysis revealed mTOR was located in both the cytosolic and SR/Mito fractions as shown (Figure 3.4). SERCA expression levels were unchanged in both the cytosolic and SR/mitochondria fractions. GAPDH and VDAC were used as loading controls and to verify the purity of the fractions.

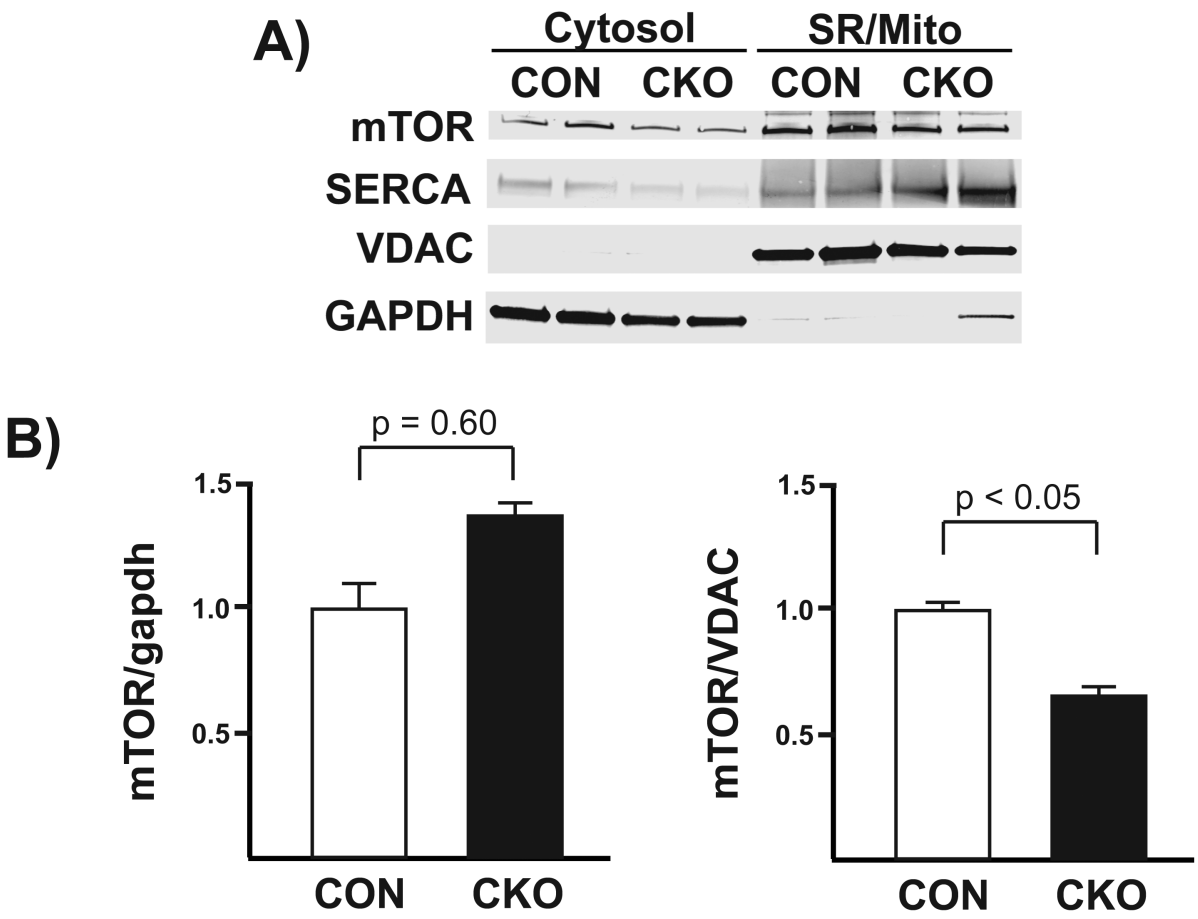

Figure 3.4. mTOR is localized in both cytosolic and subcellular fractions
A) Representative immunoblot of hearts prepared using an ultracentrifuge to obtain subcellular fractions. mTOR was present in both the cytosolic and SR/mitochondria fractions. B) Quantification of the amount of mTOR in the cytosol (left) and the SR/mitochondria fractions (right). GAPDH was used as a loading control for the cytosolic fraction while VDAC was used as the control for the SR/Mito fraction. N=4 for all groups. *p*-values are listed on graphs.

3.3.2. CMs isolated from mTOR-CKO mice have decreased contractility and a smaller calcium transient ratio.

After confirming the localization of mTOR to the SR/mitochondria fractions, I evaluated CM contraction and Ca^{2+} transients at baseline. To do this, CMs were isolated using the method described in section 3.2.1 and examined for contractility and Ca^{2+} transients using the method in 3.2.2. Using this system, I observed that CKO CMs have both weaker and slower contractions as well as a decreased Ca^{2+} transient ratio

(Figure 3.5A). Supporting this observation, quantifiable parameters of contractility and Ca^{2+} transients of CMs isolated from CKO and control mice also exhibited significant differences from each other. Peak shortening was significantly decreased in CKO CMs compared to controls while time to 90% peak shortening (TPS), and time to 90% re-lengthening (TR90) were significantly increased compared to controls (Figure 3.5B). Ca^{2+} transient ratio was also quantifiably decreased in the CKO CMs versus controls (Figure 3.4B). These data indicate CKO CMs have significantly worse contractile function and weaker Ca^{2+} transients at baseline compared to controls.

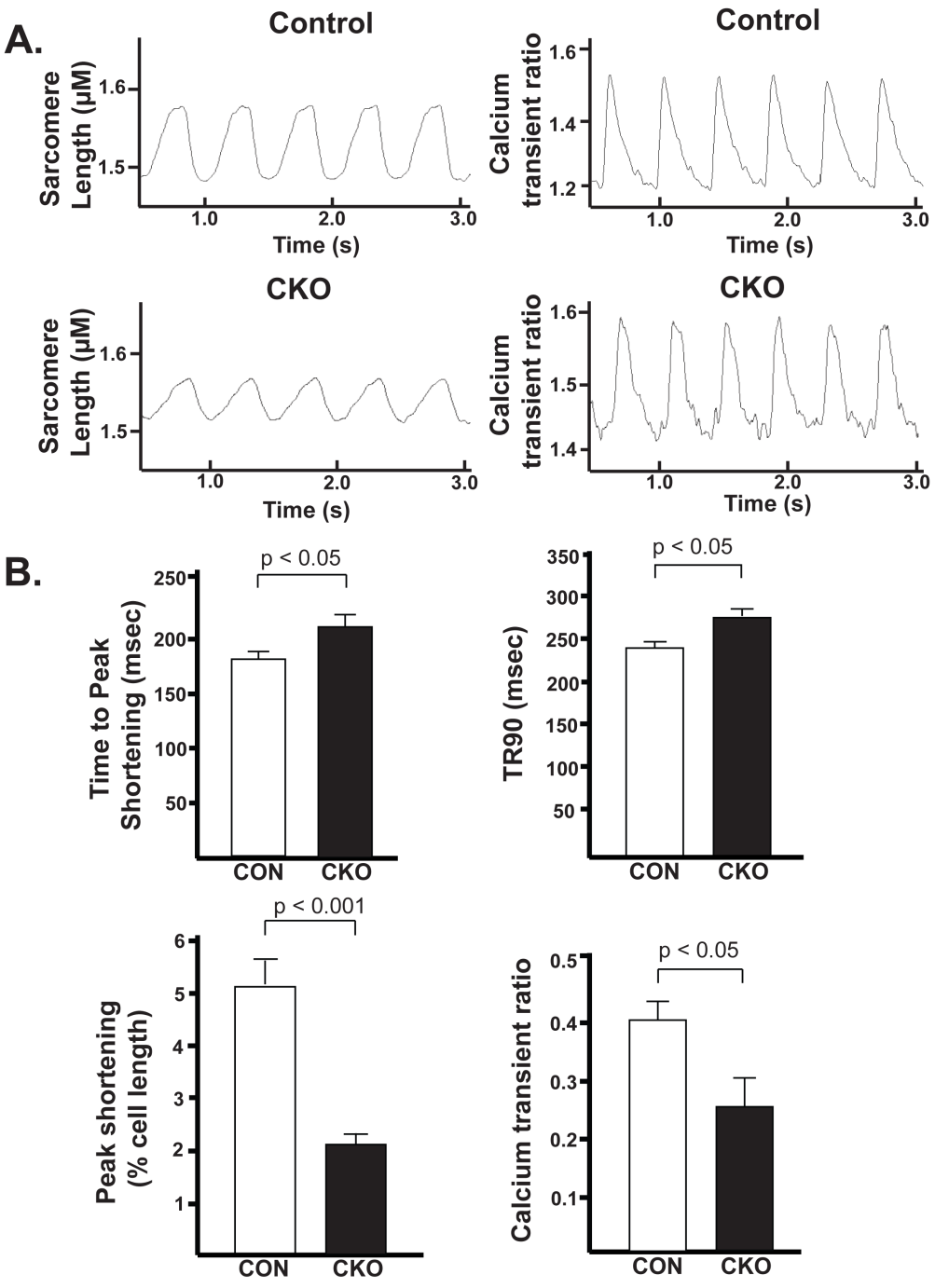

Figure 3.5. Cardiomyocytes isolated from mTOR-KO mice have weaker contractility and a smaller calcium transient ratio.
A) Representative traces of sarcomere length contraction and Ca^{2+} transients in control and mTOR-KO CMs. CKO CMs had both weaker and slower contractions as well as a lower Ca^{2+} transient ratio. B) Time to peak shortening and time to 90% relaxation were both significantly increased in CKO CMs. Peak shortening was significantly lower in CKO CMs compared to controls and Ca^{2+} transient ratio was also significantly decreased in CKO CMs. N=3 independent experiments, 8-12 cells total for both groups. p-values are all displayed on graphs.

3.3.3. Isoproterenol challenge of CKO cardiomyocytes did not show an increase in the percent of spontaneous Ca^{2+} waves and ryanodine inhibition of the ryanodine receptor did not decrease the amount of spontaneous Ca^{2+} waves.

Due to the decreased Ca^{2+} transient ratio and weaker contractions of the CKO CMs, I hypothesized mTOR may play an important role in EC-coupling. To test this hypothesis, I challenged the CKOs with 1 μM isoproterenol and ± 1 μM ryanodine at increasing pacing rates from 0.5 Hz to 4.0 Hz. Isoproterenol is a known beta-adrenergic receptor stimulator that activates PKA. PKA is known to phosphorylate the ryanodine receptor and result in increased release of Ca^{2+} from the SR. Isoproterenol can also trigger spontaneous Ca^{2+} waves (SCWs) and delayed after depolarizations (DADs) that are indicative of premature spontaneous Ca^{2+} release during diastole [138]. Based on the initial baseline IonOptix data, I hypothesized that mTOR-CKO CMs had a defect either in Ca^{2+} release or reuptake. If there was dysfunction in Ca^{2+} release, I expected the CKO CMs to possibly have increased SCW or DADs upon isoproterenol stimulation relative to controls. However, there was no difference between the CKO and control CMs and the percentage of SCW. In addition, ryanodine treatment did not decrease the amount of SCWs (Figure 3.6). Therefore, hyper-phosphorylation of the ryanodine receptor is not the cause of the weaker contractions and smaller Ca^{2+} transients.

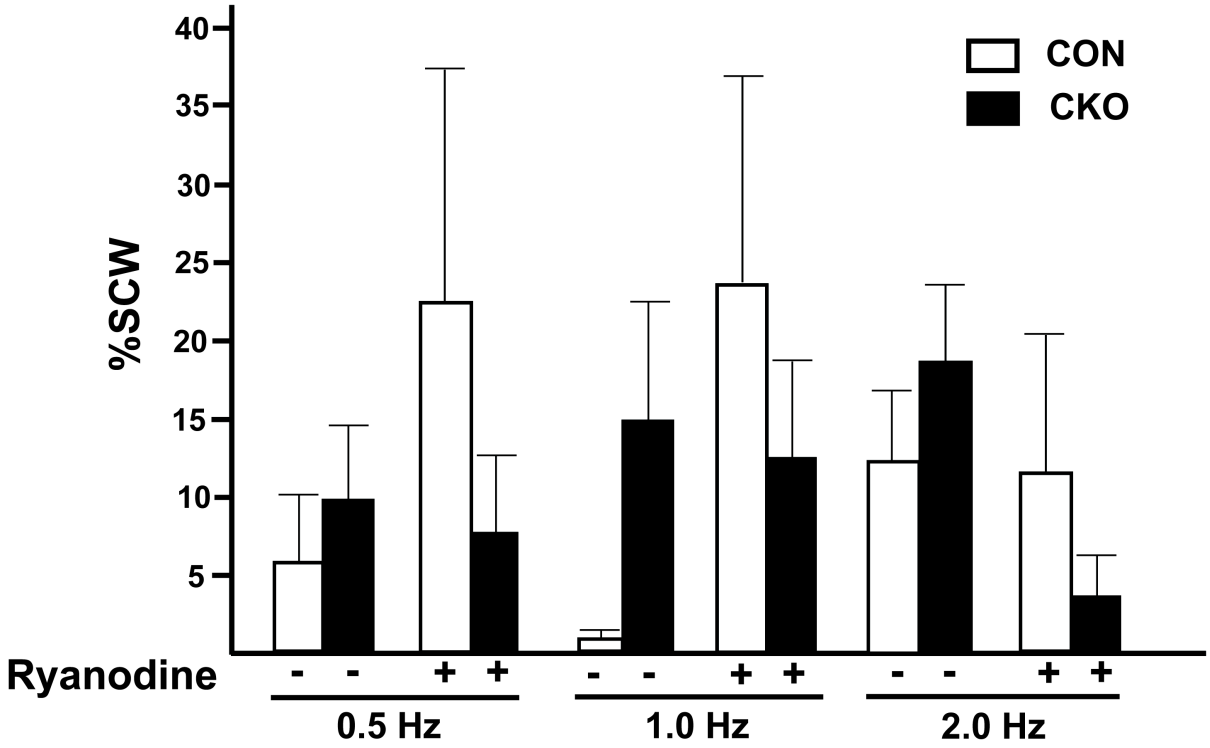

Figure 3.6. mTOR-KO CMs do not have significantly more %SCW than controls and ryanodine did not significantly decrease the percentage of SCWs.
Quantification of the number of SCW compared to the number of normal Ca^{2+} peaks to determine %SCW with and without ryanodine treatment. There was no difference in the %SCW between CKOs and controls with or without treatment. N = 7 (CON), 7(CKO), 9 (CON + ryanodine), 11 (CKO + ryanodine).

3.3.4. ,mTOR-CKO CMs do not show a change in any major EC-Coupling protein.

I next confirmed the isoproterenol data and determined that there was no change in ryanodine receptor phosphorylation. I isolated adult CMs from controls and CKO mice and performed the same fractionation protocol as figure 3.4. I blotted for phospho-ryanodine receptor (p-RYR) and total RYR. I found no significant difference in the ratio of p-RYR:RYR in CKO CMs versus controls (Figure 3.7) in either the cytosolic or SR/mitochondria fractions. There was also not find any significant difference in p-PLN or SERCA expression.

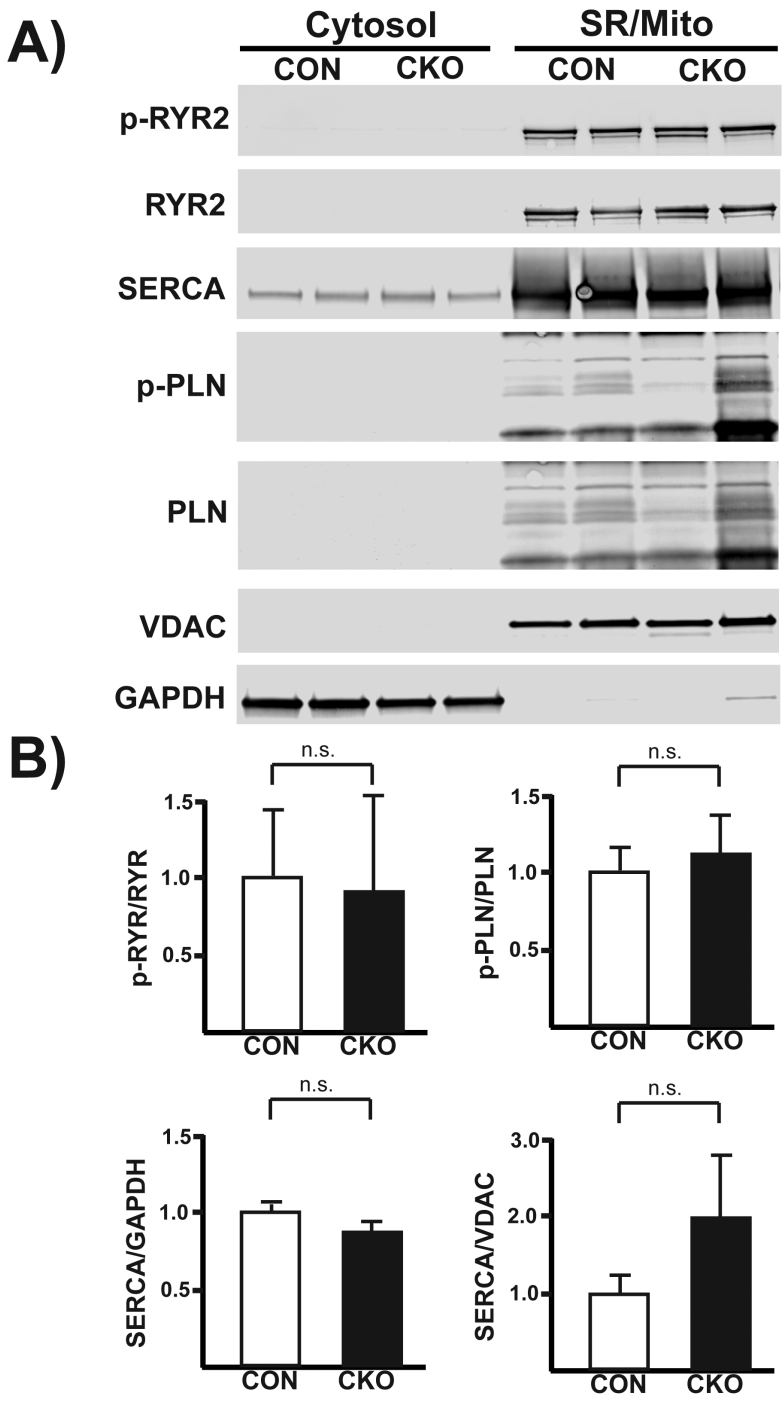

Figure 3.7. CKO hearts do not show a change in any major EC-Coupling protein.
A) Representative immunoblot from control and CKO hearts that underwent ultracentrifugation to obtain subcellular fractions. Analysis of the blots showed there was no increase in p-RYR in the CKO hearts. There was also no change in SERCA and p-PLN. VDAC was used as a loading control for the SR/mito fraction while GAPDH was used as the loading control for the cytosolic fraction. B) Quantification of the amount of p-RYR, p-PLN, and SERCA in controls and CKO hearts. N = 6 for all groups.

3.3.5. Caffeine stimulation of control and CKO cardiomyocytes showed CKO CMs have decreased relative SR Ca^{2+} content

I hypothesized that the knockout of mTOR may lead to decreased SR content and slower release and reuptake of Ca^{2+}. To test this hypothesis, I challenged CMs isolated from CKO and control mice with 10 mmol/L caffeine using the method explained in section 3.2.6. CKO CMs exhibited significantly reduced caffeine- induced Ca^{2+} transients and significantly smaller peak shortening as shown by the representative images and quantitative data (Figure 3.8). The majority of the control CMs had sharp peaks in response to caffeine as demonstrated by the representative image. On the other hand, the CKO CMs were not as responsive to the caffeine. They had wider peaks and sometimes multiple peaks as shown in the representative images (Figure 3.8A). Quantification of these peaks confirmed these observations. Peak shortening (% cell length) and Ca^{2+} transient ratio were both significantly smaller in CKO CMs (Figure 3.7B). These two indicators showed that mTOR-KO CMs had a significantly diminished response to caffeine. The smaller Ca^{2+} transient induced by caffeine in the CKO CMs also demonstrates that the relative SR Ca^{2+} content is significantly smaller than in control CMs.

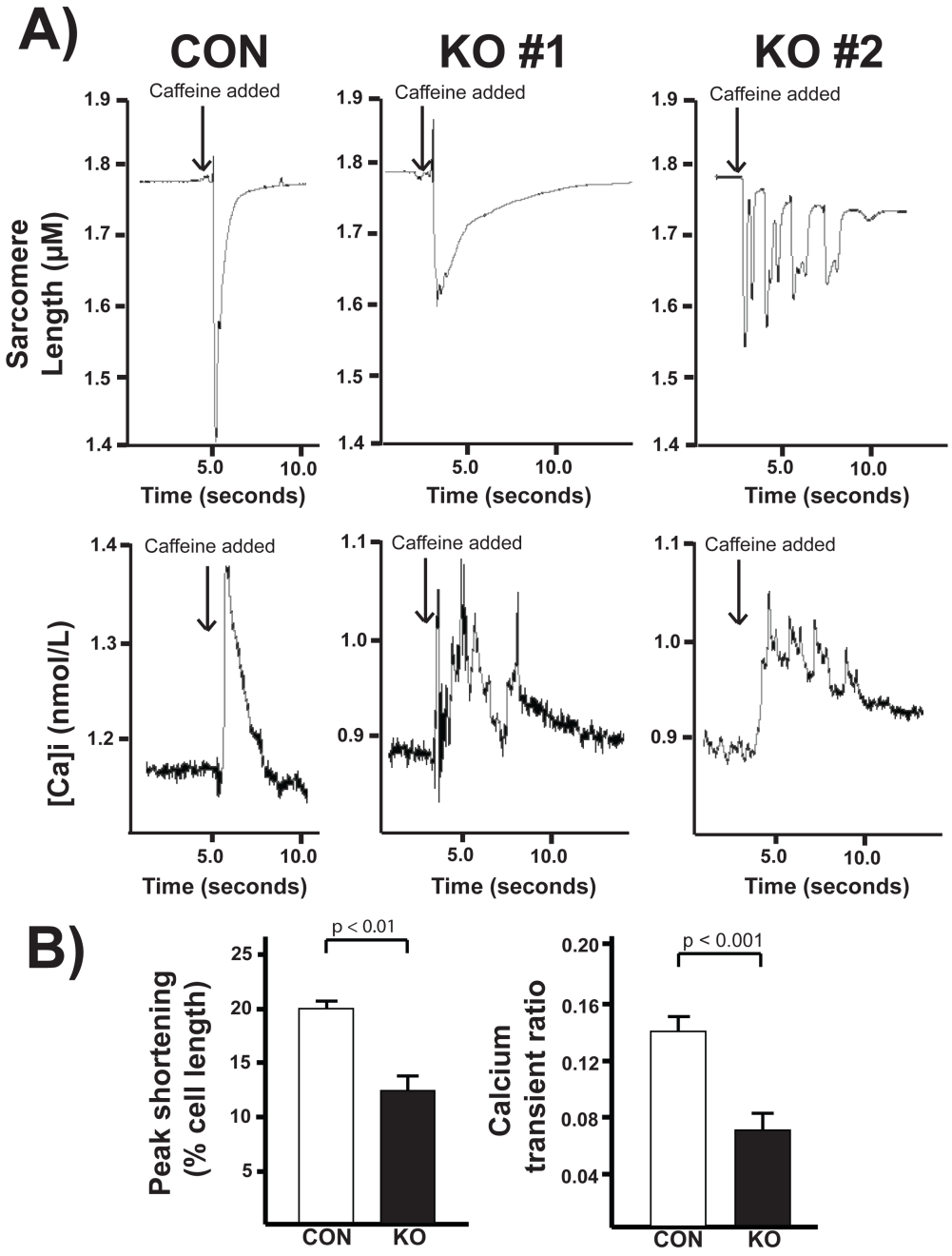

Figure 3.8. mTOR-CKO CMs have lower relative SR calcium content than controls.
A) Representative images from caffeine experiments. *Top.* Representative tracing of sarcomere length from CON and CKO CMs stimulated with caffeine. CKO peaks were smaller and sometimes had multiple contractions. *Middle.* Representative tracing of Ca^{2+} transients from CON and CKO CMs stimulated with caffeine. The CKO CM Ca^{2+} transient ratio was significantly lower than controls. *Bottom.* Quantification of the peaks resulting from caffeine stimulation. CKO CMs had significantly smaller % peak shortening and Ca^{2} transients than controls indicating the CKO CMs have a lower SR Ca^{2+} content. N = 12 cells from 3 (CON) and 4 (CKO) mice. P-values are displayed on graphs as determined by student's t-test.

3.4. Discussion

3.4.1. Summary and interpretation of results

I hypothesized that mTOR may play an important role in Ca^{2+} signaling in CMs based on other studies supporting a role for mTOR in Ca^{2+} signaling in non-muscle cell types and my own data showing mTOR was localized to both the cytosol and the SR/mitochondria. To demonstrate a functional role for mTOR in Ca^{2+} signaling, I isolated CMs from control and CKO mice and tested their baseline CM contraction/Ca^{2+} transients using our IonOptix system. The CMs isolated from CKO mice displayed significantly weaker contractions and had reduced Ca^{2+} transients (Figure 3.5). This was expected based on the *in vivo* data which showed that mTOR was necessary for cardioprotection against I/R injury. Therefore, I also expected CMs isolated from CKO mice to have worse baseline function, despite the *ex vivo* data showing that the CKO hearts recovered better in an *ex vivo* Langendorff model.

Based on the baseline IonOptix data, I hypothesized that the CKO CMs had either dysfunctional Ca^{2+} release or reuptake, possibly due to a change in one or more proteins involved in EC-Coupling. To test if Ca^{2+} release was impaired, I stimulated the CMs with the β-adrenergic agonist, isoproterenol, resulting in increased release of Ca^{2+} from the SR through RYRs. I also treated some of the cells with the RYR inhibitor, ryanodine. I speculated if RYRs were hyper-phosphorylated then inhibition of RYRs with ryanodine would decrease the amount of Ca^{2+} sparks. I found that CKO CMs did not have significantly more SCWs than control CMs (Figure 3.6). Most likely this means the weaker contractions and smaller Ca^{2+} transients are not due to the hyper-phosphorylation of RYRs. This is reinforced by the Western blot data showing there was

no significant increase in the phosphorylation of RYRs between control and CKO CMs (Figure 3.7). Therefore, the cause of the weaker contractions and smaller Ca^{2+} transients is due to another mechanism.

Since I determined that changes in the RYR receptor does not explain the differences in CKO CMs, I decided to evaluate the SR Ca^{2+} content in the CKO CMs versus control CMs. To determine the relative SR Ca^{2+} content, I stimulated the CMs with caffeine, which activates Ca^{2+}-induced Ca^{2+} release on the SR. I found significant differences in the relative SR Ca^{2+} content between the CKO CMs and the control CMs. CKO CMs had significantly less SR Ca^{2+} as demonstrated by their smaller Ca^{2+} transient ratio (Figure 3.8). A smaller amount of SR Ca^{2+} could then explain the baseline IonOptix data. Decreased expression of the IP3R as shown in Figure 2.17 could potentially be the cause. Reduced IP3R levels could destabilize MAMs resulting in increased mitochondrial Ca^{2+} uptake. This could result in less Ca^{2+} being taken up by SERCA into the SR as more Ca^{2+} than usual is in the mitochondria.

I did not investigate the Ca^{2+} reuptake in the CKO CMs, however, I did not find any evidence to investigate Ca^{2+} reuptake based on western blot data that exhibited no changes in SERCA expression or increase in phospho-phospholamban (p-PLN, Figure 3.7). Therefore, I concluded that SERCA down-regulation and/or an increase in p-PLN was likely not the cause of lower Ca^{2+} in the SR or the weaker contractions and Ca^{2+} transients I observed at baseline. The mechanism has yet to be determined though it may be through a reduction of IP3R expression.

Chapter Four

THE ROLE OF MTOR IN OTHER PATHOLOGICAL SETTINGS ESPECIALLY DIABETES MELLITUS

4.1. Introduction

4.1.1. Specific Aim 3: To define the role of cardiac mTOR in metabolic disorders such as diabetes mellitus (DM).

mTOR is an important contributor to several cellular functions and has a major role in cellular and glucose metabolism. Therefore, I studied its role in other pathological settings, especially the metabolic syndrome and DM. Indeed, patients with DM is associated with a two-fold higher risk of developing heart failure in men and a four to five-fold greater risk in women compared to healthy controls and accounts for 66% of the mortality in the first year post MI [139-141]. Even more concerning is that, despite the advanced therapeutics available, the rate of HF in patients with diabetes has increased over time [142]. Consequently, there is a need to thoroughly investigate key proteins in metabolism and cardiovascular disease such as mTOR in further detail in order to develop new therapeutic targets in DM patients.

Our previous study demonstrated that overexpression of mTOR was cardioprotective in a mouse model of obesity. Glucose tolerance and insulin resistance were comparable between mTOR-Tg and WT mice, however, functional recovery after I/R using the *ex vivo* Langendorff perfusion model was significantly better in mTOR-Tg mice on a HFD than WT mice on a HFD [8]. Overall, this study demonstrated mTOR

was significantly better for cardioprotection in a mouse model of obesity. My next objective was to verify if mTOR was an important factor involved in cardioprotection in a mouse model of obesity. As a preliminary study, I placed the control and CKO mice on a HFD for 12 weeks. Following, I evaluated these mice for hyperglycemia and obesity before subjecting their hearts to I/R injury using the Langendorff perfusion model.

4.1.2. Rationale for using a diet-induced obesity mouse model

C57BL6/J mice on a HFD display the three key risk factors of metabolic syndrome: obesity, glucose intolerance, and insulin tolerance [8, 143, 144]. These risk factors are major determinants for developing diabetes and/or MI. Genetic mouse models such as *db/db* mice are not as relevant to human obesity since they are caused by a mutation in one gene whereas human obesity is most likely mediated by multiple factors including diet, lifestyle, and genetics. Polygenic mouse models of obesity such as the New Zealand Obese (NZO) mice are available, however, a diet-induced model most closely resembles the metabolic state in humans.

4.2. Methods

4.2.1. Tamoxifen administration (injections)

At 6 weeks of age, CKO and control mice were administered a series of five tamoxifen injections over a period of one week. Thirty mg/kg/d of tamoxifen were dissolved in corn oil and given to the mice via intraperitoneal (IP) injections.

4.2.2. *High-fat diet administration.*

At 6-8 weeks of age, CKO and control mice were given either a normal chow diet (NCD) consisting of 24.7% energy from protein, 13.2% from fat, and 62.1% from carbohydrates (5053, PicoLab, St. Louis, MO) or a HFD consisting of 14.9% energy from protein, 26.0% carbohydrate, and 59.0% fat (S3282, 549.0 kcal/100 g, Bio-Serv, Frenchtown, NJ) for 12 weeks.

4.2.3. Collection of blood glucose levels.

At the end of 12 weeks, mice were fasted overnight and blood samples were drawn from the tail vein and measured using a commercially available glucose meter (OneTouch Ultra blood glucose meter, LifeScan, Milpitas, CA).

4.2.4. Statistical analysis

Results were analyzed using Graph Pad's PRISM software. Statistical tests were applied according to the experimental design as indicated in the figure legends. For comparisons of two groups, a student t-test was applied. For comparison of multiple groups, one-way ANOVA was used. Tukey's post hoc test was used as a post-test for one-way ANOVA. *P* values are also shown in the figures or graphs. All results are reported as means ± SEM.

4.3. Results

4.3.1. Mice on a HFD exhibit large body weights and high blood glucose levels relative to mice on a NCD.

After 12 weeks on HFD, control and CKO mice on a NCD and HFD were weighed. A blood glucose test was performed to determine if the mice were exhibiting hyperglycemia. As this was a preliminary study, these mice were not evaluated for glucose tolerance and insulin resistance. Body weight and blood glucose levels were found to be significantly higher in control mice on the HFD versus controls on a NCD. Body weight and blood glucose levels for the CKO mice were not significantly higher though they were trending that way (Table 5 and Figure 4.1). Most likely, the lack of significance was due to the low sample number for these mice as power analysis indicated I would need a sample size of 8 per group based on a power of 0.80 and a type 1 error rate of 0.05. Likewise, there were no significant differences in body weight and blood glucose levels between CON and CKO mice on a HFD or on a NCD (Table 5 and Figure 4.1)

Table 5. Comparison of body weight, heart weight, and HW:TB between control and CKO mice on a NCD and a HFD

	CON NCD	**CKO NCD**	**CON HFD**	**CKO HFD**
Body Weight	31.12 ± 1.37 g	31.43 ± 0.55 g	42.60 ± 3.08 g	40.40 ± 5.57 g
Heart Weight	0.19 ± 0.009 g	0.19 ± 0.019 g	0.21 ± 0.019 g	0.21 ± 0.030
HW:TB	0.0083 ± 0.0004	0.0083 ± 0.0008	0.0093 ± 0.0009	0.0092 ± 0.001

Values shown are means ± SEM. N = 7(CON NCD), 4 (CKO NCD), 6 (CON HFD), and 4(CKO HFD)

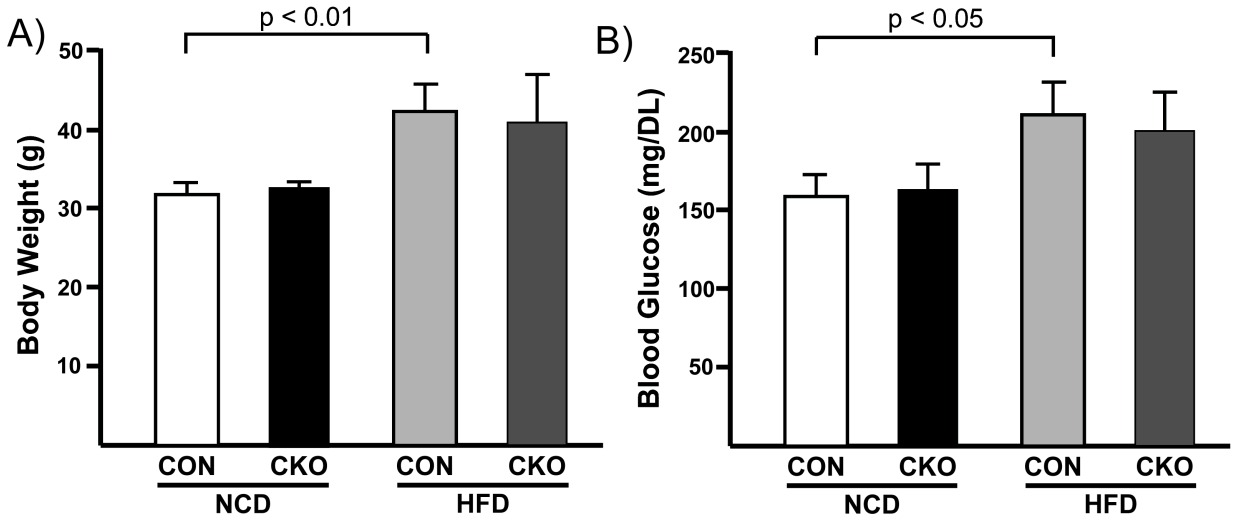

Figure 4.1. Body weight and fasting blood glucose levels are significantly higher in control mice on a HFD.
Bar graph showing control mice on a HFD had significantly increased body weight compared to controls on a NCD. B) Bar graph demonstrating CON mice on a HFD have significantly increased fasting blood glucose levels. N = 7 (CON NCD), 4 (CKO NCD), 6 (CON HFD), and 4 (CKO HFD). P-values displayed on graph.

4.3.2. CKO mice hearts recover significantly better than CON on both a NCD and a HFD.

To determine if mTOR is *necessary* to protect the heart against I/R injury in a mouse model of obesity, I next placed CKO and control mice on a HFD for 12 weeks and then evaluated their cardiac function via *ex vivo* Langendorff. I found that CKO mice recovered better then their littermate controls on both a NCD and HFD (Figure 4.4). There was also no significant difference between the recoveries of the control mice on a HFD versus a NCD and likewise between CKO mice on a HFD versus a NCD. Most likely this was due to the low sample number. A larger number may have revealed differences between these groups as power analysis indicated I would need 8 mice per

group given a power of 0.80 and a type 1 error rate of 0.05 to reliably detect a 2-fold difference in %LVDP recovery.

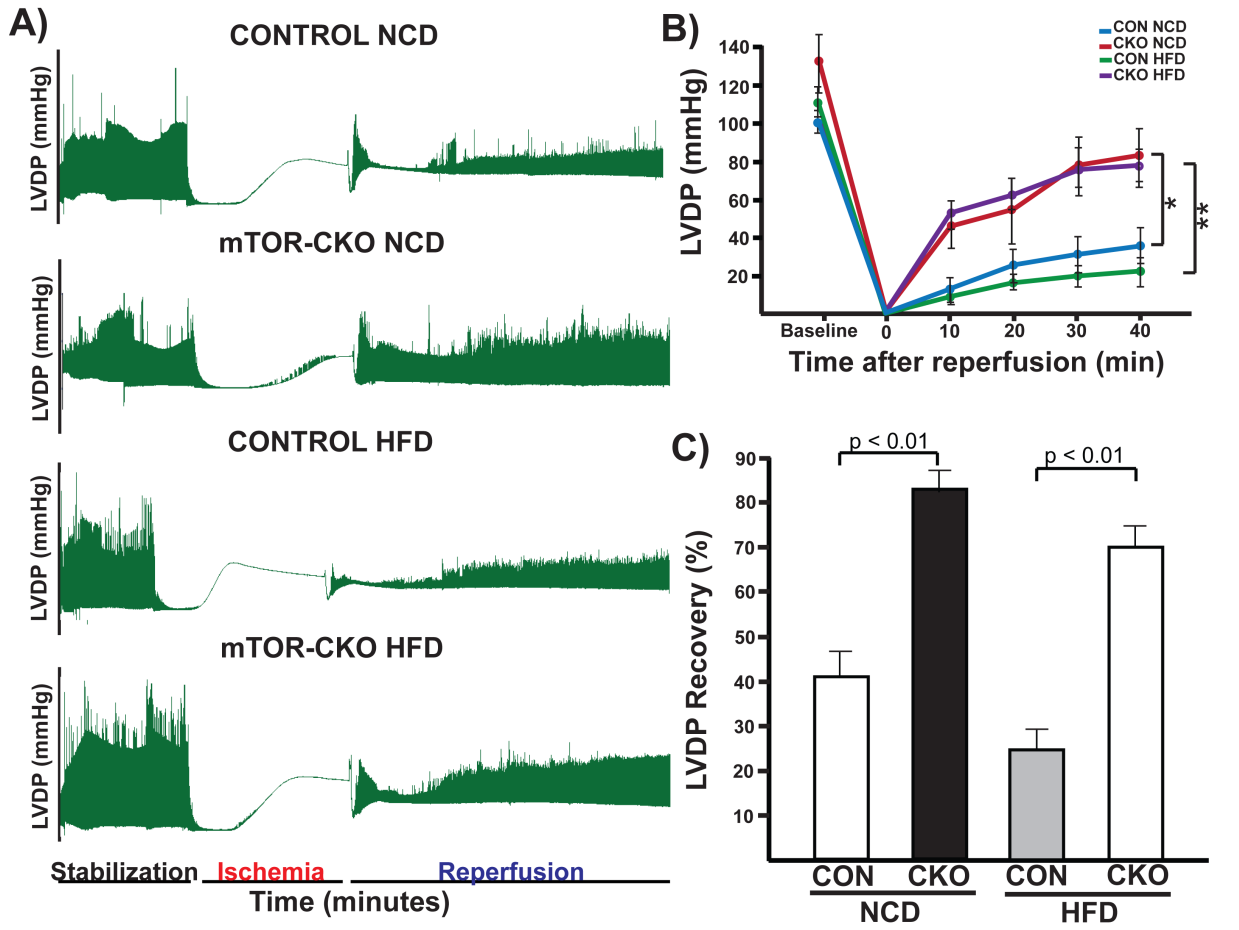

Figure 4.2. mTOR-CKO mice on a NCD and HFD recover better after I/R injury in the *ex vivo* Langendorff model.
A) Representative tracings showing the entire Langendorff experiment. B) Quantitation of the LVDP at baseline and every 10 minutes of reperfusion. mTOR-KO mice on a NCD and a HFD recovered significantly better than control mice on a NCD and HFD. C) %LVDP recovery of control and CKO mice on both a NCD and HFD. N = 7 (CON NCD), 4 (CKO NCD), 6 (CON HFD), and 4 (CKO HFD). P-values are listed on the graphs as determined by one-way ANOVA and Tukey's post hoc test.

4.4. Discussion

4.4.1. Summary and interpretation of results

Since mTOR is highly involved in glucose metabolism and fatty acid oxidation, I decided to investigate the role of mTOR in the metabolic syndrome and DM. As a

preliminary study, I placed mTOR-KO mice on a HFD along with their littermate controls for 12 weeks and then assessed them for their body weight and their blood glucose levels. I found significant changes to the body weight and blood glucose levels in the controls that were on a HFD but not in the CKOs. Most likely this was due to the low sample number of the CKO mice and if repeated in the future, the body weight and blood glucose levels would be significantly higher.

As part of the preliminary study, I subjected the mice to global ischemia-reperfusion injury using *ex vivo* Langendorff. The CKO hearts again recovered better than control hearts on both a NCD and a HFD. This was surprising as I expected the HFD to be especially detrimental to the mTOR-CKO hearts. The better recovery of the CKO hearts on a HFD in the *ex vivo* system may again be explained by the lack of insulin stimulation and lower amount of Ca^{2+} in the SR. Since there is less Ca^{2+} in the SR, there is less Ca^{2+} entering the CM during ischemia and therefore, the CKO hearts are recovering better. If insulin were given at the start of reperfusion, most likely this would result in a lower recovery for mTOR-CKO hearts on a HFD.

Chapter Five

Concluding Remarks

5.1. Summary and discussion of results

In our previous studies, overexpression of mTOR was shown to be cardioprotective against a number of different pathological stimuli including I/R injury, TAC-induced hypertrophy, and I/R injury in a mouse model of obesity [2, 7, 8]. These studies clearly established that mTOR overexpression significantly protected the heart against negative stimuli and suggested the mTOR signaling pathway was a potential therapeutic target. However, we did not establish the role of mTOR in cardioprotection and other pathological settings. Therefore, in order to demonstrate mTOR prevented cell death and left ventricular remodeling, I established a tamoxifen-inducible, CM specific mTOR-KO mouse line and studied it in a number of different functional settings. I hypothesized loss of mTOR would be detrimental to the heart in the I/R injury model. As expected, the mTOR-KO mice had reduced cardiac function and increased fibrosis just seven days after *in vivo* I/R surgery (Figure 1.4). Since our previous studies demonstrated a beneficial effect of mTOR in both *in vivo* and *ex vivo* I/R injury, I anticipated the CKO hearts would conversely have a lower %LVDP recovery than their littermate controls. However, upon subjecting these hearts to the Langendorff protocol, I found a very surprising and yet very consistent result. The mTOR-KO mice recovered significantly better than their littermate controls (Figure 2.8).

As a result of this unexpected finding, I explored the role of mTOR in cardiac physiology and EC-coupling rather than focus on cell death. I hypothesized that one of the proteins involved in CM contraction may be altered in the mTOR-CKO hearts, resulting in lower overall SR Ca^{2+} content. The lower SR Ca^{2+} and subsequent loss of external stimuli normally present *in vivo* was causing the mTOR-KO hearts recovered better after I/R injury. I tested a number of different stimuli that triggered various components of the EC-coupling pathway. First, I examined ones that increased Ca^{2+} release through ryanodine receptors such as isoproterenol and pacing. None of these significantly decreased the recovery of the mTOR-KO hearts (Figures 2.11 and 2.13). This implies the hyper-phosphorylation of the ryanodine receptor is not the cause of my hypothesized lower amount of Ca^{2+} in the SR. This was later further confirmed by western blot analysis (Figure 3.6).

Then, since mTOR is a part of the insulin-signaling pathway, I tested direct insulin stimulation. Insulin may be one of the missing external factors that are present *in vivo* that the Langendorff system lacks. I found that insulin given at reperfusion significantly decreased the recovery of the CKO hearts. One potential mechanism for insulin blunting the recovery of the CKO mice is that insulin signaling activates Ca^{2+} release from the IP3R and leads to increased mitochondrial uptake of Ca^{2+} [121, 122]. mTOR is known to associate with MAMs which requires IP3R to have MAM integrity. In MEFs that had mTORC2 knocked down, expression of the IP3R3 was found to be significantly decreased [5]. Taken together, these results show mTOR is an important contributor for cardioprotection against I/R injury although the mechanism is unclear as to why the CKO hearts recover better without insulin.

For the second aim, since the *ex vivo* data was unclear due to missing elements normally present *in vivo*, I utilized isolated CMs as our knockout is in specifically CMs to determine if mTOR helped maintain normal Ca^{2+} transients and contraction. To analyze changes in Ca^{2+} transients and contractility in mTOR-CKO CMs, I isolated CMs and studied their contraction and Ca^{2+} transients using our IonOptix system. I found that CMs isolated from mTOR-CKO mice had significantly weaker contractions and smaller Ca^{2+} transients (Figure 3.4). Consistent with my *ex vivo* data, isoproterenol stimulation did not result in significantly more spontaneous contractions between the CKO and control CMs (Figure 3.5). If RYR2 was hyper-phosphorylated in CKO CMs, isoproterenol stimulation should have resulted in increased SCWs. However, stimulation with caffeine did demonstrate there was significantly lower relative SR Ca^{2+} in CKO CMs compared with controls, although the mechanism for why there is lower SR Ca^{2+} in these CMs also remains unclear. It is possible that the lower SR Ca^{2+} and the better recovery of the CKO hearts in the *ex vivo* Langendorff system is tied to the same mechanism. This is potentially due to downregulated IP3R levels, resulting in more Ca^{2+} being taken up by the mitochondria leaving less Ca^{2+} to be taken up into the SR by SERCA.

Finally for my third aim, as a preliminary study, I investigated the role of mTOR in a mouse model of obesity by placing CKO mice and their littermate controls on a HFD for 12 weeks, since our previous study demonstrated the sufficiency for mTOR to guard against harmful cardiovascular effects in the metabolic syndrome [8]. The result was unexpected when I subjected these hearts to global ischemia. Once again, the hearts from the CKO mice recovered better then their littermate controls (Figure 4.2). This

unforeseen result could be due to missing insulin and or other external factors. It is probable that insulin stimulation of the CKO mice on a HFD would significantly blunt their recovery. Notably, the HFD CKO hearts recovered better than control hearts on a NCD.

5.2. Conclusion

This dissertation focused primarily on the role of mTOR in cardiac function, a role that has not yet been well defined in I/R injury and diabetes mellitus. This study is unique in that both mTORC1 and mTORC2 were knocked out. Most of the other studies involving mTOR have focused on either inhibiting mTORC1 through a RAPTOR knockout or by using rapamycin or its derivatives. Some studies also inhibited the expression of mTORC2 through a RICTOR knockout. However, these studies only focus on one of the mTOR complexes. Since mTOR expression is significantly up regulated in heart failure patients, we used a model that over-expressed mTOR [7]. However, it was unknown as to whether this was a compensatory or a de-compensatory response until our study demonstrated mTOR prevented cell death and helped maintain normal cardiac function in both *in vivo* and *ex vivo* models of I/R injury [2].

Since our previous report in CMs focused on the beneficial effects of mTOR over-expression, I determined the consequences of a CM-specific mTOR knockout. My studies in this dissertation clearly demonstrate loss of mTOR is detrimental to the heart in various functional pathological conditions although insulin is also required in *ex vivo* I/R injury. I also established mTOR was required to maintain normal contractions and Ca^{2+} transients *in vitro* using our IonOptix system, and that mTOR CKO CMs had lower relative SR Ca^{2+} content. However, I could not identify the mechanism responsible for

these different findings although insulin and the IP3R2 may play a key role in the overall mechanism since IP3R expression was significantly lowered in the SR/mito fractions of the CKO hearts. Based on my data and the literature, I hypothesized that loss of mTOR may lead to the following (See Figure 5.1): 1) decreased IP3R expression (Figure 2.17) and *possible* loss of MAM integrity. 2) This leads to *possible* increased mitochondrial Ca^{2+} uptake and significantly lowered SR Ca^{2+} (Figure 3.8). Lower SR Ca^{2+} then results in 3) decreased Ca^{2+} transients and weaker contractions (Figure 3.5). Without insulin stimulation, increasing release of Ca^{2+} from release channels, CKO hearts can recover better because there is less Ca^{2+} entering the mitochondria. However, with insulin, there *may* be increased Ca^{2+} release combined with possible altered MAM integrity and amplified mitochondrial Ca^{2+} uptake leading to the decreased recovery of the CKO hearts, although this is mere speculation.

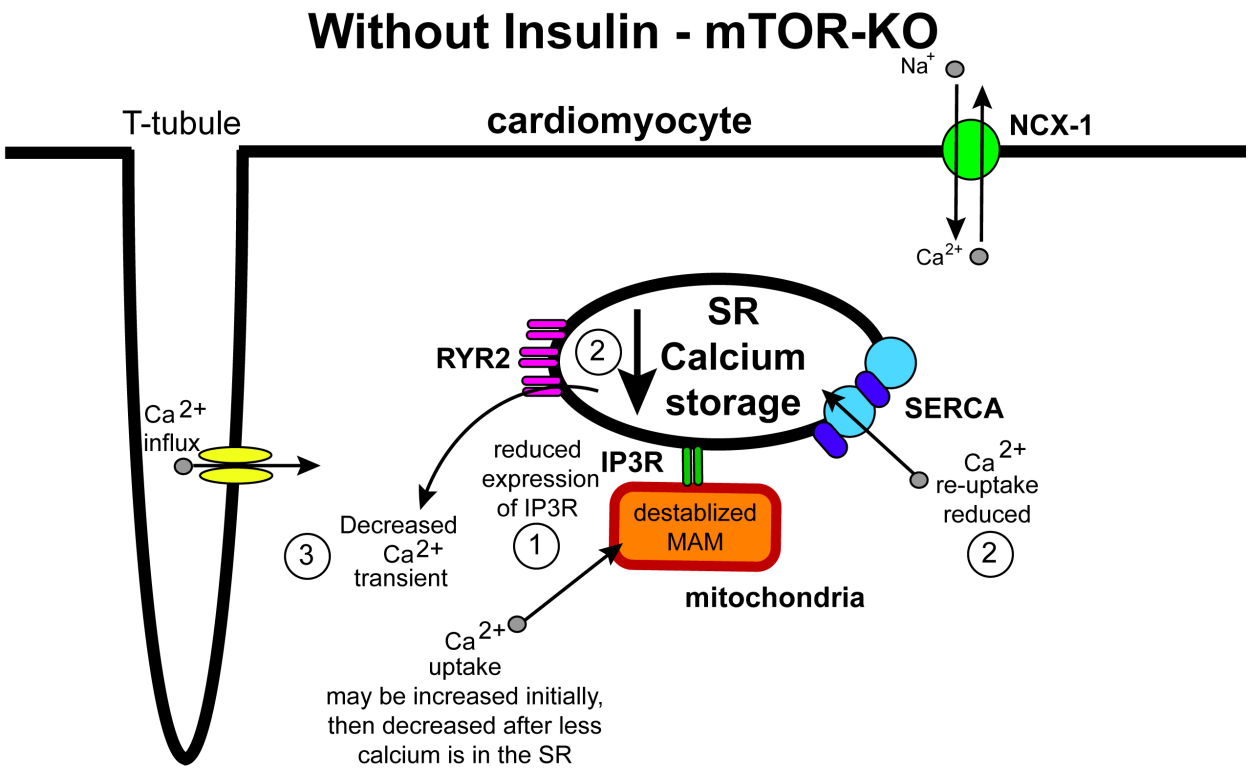

Figure 5.1. Scheme of our speculated mechanism for the findings in this dissertation. Illustration of my findings and speculated mechanism. Numbers correspond to the numbers written above in the text in section 5.2. 1) I found that loss of mTOR may lead to reduced expression of the IP3R (Figure 2.17). This could cause more Ca^{2+} to be taken up by the mitochondria, although not enough to trigger cell death. The lower amount of Ca^{2+} in the cytosol then leads to 2) reduced Ca^{2+} reuptake and SR Ca^{2+} content (Figure 3.8). This then results in 3) decreased Ca^{2+} transients and weaker contractions (Figure 3.5).

5.3. Limitations and future directions

The research described in this dissertation was primarily focused on characterizing our cardiac specific mTOR-KO mice and the role of mTOR in functional cardiovascular studies and consequently, has some limitations. Although it established clear and key differences between the CKO mice and their littermate controls and demonstrated mTOR was required for shielding the heart against adverse conditions when given insulin, it did not specifically look at whether cell death was prevented in both the *ex vivo* and *in vitro* studies. Therefore, there must be consideration that mTOR

is only partially essential for cardioprotection. Future studies are necessary to determine the necessity of mTOR in the two major forms of cell death: apoptosis and necrosis.

Another major limitation of these studies is the lack of mechanism for the findings I discovered in these experiments. I saw a decrease in IP3R expression but I did not look in-depth to determine if IP3R reduction was the cause of my findings. More thorough experimentation is needed to determine the mechanism. However, I did show a new finding in location of mTOR which is located within the SR/mitochondria and established loss of mTOR was necessary to maintain normal Ca^{2+} transients and contraction. Although a clear mechanism was not found, there is the potential for new findings based on my discoveries in this dissertation concerning a role for mTOR in SR/mito signaling. Having a clear mechanism would then allow for further studies involving mTOR and could provide new insights into potential therapeutics for different forms of heart disease such as MI, HF, and DM.

LITERATURE CITED

1. Benjamin, E.J., M.J. Blaha, S.E. Chiuve, M. Cushman, S.R. Das, R. Deo, S.D. de Ferranti, J. Floyd, M. Fornage, C. Gillespie, C.R. Isasi, M.C. Jimenez, L.C. Jordan, S.E. Judd, D. Lackland, J.H. Lichtman, L. Lisabeth, S. Liu, C.T. Longenecker, R.H. Mackey, K. Matsushita, D. Mozaffarian, M.E. Mussolino, K. Nasir, R.W. Neumar, L. Palaniappan, D.K. Pandey, R.R. Thiagarajan, M.J. Reeves, M. Ritchey, C.J. Rodriguez, G.A. Roth, W.D. Rosamond, C. Sasson, A. Towfighi, C.W. Tsao, M.B. Turner, S.S. Virani, J.H. Voeks, J.Z. Willey, J.T. Wilkins, J.H. Wu, H.M. Alger, S.S. Wong, and P. Muntner, *Heart Disease and Stroke Statistics-2017 Update: A Report From the American Heart Association.* Circulation, 2017.

2. Aoyagi, T., Y. Kusakari, C.Y. Xiao, B.T. Inouye, M. Takahashi, M. Scherrer-Crosbie, A. Rosenzweig, K. Hara, and T. Matsui, *Cardiac mTOR protects the heart against ischemia-reperfusion injury.* American journal of physiology. Heart and circulatory physiology, 2012. **303**(1): p. H75-85.

3. Hernandez, G., H. Lal, M. Fidalgo, A. Guerrero, J. Zalvide, T. Force, and C.M. Pombo, *A novel cardioprotective p38-MAPK/mTOR pathway.* Experimental cell research, 2011. **317**(20): p. 2938-49.

4. Sciarretta, S., M. Volpe, and J. Sadoshima, *Mammalian target of rapamycin signaling in cardiac physiology and disease.* Circulation research, 2014. **114**(3): p. 549-64.

5. Betz, C., D. Stracka, C. Prescianotto-Baschong, M. Frieden, N. Demaurex, and M.N. Hall, *Feature Article: mTOR complex 2-Akt signaling at mitochondria-associated endoplasmic reticulum membranes (MAM) regulates mitochondrial physiology.* Proceedings of the National Academy of Sciences of the United States of America, 2013. **110**(31): p. 12526-34.

6. Kung, G., K. Konstantinidis, and R.N. Kitsis, *Programmed necrosis, not apoptosis, in the heart.* Circulation research, 2011. **108**(8): p. 1017-36.

7. Song, X., Y. Kusakari, C.Y. Xiao, S.D. Kinsella, M.A. Rosenberg, M. Scherrer-Crosbie, K. Hara, A. Rosenzweig, and T. Matsui, *mTOR attenuates the inflammatory response in cardiomyocytes and prevents cardiac dysfunction in pathological hypertrophy.* American journal of physiology. Cell physiology, 2010. **299**(6): p. C1256-66.

8. Aoyagi, T., J.K. Higa, H. Aoyagi, N. Yorichika, B. Shimada, and T. Matsui, *Cardiac mTOR rescues the detrimental effects of diet-induced obesity in the*

heart after ischemia-reperfusion. American journal of physiology. Heart and circulatory physiology, 2015: p. ajpheart 00008 2015.

9. Zhang, D., R. Contu, M.V. Latronico, J. Zhang, R. Rizzi, D. Catalucci, S. Miyamoto, K. Huang, M. Ceci, Y. Gu, N.D. Dalton, K.L. Peterson, K.L. Guan, J.H. Brown, J. Chen, N. Sonenberg, and G. Condorelli, *MTORC1 regulates cardiac function and myocyte survival through 4E-BP1 inhibition in mice.* The Journal of clinical investigation, 2010. **120**(8): p. 2805-16.

10. Minicucci, M.F., P.S. Azevedo, B.F. Polegato, S.A. Paiva, and L.A. Zornoff, *Heart failure after myocardial infarction: clinical implications and treatment.* Clinical cardiology, 2011. **34**(7): p. 410-4.

11. Cohn, J.N., R. Ferrari, and N. Sharpe, *Cardiac remodeling--concepts and clinical implications: a consensus paper from an international forum on cardiac remodeling. Behalf of an International Forum on Cardiac Remodeling.* Journal of the American College of Cardiology, 2000. **35**(3): p. 569-82.

12. Eaton, L.W. and B.H. Bulkley, *Expansion of acute myocardial infarction: its relationship to infarct morphology in a canine model.* Circulation research, 1981. **49**(1): p. 80-8.

13. Hochman, J.S. and B.H. Bulkley, *Expansion of acute myocardial infarction: an experimental study.* Circulation, 1982. **65**(7): p. 1446-50.

14. Tan, L.B., J.E. Jalil, R. Pick, J.S. Janicki, and K.T. Weber, *Cardiac myocyte necrosis induced by angiotensin II.* Circulation research, 1991. **69**(5): p. 1185-95.

15. Weber, K.T., R. Pick, M.A. Silver, G.W. Moe, J.S. Janicki, I.H. Zucker, and P.W. Armstrong, *Fibrillar collagen and remodeling of dilated canine left ventricle.* Circulation, 1990. **82**(4): p. 1387-401.

16. Villarreal, F.J., N.N. Kim, G.D. Ungab, M.P. Printz, and W.H. Dillmann, *Identification of functional angiotensin II receptors on rat cardiac fibroblasts.* Circulation, 1993. **88**(6): p. 2849-61.

17. Tousoulis, D., A.M. Kampoli, N. Papageorgiou, C. Antoniades, G. Siasos, G. Latsios, E. Tsiamis, and C. Stefanadis, *Matrix metallopropteinases in heart failure.* Current topics in medicinal chemistry, 2012. **12**(10): p. 1181-91.

18. Wu, E., J.T. Ortiz, P. Tejedor, D.C. Lee, C. Bucciarelli-Ducci, P. Kansal, J.C. Carr, T.A. Holly, D. Lloyd-Jones, F.J. Klocke, and R.O. Bonow, *Infarct size by contrast enhanced cardiac magnetic resonance is a stronger predictor of*

outcomes than left ventricular ejection fraction or end-systolic volume index: prospective cohort study. Heart, 2008. **94**(6): p. 730-6.

19. Kwong, R.Y., A.K. Chan, K.A. Brown, C.W. Chan, H.G. Reynolds, S. Tsang, and R.B. Davis, *Impact of unrecognized myocardial scar detected by cardiac magnetic resonance imaging on event-free survival in patients presenting with signs or symptoms of coronary artery disease.* Circulation, 2006. **113**(23): p. 2733-43.

20. Anversa, P., G. Olivetti, and J.M. Capasso, *Cellular basis of ventricular remodeling after myocardial infarction.* The American journal of cardiology, 1991. **68**(14): p. 7D-16D.

21. Cohn, J.N., G.R. Johnson, R. Shabetai, H. Loeb, F. Tristani, T. Rector, R. Smith, and R. Fletcher, *Ejection fraction, peak exercise oxygen consumption, cardiothoracic ratio, ventricular arrhythmias, and plasma norepinephrine as determinants of prognosis in heart failure. The V-HeFT VA Cooperative Studies Group.* Circulation, 1993. **87**(6 Suppl): p. VI5-16.

22. White, H.D., R.M. Norris, M.A. Brown, P.W. Brandt, R.M. Whitlock, and C.J. Wild, *Left ventricular end-systolic volume as the major determinant of survival after recovery from myocardial infarction.* Circulation, 1987. **76**(1): p. 44-51.

23. Cafferkey, R., P.R. Young, M.M. McLaughlin, D.J. Bergsma, Y. Koltin, G.M. Sathe, L. Faucette, W.K. Eng, R.K. Johnson, and G.P. Livi, *Dominant missense mutations in a novel yeast protein related to mammalian phosphatidylinositol 3-kinase and VPS34 abrogate rapamycin cytotoxicity.* Molecular and cellular biology, 1993. **13**(10): p. 6012-23.

24. Kunz, J., R. Henriquez, U. Schneider, M. Deuter-Reinhard, N.R. Movva, and M.N. Hall, *Target of rapamycin in yeast, TOR2, is an essential phosphatidylinositol kinase homolog required for G1 progression.* Cell, 1993. **73**(3): p. 585-96.

25. Brown, E.J., M.W. Albers, T.B. Shin, K. Ichikawa, C.T. Keith, W.S. Lane, and S.L. Schreiber, *A mammalian protein targeted by G1-arresting rapamycin-receptor complex.* Nature, 1994. **369**(6483): p. 756-8.

26. Sabatini, D.M., H. Erdjument-Bromage, M. Lui, P. Tempst, and S.H. Snyder, *RAFT1: a mammalian protein that binds to FKBP12 in a rapamycin-dependent fashion and is homologous to yeast TORs.* Cell, 1994. **78**(1): p. 35-43.

27. Sabers, C.J., M.M. Martin, G.J. Brunn, J.M. Williams, F.J. Dumont, G. Wiederrecht, and R.T. Abraham, *Isolation of a protein target of the FKBP12-*

rapamycin complex in mammalian cells. The Journal of biological chemistry, 1995. **270**(2): p. 815-22.

28. Avruch, J., K. Hara, Y. Lin, M. Liu, X. Long, S. Ortiz-Vega, and K. Yonezawa, *Insulin and amino-acid regulation of mTOR signaling and kinase activity through the Rheb GTPase.* Oncogene, 2006. **25**(48): p. 6361-72.

29. Yang, H., D.G. Rudge, J.D. Koos, B. Vaidialingam, H.J. Yang, and N.P. Pavletich, *mTOR kinase structure, mechanism and regulation.* Nature, 2013. **497**(7448): p. 217-23.

30. Laplante, M. and D.M. Sabatini, *mTOR signaling in growth control and disease.* Cell, 2012. **149**(2): p. 274-93.

31. Jewell, J.L., R.C. Russell, and K.L. Guan, *Amino acid signalling upstream of mTOR.* Nature reviews. Molecular cell biology, 2013. **14**(3): p. 133-9.

32. Kim, D.H., D.D. Sarbassov, S.M. Ali, J.E. King, R.R. Latek, H. Erdjument-Bromage, P. Tempst, and D.M. Sabatini, *mTOR interacts with raptor to form a nutrient-sensitive complex that signals to the cell growth machinery.* Cell, 2002. **110**(2): p. 163-75.

33. Kim, D.H., D.D. Sarbassov, S.M. Ali, R.R. Latek, K.V. Guntur, H. Erdjument-Bromage, P. Tempst, and D.M. Sabatini, *GbetaL, a positive regulator of the rapamycin-sensitive pathway required for the nutrient-sensitive interaction between raptor and mTOR.* Molecular cell, 2003. **11**(4): p. 895-904.

34. Sancak, Y., C.C. Thoreen, T.R. Peterson, R.A. Lindquist, S.A. Kang, E. Spooner, S.A. Carr, and D.M. Sabatini, *PRAS40 is an insulin-regulated inhibitor of the mTORC1 protein kinase.* Molecular cell, 2007. **25**(6): p. 903-15.

35. Peterson, T.R., M. Laplante, C.C. Thoreen, Y. Sancak, S.A. Kang, W.M. Kuehl, N.S. Gray, and D.M. Sabatini, *DEPTOR is an mTOR inhibitor frequently overexpressed in multiple myeloma cells and required for their survival.* Cell, 2009. **137**(5): p. 873-86.

36. Sarbassov, D.D., S.M. Ali, D.H. Kim, D.A. Guertin, R.R. Latek, H. Erdjument-Bromage, P. Tempst, and D.M. Sabatini, *Rictor, a novel binding partner of mTOR, defines a rapamycin-insensitive and raptor-independent pathway that regulates the cytoskeleton.* Current biology : CB, 2004. **14**(14): p. 1296-302.

37. Jacinto, E., V. Facchinetti, D. Liu, N. Soto, S. Wei, S.Y. Jung, Q. Huang, J. Qin, and B. Su, *SIN1/MIP1 maintains rictor-mTOR complex integrity and regulates Akt phosphorylation and substrate specificity.* Cell, 2006. **127**(1): p. 125-37.

38. Pearce, L.R., X. Huang, J. Boudeau, R. Pawlowski, S. Wullschleger, M. Deak, A.F. Ibrahim, R. Gourlay, M.A. Magnuson, and D.R. Alessi, *Identification of Protor as a novel Rictor-binding component of mTOR complex-2.* The Biochemical journal, 2007. **405**(3): p. 513-22.

39. Wullschleger, S., R. Loewith, and M.N. Hall, *TOR signaling in growth and metabolism.* Cell, 2006. **124**(3): p. 471-84.

40. Kapahi, P., D. Chen, A.N. Rogers, S.D. Katewa, P.W. Li, E.L. Thomas, and L. Kockel, *With TOR, less is more: a key role for the conserved nutrient-sensing TOR pathway in aging.* Cell metabolism, 2010. **11**(6): p. 453-65.

41. Laplante, M. and D.M. Sabatini, *Regulation of mTORC1 and its impact on gene expression at a glance.* Journal of cell science, 2013. **126**(Pt 8): p. 1713-9.

42. Johnson, S.C., P.S. Rabinovitch, and M. Kaeberlein, *mTOR is a key modulator of ageing and age-related disease.* Nature, 2013. **493**(7432): p. 338-45.

43. Sancak, Y., T.R. Peterson, Y.D. Shaul, R.A. Lindquist, C.C. Thoreen, L. Bar-Peled, and D.M. Sabatini, *The Rag GTPases bind raptor and mediate amino acid signaling to mTORC1.* Science, 2008. **320**(5882): p. 1496-501.

44. Blommaart, E.F., J.J. Luiken, P.J. Blommaart, G.M. van Woerkom, and A.J. Meijer, *Phosphorylation of ribosomal protein S6 is inhibitory for autophagy in isolated rat hepatocytes.* The Journal of biological chemistry, 1995. **270**(5): p. 2320-6.

45. Hara, K., K. Yonezawa, Q.P. Weng, M.T. Kozlowski, C. Belham, and J. Avruch, *Amino acid sufficiency and mTOR regulate p70 S6 kinase and eIF-4E BP1 through a common effector mechanism.* The Journal of biological chemistry, 1998. **273**(23): p. 14484-94.

46. Laplante, M. and D.M. Sabatini, *mTOR signaling at a glance.* Journal of cell science, 2009. **122**(Pt 20): p. 3589-94.

47. Wang, L., T.E. Harris, R.A. Roth, and J.C. Lawrence, Jr., *PRAS40 regulates mTORC1 kinase activity by functioning as a direct inhibitor of substrate binding.* The Journal of biological chemistry, 2007. **282**(27): p. 20036-44.

48. Manning, B.D., A.R. Tee, M.N. Logsdon, J. Blenis, and L.C. Cantley, *Identification of the tuberous sclerosis complex-2 tumor suppressor gene product tuberin as a target of the phosphoinositide 3-kinase/akt pathway.* Molecular cell, 2002. **10**(1): p. 151-62.

49. Garami, A., F.J. Zwartkruis, T. Nobukuni, M. Joaquin, M. Roccio, H. Stocker, S.C. Kozma, E. Hafen, J.L. Bos, and G. Thomas, *Insulin activation of Rheb, a mediator of mTOR/S6K/4E-BP signaling, is inhibited by TSC1 and 2.* Molecular cell, 2003. **11**(6): p. 1457-66.

50. Saxton, R.A. and D.M. Sabatini, *mTOR Signaling in Growth, Metabolism, and Disease.* Cell, 2017. **168**(6): p. 960-976.

51. Gan, X., J. Wang, C. Wang, E. Sommer, T. Kozasa, S. Srinivasula, D. Alessi, S. Offermanns, M.I. Simon, and D. Wu, *PRR5L degradation promotes mTORC2-mediated PKC-delta phosphorylation and cell migration downstream of Galpha12.* Nature cell biology, 2012. **14**(7): p. 686-96.

52. Li, X. and T. Gao, *mTORC2 phosphorylates protein kinase Czeta to regulate its stability and activity.* EMBO reports, 2014. **15**(2): p. 191-8.

53. Sarbassov, D.D., D.A. Guertin, S.M. Ali, and D.M. Sabatini, *Phosphorylation and regulation of Akt/PKB by the rictor-mTOR complex.* Science, 2005. **307**(5712): p. 1098-101.

54. Shioi, T., J.R. McMullen, O. Tarnavski, K. Converso, M.C. Sherwood, W.J. Manning, and S. Izumo, *Rapamycin attenuates load-induced cardiac hypertrophy in mice.* Circulation, 2003. **107**(12): p. 1664-70.

55. McMullen, J.R., M.C. Sherwood, O. Tarnavski, L. Zhang, A.L. Dorfman, T. Shioi, and S. Izumo, *Inhibition of mTOR signaling with rapamycin regresses established cardiac hypertrophy induced by pressure overload.* Circulation, 2004. **109**(24): p. 3050-5.

56. Khan, S., F. Salloum, A. Das, L. Xi, G.W. Vetrovec, and R.C. Kukreja, *Rapamycin confers preconditioning-like protection against ischemia-reperfusion injury in isolated mouse heart and cardiomyocytes.* Journal of molecular and cellular cardiology, 2006. **41**(2): p. 256-64.

57. Das, A., F.N. Salloum, D. Durrant, R. Ockaili, and R.C. Kukreja, *Rapamycin protects against myocardial ischemia-reperfusion injury through JAK2-STAT3 signaling pathway.* Journal of molecular and cellular cardiology, 2012. **53**(6): p. 858-69.

58. Buss, S.J., S. Muenz, J.H. Riffel, P. Malekar, M. Hagenmueller, C.S. Weiss, F. Bea, R. Bekeredjian, M. Schinke-Braun, S. Izumo, H.A. Katus, and S.E. Hardt, *Beneficial effects of Mammalian target of rapamycin inhibition on left ventricular remodeling after myocardial infarction.* Journal of the American College of Cardiology, 2009. **54**(25): p. 2435-46.

59. Cittadini, A., M.G. Monti, V. Petrillo, G. Esposito, G. Imparato, A. Luciani, F. Urciuolo, E. Bobbio, C.F. Natale, L. Sacca, and P.A. Netti, *Complementary therapeutic effects of dual delivery of insulin-like growth factor-1 and vascular endothelial growth factor by gelatin microspheres in experimental heart failure.* European journal of heart failure, 2011. **13**(12): p. 1264-74.

60. Jonassen, A.K., M.N. Sack, O.D. Mjos, and D.M. Yellon, *Myocardial protection by insulin at reperfusion requires early administration and is mediated via Akt and p70s6 kinase cell-survival signaling.* Circulation research, 2001. **89**(12): p. 1191-8.

61. Ge, Y., M.S. Yoon, and J. Chen, *Raptor and Rheb negatively regulate skeletal myogenesis through suppression of insulin receptor substrate 1 (IRS1).* The Journal of biological chemistry, 2011. **286**(41): p. 35675-82.

62. Harrington, L.S., G.M. Findlay, and R.F. Lamb, *Restraining PI3K: mTOR signalling goes back to the membrane.* Trends in biochemical sciences, 2005. **30**(1): p. 35-42.

63. Volkers, M., M.H. Konstandin, S. Doroudgar, H. Toko, P. Quijada, S. Din, A. Joyo, L. Ornelas, K. Samse, D.J. Thuerauf, N. Gude, C.C. Glembotski, and M.A. Sussman, *Mechanistic target of rapamycin complex 2 protects the heart from ischemic damage.* Circulation, 2013. **128**(19): p. 2132-44.

64. Wu, X., Y. Cao, J. Nie, H. Liu, S. Lu, X. Hu, J. Zhu, X. Zhao, J. Chen, X. Chen, Z. Yang, and X. Li, *Genetic and pharmacological inhibition of Rheb1-mTORC1 signaling exerts cardioprotection against adverse cardiac remodeling in mice.* The American journal of pathology, 2013. **182**(6): p. 2005-14.

65. Bers, D.M., *Calcium cycling and signaling in cardiac myocytes.* Annual review of physiology, 2008. **70**: p. 23-49.

66. Scoote, M., P.A. Poole-Wilson, and A.J. Williams, *The therapeutic potential of new insights into myocardial excitation-contraction coupling.* Heart, 2003. **89**(4): p. 371-6.

67. Fearnley, C.J., H.L. Roderick, and M.D. Bootman, *Calcium signaling in cardiac myocytes.* Cold Spring Harbor perspectives in biology, 2011. **3**(11): p. a004242.

68. Fabiato, A., *Calcium-induced release of calcium from the cardiac sarcoplasmic reticulum.* The American journal of physiology, 1983. **245**(1): p. C1-14.

69. Cheng, H., W.J. Lederer, and M.B. Cannell, *Calcium sparks: elementary events underlying excitation-contraction coupling in heart muscle.* Science, 1993. **262**(5134): p. 740-4.

70. Brittsan, A.G., K.S. Ginsburg, G. Chu, A. Yatani, B.M. Wolska, A.G. Schmidt, M. Asahi, D.H. MacLennan, D.M. Bers, and E.G. Kranias, *Chronic SR Ca2+-ATPase inhibition causes adaptive changes in cellular Ca2+ transport.* Circulation research, 2003. **92**(7): p. 769-76.

71. Ke, Y., L. Wang, W.G. Pyle, P.P. de Tombe, and R.J. Solaro, *Intracellular localization and functional effects of P21-activated kinase-1 (Pak1) in cardiac myocytes.* Circulation research, 2004. **94**(2): p. 194-200.

72. Moss, R.L., M. Razumova, and D.P. Fitzsimons, *Myosin crossbridge activation of cardiac thin filaments: implications for myocardial function in health and disease.* Circulation research, 2004. **94**(10): p. 1290-300.

73. Tyska, M.J. and D.M. Warshaw, *The myosin power stroke.* Cell motility and the cytoskeleton, 2002. **51**(1): p. 1-15.

74. Bers, D.M., *Cardiac excitation-contraction coupling.* Nature, 2002. **415**(6868): p. 198-205.

75. Hobai, I.A. and B. O'Rourke, *Decreased sarcoplasmic reticulum calcium content is responsible for defective excitation-contraction coupling in canine heart failure.* Circulation, 2001. **103**(11): p. 1577-84.

76. Lindner, M., E. Erdmann, and D.J. Beuckelmann, *Calcium content of the sarcoplasmic reticulum in isolated ventricular myocytes from patients with terminal heart failure.* Journal of molecular and cellular cardiology, 1998. **30**(4): p. 743-9.

77. Schwinger, R.H., G. Munch, B. Bolck, P. Karczewski, E.G. Krause, and E. Erdmann, *Reduced Ca(2+)-sensitivity of SERCA 2a in failing human myocardium due to reduced serin-16 phospholamban phosphorylation.* Journal of molecular and cellular cardiology, 1999. **31**(3): p. 479-91.

78. Kranias, E.G. and R.J. Hajjar, *Modulation of cardiac contractility by the phospholamban/SERCA2a regulatome.* Circulation research, 2012. **110**(12): p. 1646-60.

79. Schmidt, U., R.J. Hajjar, C.S. Kim, D. Lebeche, A.A. Doye, and J.K. Gwathmey, *Human heart failure: cAMP stimulation of SR Ca(2+)-ATPase activity and phosphorylation level of phospholamban.* The American journal of physiology, 1999. **277**(2 Pt 2): p. H474-80.

80. Nicolaou, P. and E.G. Kranias, *Role of PP1 in the regulation of Ca cycling in cardiac physiology and pathophysiology.* Frontiers in bioscience, 2009. **14**: p. 3571-85.

81. Hasenfuss, G., H. Reinecke, R. Studer, M. Meyer, B. Pieske, J. Holtz, C. Holubarsch, H. Posival, H. Just, and H. Drexler, *Relation between myocardial function and expression of sarcoplasmic reticulum Ca(2+)-ATPase in failing and nonfailing human myocardium.* Circulation research, 1994. **75**(3): p. 434-42.

82. Bers, D.M., *Ryanodine receptor S2808 phosphorylation in heart failure: smoking gun or red herring.* Circulation research, 2012. **110**(6): p. 796-9.

83. Marks, A.R., S. Reiken, and S.O. Marx, *Progression of heart failure: is protein kinase a hyperphosphorylation of the ryanodine receptor a contributing factor?* Circulation, 2002. **105**(3): p. 272-5.

84. Marks, A.R., S. Priori, M. Memmi, K. Kontula, and P.J. Laitinen, *Involvement of the cardiac ryanodine receptor/calcium release channel in catecholaminergic polymorphic ventricular tachycardia.* Journal of cellular physiology, 2002. **190**(1): p. 1-6.

85. Pogwizd, S.M., K. Schlotthauer, L. Li, W. Yuan, and D.M. Bers, *Arrhythmogenesis and contractile dysfunction in heart failure: Roles of sodium-calcium exchange, inward rectifier potassium current, and residual beta-adrenergic responsiveness.* Circulation research, 2001. **88**(11): p. 1159-67.

86. Bers, D.M., *Altered cardiac myocyte Ca regulation in heart failure.* Physiology, 2006. **21**: p. 380-7.

87. Baines, C.P., *Role of the mitochondrion in programmed necrosis.* Frontiers in physiology, 2010. **1**: p. 156.

88. Crompton, M., A. Costi, and L. Hayat, *Evidence for the presence of a reversible Ca2+-dependent pore activated by oxidative stress in heart mitochondria.* The Biochemical journal, 1987. **245**(3): p. 915-8.

89. Nakayama, H., X. Chen, C.P. Baines, R. Klevitsky, X. Zhang, H. Zhang, N. Jaleel, B.H. Chua, T.E. Hewett, J. Robbins, S.R. Houser, and J.D. Molkentin,

Ca2+- and mitochondrial-dependent cardiomyocyte necrosis as a primary mediator of heart failure. The Journal of clinical investigation, 2007. **117**(9): p. 2431-44.

90. Zamzami, N. and G. Kroemer, *The mitochondrion in apoptosis: how Pandora's box opens.* Nature reviews. Molecular cell biology, 2001. **2**(1): p. 67-71.

91. Crompton, M., E. Barksby, N. Johnson, and M. Capano, *Mitochondrial intermembrane junctional complexes and their involvement in cell death.* Biochimie, 2002. **84**(2-3): p. 143-52.

92. Halestrap, A.P., *Calcium, mitochondria and reperfusion injury: a pore way to die.* Biochemical Society transactions, 2006. **34**(Pt 2): p. 232-7.

93. Griffiths, E.J. and A.P. Halestrap, *Mitochondrial non-specific pores remain closed during cardiac ischaemia, but open upon reperfusion.* The Biochemical journal, 1995. **307 (Pt 1)**: p. 93-8.

94. Gant, J.C., K.C. Chen, C.M. Norris, I. Kadish, O. Thibault, E.M. Blalock, N.M. Porter, and P.W. Landfield, *Disrupting function of FK506-binding protein 1b/12.6 induces the Ca(2)+-dysregulation aging phenotype in hippocampal neurons.* The Journal of neuroscience : the official journal of the Society for Neuroscience, 2011. **31**(5): p. 1693-703.

95. MacMillan, D. and J.G. McCarron, *Regulation by FK506 and rapamycin of Ca2+ release from the sarcoplasmic reticulum in vascular smooth muscle: the role of FK506 binding proteins and mTOR.* British journal of pharmacology, 2009. **158**(4): p. 1112-20.

96. MacMillan, D., S. Currie, and J.G. McCarron, *FK506-binding protein (FKBP12) regulates ryanodine receptor-evoked Ca2+ release in colonic but not aortic smooth muscle.* Cell calcium, 2008. **43**(6): p. 539-49.

97. Martin-Cano, F.E., C. Camello-Almaraz, D. Hernandez, M.J. Pozo, and P.J. Camello, *mTOR pathway and Ca(2)(+) stores mobilization in aged smooth muscle cells.* Aging, 2013. **5**(5): p. 339-46.

98. Regimbald-Dumas, Y., M.O. Fregeau, and G. Guillemette, *Mammalian target of rapamycin (mTOR) phosphorylates inositol 1,4,5-trisphosphate receptor type 2 and increases its Ca(2+) release activity.* Cellular signalling, 2011. **23**(1): p. 71-9.

99. Bultynck, G., P. De Smet, D. Rossi, G. Callewaert, L. Missiaen, V. Sorrentino, H. De Smedt, and J.B. Parys, *Characterization and mapping of the 12 kDa FK506-*

binding protein (FKBP12)-binding site on different isoforms of the ryanodine receptor and of the inositol 1,4,5-trisphosphate receptor. The Biochemical journal, 2001. **354**(Pt 2): p. 413-22.

100. Decuypere, J.P., D. Kindt, T. Luyten, K. Welkenhuyzen, L. Missiaen, H. De Smedt, G. Bultynck, and J.B. Parys, *mTOR-Controlled Autophagy Requires Intracellular Ca(2+) Signaling.* PloS one, 2013. **8**(4): p. e61020.

101. Grundy, S.M., H.B. Brewer, Jr., J.I. Cleeman, S.C. Smith, Jr., and C. Lenfant, *Definition of metabolic syndrome: Report of the National Heart, Lung, and Blood Institute/American Heart Association conference on scientific issues related to definition.* Circulation, 2004. **109**(3): p. 433-8.

102. Aronson, D., A. Musallam, J. Lessick, S. Dabbah, S. Carasso, H. Hammerman, S. Reisner, Y. Agmon, and D. Mutlak, *Impact of diastolic dysfunction on the development of heart failure in diabetic patients after acute myocardial infarction.* Circulation. Heart failure, 2010. **3**(1): p. 125-31.

103. Kannel, W.B., M. Hjortland, and W.P. Castelli, *Role of diabetes in congestive heart failure: the Framingham study.* The American journal of cardiology, 1974. **34**(1): p. 29-34.

104. Guo, S., *Insulin signaling, resistance, and the metabolic syndrome: insights from mouse models into disease mechanisms.* The Journal of endocrinology, 2014. **220**(2): p. T1-T23.

105. Fraenkel, M., M. Ketzinel-Gilad, Y. Ariav, O. Pappo, M. Karaca, J. Castel, M.F. Berthault, C. Magnan, E. Cerasi, N. Kaiser, and G. Leibowitz, *mTOR inhibition by rapamycin prevents beta-cell adaptation to hyperglycemia and exacerbates the metabolic state in type 2 diabetes.* Diabetes, 2008. **57**(4): p. 945-57.

106. Reichelt, M.E., L. Willems, J.N. Peart, K.J. Ashton, G.P. Matherne, M.R. Blackburn, and J.P. Headrick, *Modulation of ischaemic contracture in mouse hearts: a 'supraphysiological' response to adenosine.* Experimental physiology, 2007. **92**(1): p. 175-85.

107. Madisen, L., T.A. Zwingman, S.M. Sunkin, S.W. Oh, H.A. Zariwala, H. Gu, L.L. Ng, R.D. Palmiter, M.J. Hawrylycz, A.R. Jones, E.S. Lein, and H. Zeng, *A robust and high-throughput Cre reporting and characterization system for the whole mouse brain.* Nature neuroscience, 2010. **13**(1): p. 133-40.

108. Liao, R., B.K. Podesser, and C.C. Lim, *The continuing evolution of the Langendorff and ejecting murine heart: new advances in cardiac phenotyping.*

American journal of physiology. Heart and circulatory physiology, 2012. **303**(2): p. H156-67.

109. Gangloff, Y.G., M. Mueller, S.G. Dann, P. Svoboda, M. Sticker, J.F. Spetz, S.H. Um, E.J. Brown, S. Cereghini, G. Thomas, and S.C. Kozma, *Disruption of the mouse mTOR gene leads to early postimplantation lethality and prohibits embryonic stem cell development.* Molecular and cellular biology, 2004. **24**(21): p. 9508-16.

110. Matsui, T., L. Li, J.C. Wu, S.A. Cook, T. Nagoshi, M.H. Picard, R. Liao, and A. Rosenzweig, *Phenotypic spectrum caused by transgenic overexpression of activated Akt in the heart.* The Journal of biological chemistry, 2002. **277**(25): p. 22896-901.

111. Nagoshi, T., T. Matsui, T. Aoyama, A. Leri, P. Anversa, L. Li, W. Ogawa, F. del Monte, J.K. Gwathmey, L. Grazette, B.A. Hemmings, D.A. Kass, H.C. Champion, and A. Rosenzweig, *PI3K rescues the detrimental effects of chronic Akt activation in the heart during ischemia/reperfusion injury.* The Journal of clinical investigation, 2005. **115**(8): p. 2128-38.

112. Reichelt, M.E., L. Willems, B.A. Hack, J.N. Peart, and J.P. Headrick, *Cardiac and coronary function in the Langendorff-perfused mouse heart model.* Experimental physiology, 2009. **94**(1): p. 54-70.

113. Desai, B.N., B.R. Myers, and S.L. Schreiber, *FKBP12-rapamycin-associated protein associates with mitochondria and senses osmotic stress via mitochondrial dysfunction.* Proceedings of the National Academy of Sciences of the United States of America, 2002. **99**(7): p. 4319-24.

114. Atkin, J., L. Halova, J. Ferguson, J.R. Hitchin, A. Lichawska-Cieslar, A.M. Jordan, J. Pines, C. Wellbrock, and J. Petersen, *Torin1-mediated TOR kinase inhibition reduces Wee1 levels and advances mitotic commitment in fission yeast and HeLa cells.* Journal of cell science, 2014. **127**(Pt 6): p. 1346-56.

115. Wang, L., R.C. Myles, N.M. De Jesus, A.K. Ohlendorf, D.M. Bers, and C.M. Ripplinger, *Optical mapping of sarcoplasmic reticulum Ca2+ in the intact heart: ryanodine receptor refractoriness during alternans and fibrillation.* Circulation research, 2014. **114**(9): p. 1410-21.

116. Grimm, M., H. Ling, A. Willeford, L. Pereira, C.B. Gray, J.R. Erickson, S. Sarma, J.L. Respress, X.H. Wehrens, D.M. Bers, and J.H. Brown, *CaMKIIdelta mediates beta-adrenergic effects on RyR2 phosphorylation and SR Ca(2+) leak and the pathophysiological response to chronic beta-adrenergic stimulation.* Journal of molecular and cellular cardiology, 2015. **85**: p. 282-91.

117. Kushnir, A., J. Shan, M.J. Betzenhauser, S. Reiken, and A.R. Marks, *Role of CaMKIIdelta phosphorylation of the cardiac ryanodine receptor in the force frequency relationship and heart failure.* Proceedings of the National Academy of Sciences of the United States of America, 2010. **107**(22): p. 10274-9.

118. Edwards, J.N. and L.A. Blatter, *Cardiac alternans and intracellular calcium cycling.* Clinical and experimental pharmacology & physiology, 2014. **41**(7): p. 524-32.

119. Koretsune, Y. and E. Marban, *Mechanism of ischemic contracture in ferret hearts: relative roles of [Ca2+]i elevation and ATP depletion.* The American journal of physiology, 1990. **258**(1 Pt 2): p. H9-16.

120. Kingsley, P.B., E.Y. Sako, M.Q. Yang, S.D. Zimmer, K. Ugurbil, J.E. Foker, and A.H. From, *Ischemic contracture begins when anaerobic glycolysis stops: a 31P-NMR study of isolated rat hearts.* The American journal of physiology, 1991. **261**(2 Pt 2): p. H469-78.

121. Contreras-Ferrat, A., S. Lavandero, E. Jaimovich, and A. Klip, *Calcium signaling in insulin action on striated muscle.* Cell calcium, 2014. **56**(5): p. 390-6.

122. Gutierrez, T., V. Parra, R. Troncoso, C. Pennanen, A. Contreras-Ferrat, C. Vasquez-Trincado, P.E. Morales, C. Lopez-Crisosto, C. Sotomayor-Flores, M. Chiong, B.A. Rothermel, and S. Lavandero, *Alteration in mitochondrial Ca(2+) uptake disrupts insulin signaling in hypertrophic cardiomyocytes.* Cell communication and signaling : CCS, 2014. **12**: p. 68.

123. MacMillan, D., S. Currie, K.N. Bradley, T.C. Muir, and J.G. McCarron, *In smooth muscle, FK506-binding protein modulates IP3 receptor-evoked Ca2+ release by mTOR and calcineurin.* Journal of cell science, 2005. **118**(Pt 23): p. 5443-51.

124. Kisfalvi, K., O. Rey, S.H. Young, J. Sinnett-Smith, and E. Rozengurt, *Insulin potentiates Ca2+ signaling and phosphatidylinositol 4,5-bisphosphate hydrolysis induced by Gq protein-coupled receptor agonists through an mTOR-dependent pathway.* Endocrinology, 2007. **148**(7): p. 3246-57.

125. Werdich, A.A., E.A. Lima, I. Dzhura, M.V. Singh, J. Li, M.E. Anderson, and F.J. Baudenbacher, *Differential effects of phospholamban and Ca2+/calmodulin-dependent kinase II on [Ca2+]i transients in cardiac myocytes at physiological stimulation frequencies.* American journal of physiology. Heart and circulatory physiology, 2008. **294**(5): p. H2352-62.

126. Parra, V., H.E. Verdejo, M. Iglewski, A. Del Campo, R. Troncoso, D. Jones, Y. Zhu, J. Kuzmicic, C. Pennanen, C. Lopez-Crisosto, F. Jana, J. Ferreira, E.

Noguera, M. Chiong, D.A. Bernlohr, A. Klip, J.A. Hill, B.A. Rothermel, E.D. Abel, A. Zorzano, and S. Lavandero, *Insulin stimulates mitochondrial fusion and function in cardiomyocytes via the Akt-mTOR-NFkappaB-Opa-1 signaling pathway.* Diabetes, 2014. **63**(1): p. 75-88.

127. Gorski, P.A., D.K. Ceholski, and R.J. Hajjar, *Altered myocardial calcium cycling and energetics in heart failure--a rational approach for disease treatment.* Cell metabolism, 2015. **21**(2): p. 183-94.

128. Lou, Q., A. Janardhan, and I.R. Efimov, *Remodeling of calcium handling in human heart failure.* Advances in experimental medicine and biology, 2012. **740**: p. 1145-74.

129. Grynkiewicz, G., M. Poenie, and R.Y. Tsien, *A new generation of Ca2+ indicators with greatly improved fluorescence properties.* The Journal of biological chemistry, 1985. **260**(6): p. 3440-50.

130. Takahashi, A., P. Camacho, J.D. Lechleiter, and B. Herman, *Measurement of intracellular calcium.* Physiological reviews, 1999. **79**(4): p. 1089-125.

131. Domeier, T.L., C.J. Roberts, A.K. Gibson, L.M. Hanft, K.S. McDonald, and S.S. Segal, *Dantrolene suppresses spontaneous Ca2+ release without altering excitation-contraction coupling in cardiomyocytes of aged mice.* American journal of physiology. Heart and circulatory physiology, 2014. **307**(6): p. H818-29.

132. Fernandez-Velasco, M., A. Rueda, N. Rizzi, J.P. Benitah, B. Colombi, C. Napolitano, S.G. Priori, S. Richard, and A.M. Gomez, *Increased Ca2+ sensitivity of the ryanodine receptor mutant RyR2R4496C underlies catecholaminergic polymorphic ventricular tachycardia.* Circulation research, 2009. **104**(2): p. 201-9, 12p following 209.

133. Varro, A., N. Negretti, S.B. Hester, and D.A. Eisner, *An estimate of the calcium content of the sarcoplasmic reticulum in rat ventricular myocytes.* Pflugers Archiv : European journal of physiology, 1993. **423**(1-2): p. 158-60.

134. Trafford, A.W., M.E. Diaz, and D.A. Eisner, *A novel, rapid and reversible method to measure Ca buffering and time-course of total sarcoplasmic reticulum Ca content in cardiac ventricular myocytes.* Pflugers Archiv : European journal of physiology, 1999. **437**(3): p. 501-3.

135. Porta, M., A.V. Zima, A. Nani, P.L. Diaz-Sylvester, J.A. Copello, J. Ramos-Franco, L.A. Blatter, and M. Fill, *Single ryanodine receptor channel basis of caffeine's action on Ca2+ sparks.* Biophysical journal, 2011. **100**(4): p. 931-8.

136. Shi, J., J. Guan, B. Jiang, D.A. Brenner, F. Del Monte, J.E. Ward, L.H. Connors, D.B. Sawyer, M.J. Semigran, T.E. Macgillivray, D.C. Seldin, R. Falk, and R. Liao, *Amyloidogenic light chains induce cardiomyocyte contractile dysfunction and apoptosis via a non-canonical p38alpha MAPK pathway.* Proceedings of the National Academy of Sciences of the United States of America, 2010. **107**(9): p. 4188-93.

137. Zhang, T., T. Guo, S. Mishra, N.D. Dalton, E.G. Kranias, K.L. Peterson, D.M. Bers, and J.H. Brown, *Phospholamban ablation rescues sarcoplasmic reticulum Ca(2+) handling but exacerbates cardiac dysfunction in CaMKIIdelta(C) transgenic mice.* Circulation research, 2010. **106**(2): p. 354-62.

138. Faggioni, M., H.S. Hwang, C. van der Werf, I. Nederend, P.J. Kannankeril, A.A. Wilde, and B.C. Knollmann, *Accelerated sinus rhythm prevents catecholaminergic polymorphic ventricular tachycardia in mice and in patients.* Circulation research, 2013. **112**(4): p. 689-97.

139. Baliga, V. and R. Sapsford, *Review article: Diabetes mellitus and heart failure--an overview of epidemiology and management.* Diabetes & vascular disease research : official journal of the International Society of Diabetes and Vascular Disease, 2009. **6**(3): p. 164-71.

140. Jaffe, A.S., J.J. Spadaro, K. Schechtman, R. Roberts, E.M. Geltman, and B.E. Sobel, *Increased congestive heart failure after myocardial infarction of modest extent in patients with diabetes mellitus.* American heart journal, 1984. **108**(1): p. 31-7.

141. Bui, A.L., T.B. Horwich, and G.C. Fonarow, *Epidemiology and risk profile of heart failure.* Nature reviews. Cardiology, 2011. **8**(1): p. 30-41.

142. From, A.M., C.L. Leibson, F. Bursi, M.M. Redfield, S.A. Weston, S.J. Jacobsen, R.J. Rodeheffer, and V.L. Roger, *Diabetes in heart failure: prevalence and impact on outcome in the population.* The American journal of medicine, 2006. **119**(7): p. 591-9.

143. Wang, C.Y. and J.K. Liao, *A mouse model of diet-induced obesity and insulin resistance.* Methods in molecular biology, 2012. **821**: p. 421-33.

144. Kanasaki, K. and D. Koya, *Biology of obesity: lessons from animal models of obesity.* Journal of biomedicine & biotechnology, 2011. **2011**: p. 197636.